Competitive Aromatic Carbon Fluorine Bond Activation and Carbon Hydrogen Bond Activation of Fluorobenzenes by Rhodium(III) Porphyrins

LEE, Man Ho

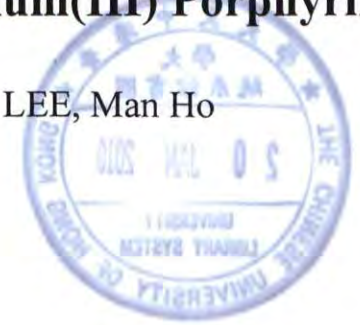

Thesis Submitted to the Department of Chemistry in Partial Fulfillment of the Requirement of the Degree of
Master of Philosophy
in
Chemistry

October 2008

Thesis/Assessment Committee

Professor MAK, Chung Wai Thomas (Chair)

Professor CHAN, Kin Shing (Thesis Supervisor)

Professor MIAO, Qian (Committee Member)

Professor LIN, Ying-Chih (External Examiner)

Table of Contents

Acknowledgement

First and foremost, I would like to express my most sincere gratitude to my supervisor, Prof. Kin Shing Chan, for his invaluable advice, patient guidance, and enthusiasm in my postgraduate studies throughout my research work. He inspired me much in learning how to utilize fundamental chemical knowledge in my research.

I would also like to give thanks to all members of the Department of Chemistry for their help and technical support in all circumstances.

Thanks are also given to all my dear former and current group members: Dr. Yin Ki Jenkins Tsang, Mr. Tsz Ho Lai, Mr. Peng Fai Chiu, Ms. Bao Zhu Li, Mr. Yun Wai Chan, Mr. Chi Wai Cheung, Mr. Kwong Shing Choi, Mr. Hong Sang Fung, Mr. Chung Yin Chan and Ms. Ching Chi Au for their encouragement and helpful discussion. I wish them continued success in their research and career.

I have to specially thank my family for their unfailing support and love. Without their love and understanding, I would not be able to finish the course of my study.

August, 2008.

Man Ho Lee

Department of Chemistry

The Chinese University of Hong Kong

Abbreviations

δ	: chemical shift	K	: equilibrium constant
Anal	: analytical	m	: multiplet (NMR)
Ar	: aryl	M^+	: molecular ion
Bn	: benzyl	M	: molarity
BDE.	: bond dissocication energy	Me	: methyl
br s	: broad singlet (NMR)	mg	: milligram (s)
^{t}Bu	: *tert*-butyl	min	: minute (s)
Calcd.	: calculated	mL	: milliliter (s)
CHA	: carbon hydrogen bond activation	mmol	: milimole (s)
CCA	: carbon carbon bond activation	MS	: mass spectrometry
d	: day (s)	NBS	: N-bromosuccinimide
d	: doublet (NMR)	NMR	: nuclear magnetic resonance
FABMS	: fast atom bombardment mass spectrometry	ppm	: part per million
ESI	: electrospray ionization	Ph	: phenyl
g	: gram (s)	PhCN	: benzonitrile
h	: hour (s)	R	: alkyl group
HRMS	: high resolution mass spectrometry	r.t.	: room temperature
Hz	: hertz	s	: singlet (NMR)
J	: coupling constant	t	: triplet (NMR)

Abstract

Aromatic carbon-fluorine bond activation (CFA) and selective aromatic carbon-hydrogen bond activation (CHA) were found in the reactions of fluoro-substituted benzenes with Rh(por)Cl (por = porphyrinate) in the presence of base to give aryl rhodium porphyrin complexes.

The aromatic carbon-fluorine bond of fluorobenzene was activated by Rh(ttp)Cl at 120 °C in basic media in 48% yield in solvent-free conditions. When the reaction was carried out in benzene as solvent, both the solubility and yield were improved. Competitive carbon-fluorine bond and carbon-hydrogen bond activations were shown in reactions between Rh(ttp)Cl and several fluorobenzenes bearing two and three fluorine atoms. The carbon-hydrogen bond activation also showed an *ortho*-selectivity to yield ortho-fluoroaryl rhodium porphyrin complexes.

摘要

碱性条件下，Rh(por)Cl (por 代表卟啉) 可进行芳香族碳氟键活化(CFA)，亦可进行选择性芳香族碳氢键活化(CHA)，得到芳基铑卟啉络合物。

碱性条件下，当反应温度为 120℃时，在非溶剂条件下，氟苯的芳香族碳氟键可被 Rh(ttp)Cl 活化，产率为 48%。在以苯为溶剂的条件下， 溶解性和产率都得到提高。碳氟键与碳氢键的竞争性可以在 Rh(ttp)Cl 与一些带有二个或三个氟原子的氟苯的反应中得到体现。碳氢键活化还显示了邻位选择性，从而得到邻位氟芳基铑卟啉络合物。

Chapter 1 Introduction

1.1 Definition of Aromatic Bond Activation

Aromatic bond activation is defined as the activation of the aromatic carbon-hydrogen, -halogen, -nitrogen, and -oxygen bonds by transition metal complexes to give transition metal aryls (eq. 1.1).

$$M + Ar\text{-}X \longrightarrow Ar\text{-}M\text{-}X \text{ or } Ar\text{-}M \qquad (1.1)$$

X = H, F, etc.

1.2 Application of Aromatic Carbon Fluorine Bond Activation

The activation of aromatic carbon-iodine, -bromine and –chlorine bonds are the key steps in the catalytic cross-couplings for the bi-aryl synthesis.[1] However, due to the great strength of aromatic carbon-fluorine bond, the synthesis of bi-aryls via the aromatic carbon-fluorine activation remains less-developed with only a few reported examples.[2,3,4,5]

Kambe et al.[2] reported the selective cross-coupling of arylfluorides by $NiCl_2$(dppf) catalyst via the activation of C-F bond (eq. 1.2).[2]

$$Ph\text{-}F + PhMgBr \xrightarrow[\text{1,3-butadiene, 25 °C, 24 h}]{\text{8 mol\% } NiCl_2(dppf)} Ph\text{-}Ph \quad 27\% \qquad (1.2)$$

Another example was demonstrated by Mongin et al.[3] to achieve the selective synthesis of heterocyclic bi-aryls by nickel(0) catalyst in the reactions of

phenylmangnesium bromides with fluoroazines and fluorodiazines at room temperature (eq. 1.3).[3]

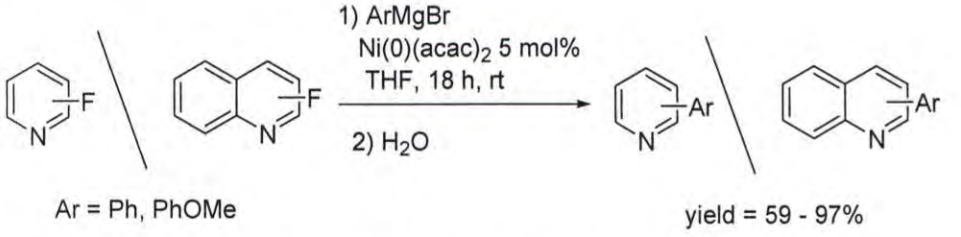

(1.3)

1.3 Mechanisms of Aromatic Bond Activation

Transition-metal-mediated aromatic carbon-halogen and carbon-hydrogen bonds activations usually occur via one of the following mechanistic pathways: 1) oxidative addition onto a metal centre, 2) electrophilic aromatic substitution with metal complexes, 3) nucleophilic aromatic substitution (S_NAr) with classical 1x2-electron pathway, 4) nucleophilic aromatic substitution with non-classical 2x1 electron transfer pathway, 5) halogen atom abstraction reaction, and 6) 1,2-addition into a metal-carbon bond (Table 1.1).

1.3.1 Oxidative Addition

Oxidative addition of an aromatic carbon-halogen or carbon-hydrogen bond involves the formal 2e oxidation of an electronically unsaturated metal centre via the cleavage of an aromatic C-H bond or aromatic C-X bond and the concurrent formation of a metal-carbon and a metal-hydrogen or metal-hydride bond (eq. 1.4). The oxidative addition of C-H occurs in the presence of *d*-electrons on the metal center, and hence this process is more common for low-valent transition metals.[6,7]

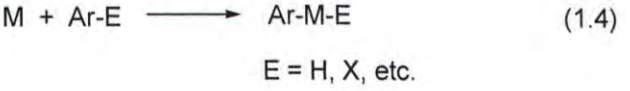

(1.4)

Table 1.1 Mechanistic Schemes Involved in Aromatic Bond Activation

Mechanistic Scheme		General Scheme	
		C-H Activation	C-F Activation
1	Oxidative Addition	M + Ar-H → Ar-M-H	M + Ar-X → Ar-M-X
2	Electrophilic Aromatic Substitution	M^+ + Ar-H → Ar-M + H^+	nil
3	Nucleophilic Aromatic Substitution -classical	Nil	M^- + Ar-X → Ar-M + X^-
4	Nucleophilic Aromatic Substitution –non-classical Electron Transfer Pathway	Nil	M^- + Ar-X → M· + Ar-X^-· Ar-X^-· → Ar· + X^- M· + Ar· → M-Ar
5	Halogen Atom Abstraction	Nil	M· + Ar-X → Ar-M + X·
6	1,2-Addition	M=C + Ar-H → Ar-M-C-H	M=C + Ar-X → Ar-M-C-X

Aromatic C-H activation via oxidative addition was discovered by Bergman and co-workers from a low valent iridium(I) complex intermediate **1** to achieve the iridium(III) product **2** (eq. 1.5).[7]

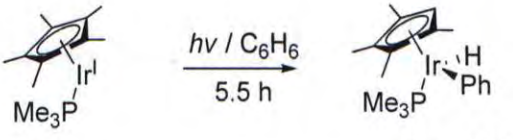

1 **2** 67% (1.5)

The oxidative addition of aromatic C-F bonds can occur in other low valent transition metal complexes. Jones and co-workers demonstrated the oxidation addition of an aromatic C-F bond into a low valent zirconium(II) complex to yield the Zr(IV) product (eq. 1.6).[8]

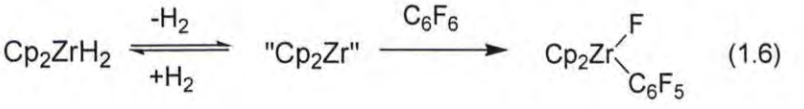

(1.6)

1.3.2 Electrophilic Aromatic Substitution

Electrophilic aromatic substitution (S_EAr) is another pathway to activate an aromatic bond. It involves the substitution of an aromatic hydrogen (in the form of proton) with an electrophilic reagent (eq. 1.7). Regioselectivity is an issue for substituted arenes where classical electrophilic aromatic substitution product(s) often form.[9]

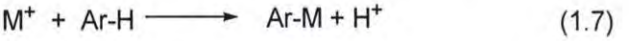

(1.7)

He and co-workers[10] demonstrated this type of reaction of gold(III) chloride with mesitylene through the formation of the arenium ion intermediate **3**[10] (Scheme 1).

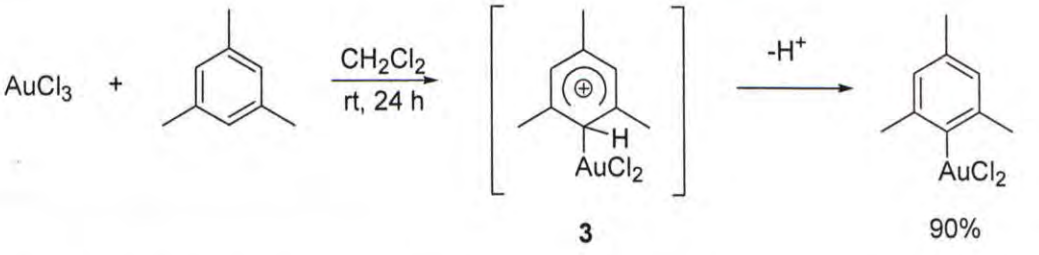

3 90%

Scheme 1. Electrophilic Aromatic Substitution of Aromatic C-H Bond by Gold(III) **3**.

Halogens always leave as anions, so they do not usually participate in this reaction pathway.

1.3.3 Nucleophilic Aromatic Substitution

Nucleophilic aromatic substitution (S_NAr) is also a viable type of aromatic bond activation. A metal complex acts as the nucleophile to replace the hydride and halide. The low valent metal complex must possess high electron density in order to have the lone pair electron for the nucleophilic attack to the sp^2 aromatic carbon (eq. 1.8).[11]

$$M^- + Ar\text{-}F \longrightarrow Ar\text{-}M + F^- \qquad (1.8)$$

No example has been reported for aromatic C-H activation via the S_NAr to generate a hydride due to the high reactivity of hydride and the poor leaving group property.

Yu et al.[12] reported the S_NAr type electron transfer C-F activation of fluoroarenes by palladium(0) metal complex **4** and forming the corresponding oxidative addition product **6**.[12] Although a interaction between palladium center and fluorine was proposed, no spectrometry evidence was yet detected in the course of reaction.

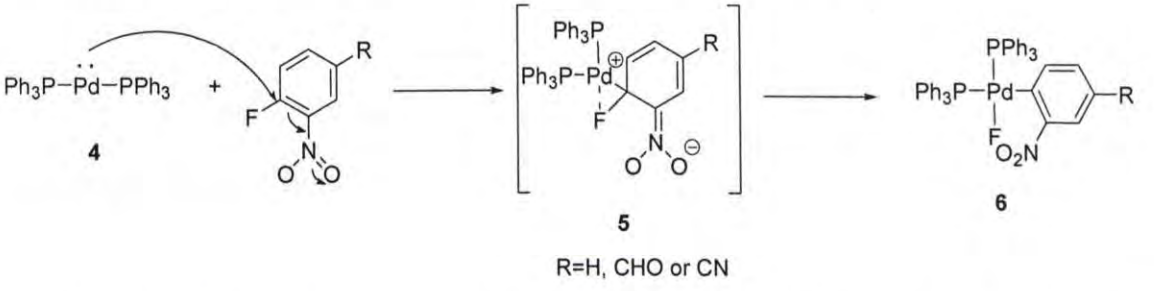

Scheme 3. Nucleophilic Aromatic Substitution of Aromatic C-F bond by Palladium(0) **4**.

A recent example of nucleophilic aromatic substitution involves the reaction of iridium(I) complex with perfluoroarenes to form the corresponding substituted product with the loss of fluoride ion (eq. 1.9).[13]

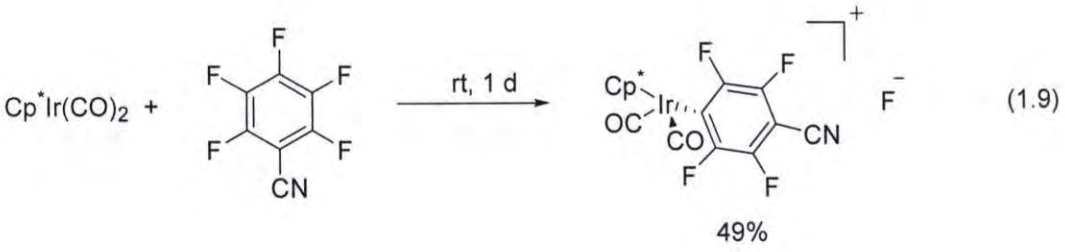

(1.9)

1.3.4 Halogen Atom Abstraction

Halogen atom abstraction involves the abstraction of a halogen atom from homolytic cleavage of the aromatic carbon-halogen bond by a metal complex (eq. 1.10).[11]

$$2M + Ar\text{-}X \longrightarrow M\text{-}Ar + M\text{-}X \qquad (1.10)$$

$$M + Ar\text{-}X \longrightarrow M\text{-}X + Ar\cdot \qquad (1.10.1)$$

$$Ar\cdot + M \longrightarrow Ar\text{-}M \qquad (1.10.2)$$

Halpern and co-workers[14] reported the activation of aryl iodide via the iodine atom abstraction pathway by an 17 electrons cobalt(II) complex. The by-product, pyridine radical was reacted with another 17 electrons cobalt(II) complex to yield the cobalt aryl complex (eq. 1.11).[14]

$$2Co(CN)_5^{3-} + 2\ PyI \xrightarrow{50\ ^\circ C,\ 16\ h} Co(CN)_5I^{3-} + Co(CN)_5Py^{2-} \qquad (1.11)$$

95%

Halogen atom abstraction is normally occurred in aliphatic halides by metal complexes. Fluorine always leaves as fluoride ion due to its high electronegativity.[15]

1.3.5 1,2-Addition

1,2-Addition into metal carbon double bond is common for aromatic C-H activations for early to mid-transition metal complexes. Legzdins and co-workers[16] reported the activation of the C-H bond of benzene by the tungsten akylidiene complex generated from the thermolysis of **7** to give product **9**[16] (Scheme 4).

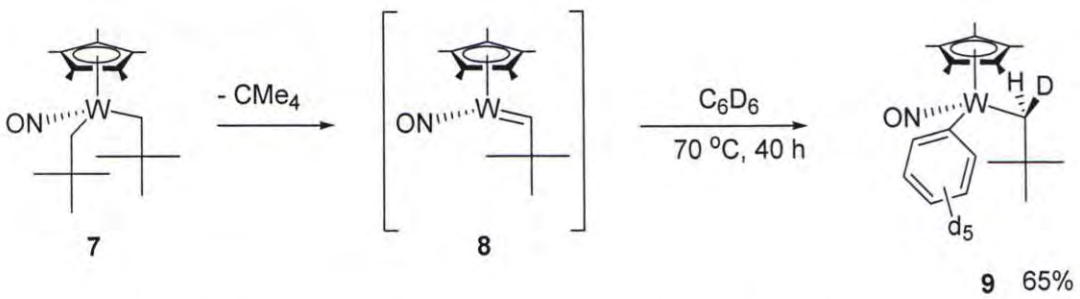

Scheme 4. Addition of Aromatic C-H Bond into W=C Linkage

1.4 Difficulties in Aromatic Bond Activations

The well-known properties of the fluorine atom is the highest electronegativity in the Pauling's electronegativity scale (4.0) and the strong bond strength character of the carbon-fluorine bond.[17] This chemical inertness and the high thermal stability make the chemistry of fluorocarbons a specialized field, an area of research that has attracted the attention of both inorganic and organometallic chemists to overcome the chemical and intellectual challenges of C-F bond activation. Furthermore, fluorocarbons are reluctant to coordinate to metal centers and making the activation kinetically difficult.[18,19]

Compared with aromatic C-F activation, aromatic C-H activation has a longer history and has received more attention in the research field. The aromatic C-H bonds are kinetically reactive even though the aromatic C-H bonds are strong (bond energy ca. 90 – 110 kcalmol^{-1}),[20,21] non-polarized, and very poor Lewis acids or bases.[22] Usually the activation is highly facilitated by the precoordination of the ring electrons to the metal center.

1.4.1 Thermodynamic Estimation

The estimation of the thermodynamics of CFA and CHA are outlined in Scheme 5. Similar calculations of other fluorobenzenes are listed in Table 1.2.

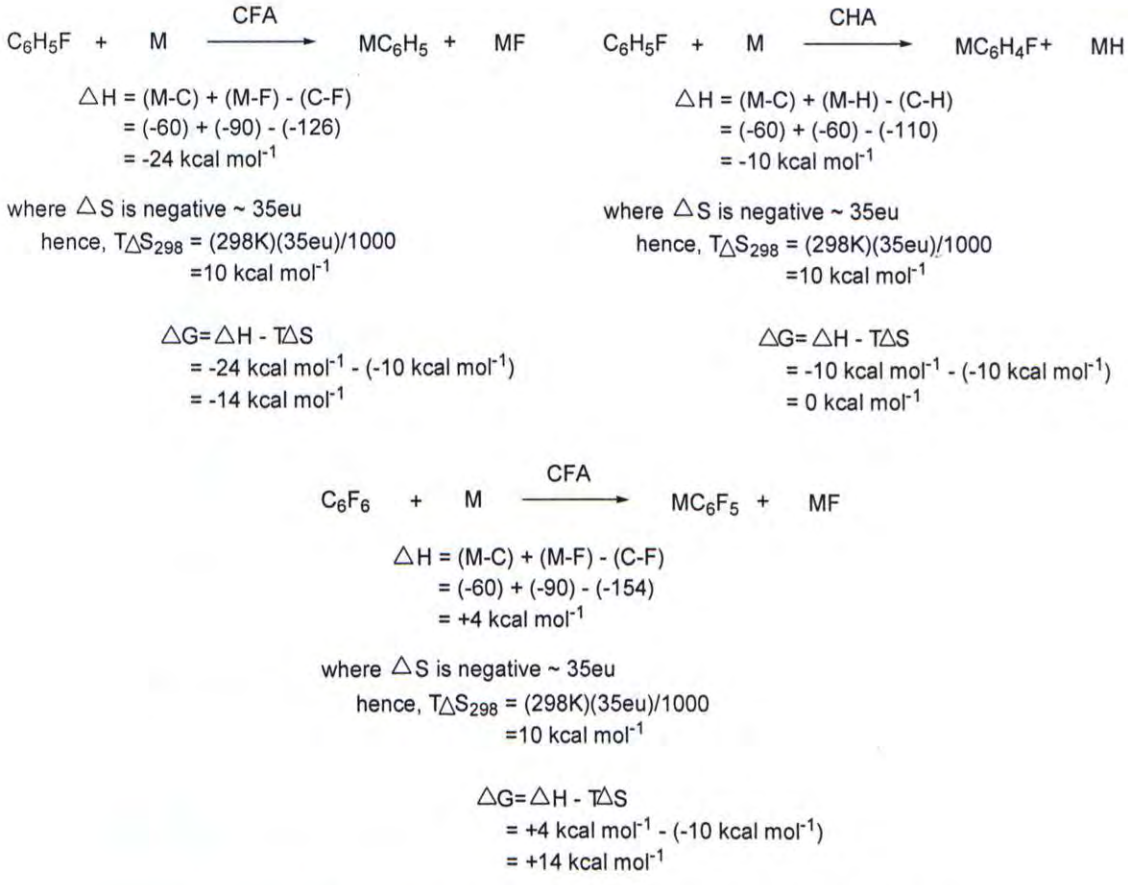

Scheme 5. Thermodynamic Estimation of CFA and CHA

Table 1.2 Thermodynamic Estimation of CFA and CHA

Entry	Fluoro-benzene	BDE of C-F bond / kcal mol^{-1}	BDE of C-H bond / kcal mol^{-1}	Gas phase pK_a of C-H (ΔG^o_g/ kcal mol^{-1})	CFA ΔG_{298} / kcal mol^{-1}	CHA ΔG_{298} / kcal mol^{-1}
1		NA	110[a]	390.4[b]	NA	0
2	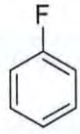	126[a]	110[a]	378.6[b]	-14	0
3	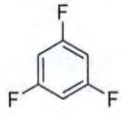	138[c]	117[c]	361.4[b]	-2	7
4	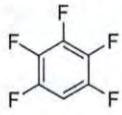	150[d]	125[d]	349[b]	10	15
5	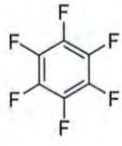	154[c]	NA	NA	14	NA

[a] Reference 23(b); [b] Reference 26; [c] Reference 23(a); [d] Reference 25.

The BDE of the C-F bond of fluorobenzene is 126 kcal mol^{-1} while the BDE of the C-H bond is 110 kcal mol^{-1}. In the case of hexafluorobenzene, the BDE of C-F bond is up to 154 kcal mol^{-1}.[23] The Rh-C bond in Rh(oep)C(O)H and the Rh-H bond in Rh(oep)H are both about 60 kcal mol^{-1}.[24] The M-F is normally higher than the M-H bond by 30 kcal mol^{-1} for *d*-block transition metal complex,[25] which is around 90 kcal mol^{-1} for this computation and the types of bond strength are listed in Table 1.3.

Table 1.3 Rhodium Bond Strength

Compound for Reference	Bond Type	Bond Strength / kcalmol^{-1}
Rh(oep)C(O)H	Rh-C bond	60[a]
Rh(oep)H	Rh-H bond	60[a]
Gerenal Transition Metal Complexes	Rh-F bond	90[b]

[a] Reference 24; [b] Reference 25

For reference, the gas phase acidities of fluorobenzenes are listed in Table 1.2.[24] The ΔS is around -35 eu at 298 K[25] and the ΔG_{298} of the CFA of fluorobenzene is estimated to be -14 kcal mol^{-1} while that of the CHA of fluorobenzene is equal or less than 0 kcal mol^{-1}. Therefore, the CFA reaction is thermodynamically more favorable process than CHA.

In the case of penta- and hexafluorobenzene, due to the stronger C-F bond, the ΔG_{298} of the CFA is positive. The Rh-C bond in Rh(ttp)C_6F_5 also expected to be stronger than that in Rh(ttp)C_6H_5. The same results are observed in ΔG_{298} of the CHA in 1,3,5-tri and pentafluorobenzene.

1.4.2 Aromatic Carbon-Fluorine Bond Activation by Transition Metal Complexes

A brief review in chronological order of the activation of C-F bonds by transition metal complexes is given below. For more pertinent reviews, the reviews by Richmond[28] and Torrens[29] should be consulted.

1.4.2.1 Examples of Aromatic C-F Activation in 1970s

In 1973, the activation of aromatic C-F bond has been realized in the cross-coupling reaction of fluorobenzene with *i*-C_3H_7MgCl. Treatment of an ether solution of *i*-C_3H_7MgCl with fluorobenzene in the presence of the $Ni(Me_2PCH_2CH_2PMe_2)Cl_2$ catalyst afford a mixture of three cross-coupling products, **10**, **11**, and **12** in 62% overall yield (eq. 1.12).[30] The key step in this transformation has been proposed to be the oxidative addition of the C-F bond in fluorobenzene at Ni(0) prior to the cross-coupling step and isomerization of aryls.

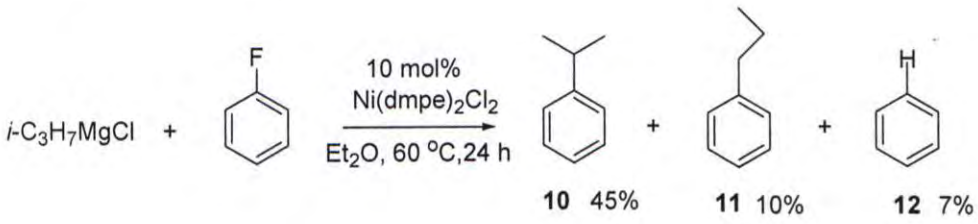

(1.12)

Another discovery of CFA was made by Stone and co-workers[31] in 1976 in the reaction of 3,5-$(CH_3OCO)_2C_6H_3N{=}NC_6F_5$ with $CpRu(PPh_3)_2(CH_3)$ to give 21% yield of **13** via the chelation-assisted metalation of the C_6F_5 ring (eq. 1.13).[31]

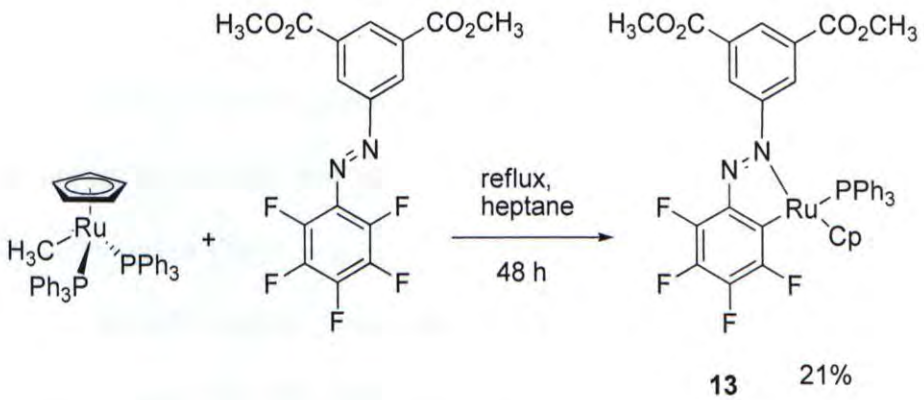

(1.13)

1.4.2.2 Examples of Aromatic C-F Activation in 1980s

In 1987, $W(CO)_3(NCEt)_3$ was reported to undergo facile oxidative addition of an aromatic C-F bond in the compound **14**. After ligand substitution of 2 equivalent of ligand EtCN of **14,** the intermediate **15** is formed. The C-F bond activation occurs intramolecularly to give the tungsten(II) product **16** in 69% yield[32] (Scheme 6).

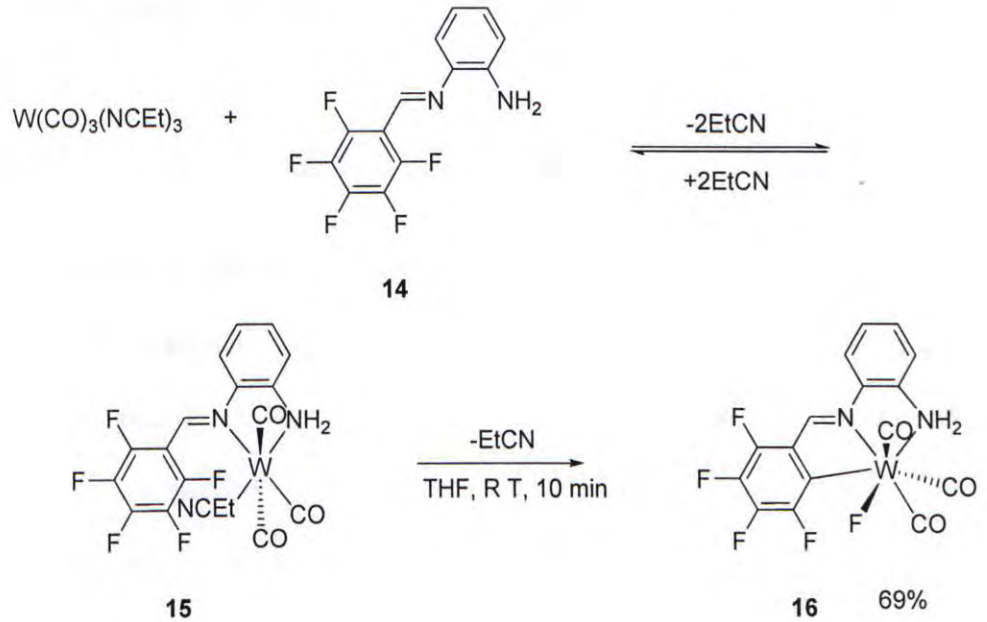

Scheme 6. Oxidative addition of aromatic C-F bond into tungsten(0) complex.

These transformations in 1970s and 1980s serve to provide more understanding of the nature of oxidative addition of fluoroarenes and started the fast growth of aromatic C-F activations in 1990s.

Transition-metal fluoroarene coordination compounds are rare. Carbtree and co-workers[33] provided the first spectroscopic evidence of fluoroarene coordination in solution with the observation of a significant upfield shift of 46 ppm (from -126 to -172 ppm) in ^{19}F NMR spectrum for the 8-fluoroquinoline-iridium complex **17**. This landmark

discovery provides an important spectroscopic tool for seeking other examples of the coordination of fluorine to a metal center in further mechanistic understanding of the activation of aromatic C-F bonds (eq. 1.14).[33]

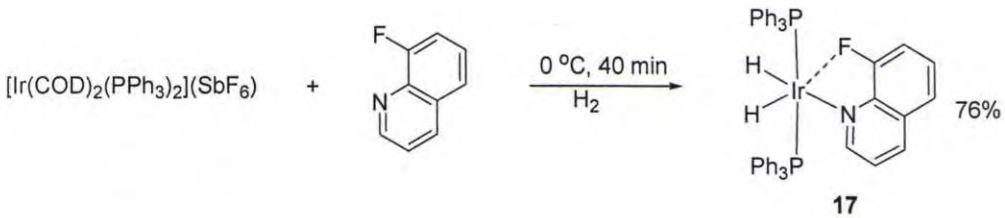

17 (1.14)

1.4.2.4 Examples of Aromatic C-F Activation in 1990s

In 1991, Milstein and co-workers[34] reported the thermolysis of $(Me)Ir(PEt_3)_3$ in hexafluorobenzene at 60 °C to afford **18** with the elimination of CH_4 and C_2H_4. The formation of a strong P-F bond overcomes the energetics of breaking the C-F and P-C bonds and a radical mechanism was proposed for this C-F activation[34] (eq. 1.15, Scheme 7).

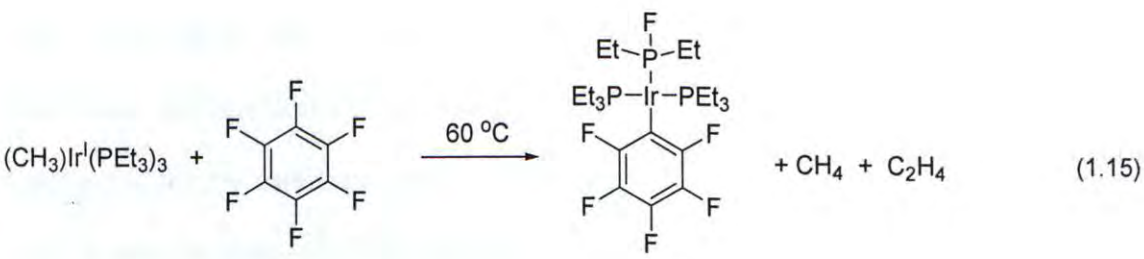

18 (1.15)

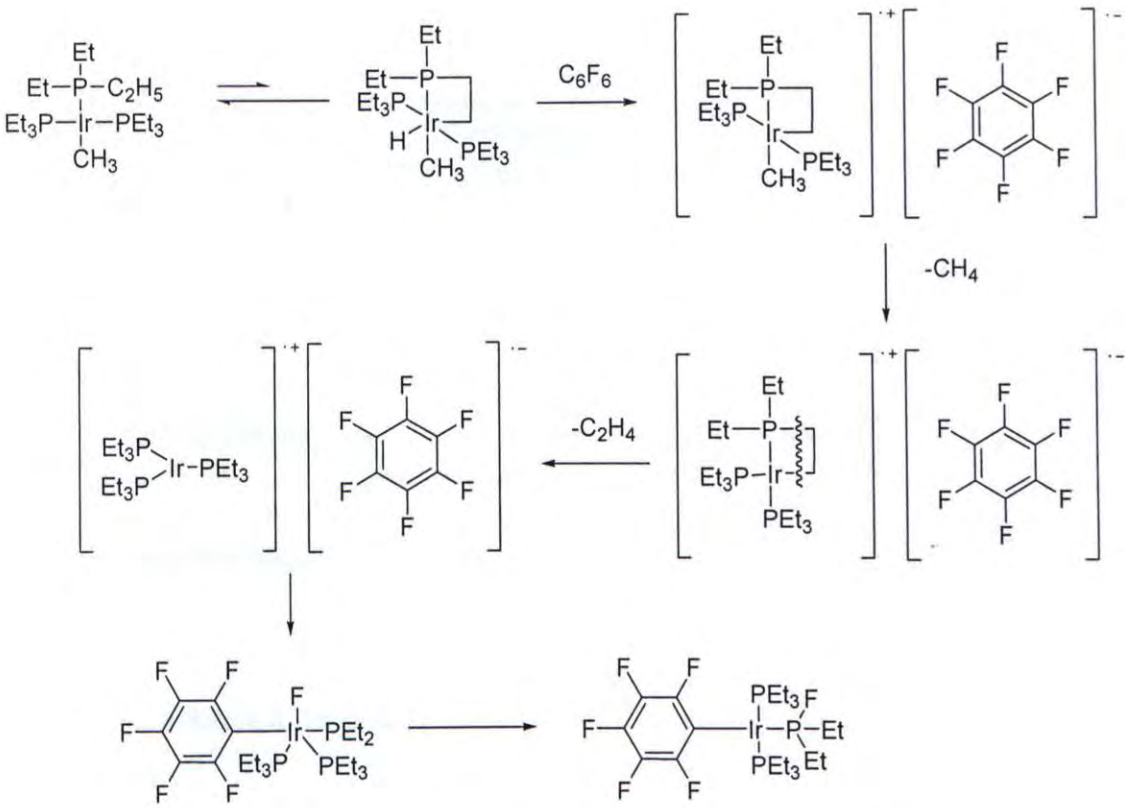

Scheme 7. Proposed Mechanism of C-F Activation by $(Me)Ir(PEt_3)_3$.

In 1997, Edelbach and Jones[35] demonstrated that the high valent rhodium complex $[Cp^*Rh(PMe_3)H_2]$ reacts with C_6F_6 in pyridine or 1:1 pyridine/benzene to give the C-F cleavage product $[Cp^*Rh(PMe)_3(C_6F_5)H]$ in 50% yield (eq. 1.16). Kinetic studies reveal that the reaction has autocatalytic character, and fluoride ion is shown to be responsible for the catalysis. The $[Cp^*Rh(PMe_3)H_2]$ intially reacts with a base (pyridine or F^-) to give the anion $[Cp^*Rh(PMe_3)H]^-$, which then reacts rapidly with C_6F_6 to give the C-F cleavage products as $[Cp^*Rh(PMe_3)(C_6F_5)H]$ via nucleophilic aromatic substitution. The fluoride ion continues the cycle by deprotonating $[Cp^*Rh(PMe_3)H_2]$[35] (Scheme 8).

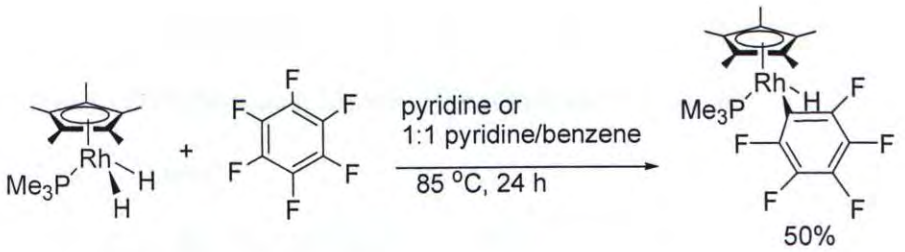

$$Cp^*Rh(PMe_3)H_2 + base \underset{(\text{Base} = F^-, \text{pyridine})}{\overset{\text{fast}}{\rightleftharpoons}} [Cp^*Rh(PMe_3)H]^- + baseH^+$$

$$[Cp^*Rh(PMe_3)H]^- + \text{aryl-F} \xrightarrow{\text{slow}} [Cp^*Rh(PMe_3)(\text{aryl-F})H] + F^-$$

$$F^- + baseH^+ \overset{\text{fast}}{\rightleftharpoons} base{\cdot}HF$$

Scheme 8. Proposed Mechanism of C-F activation of $Cp^*Rh(PMe_3)H_2$.

There are examples of catalytic C-F activations of fluorinated alkenes,[36,37] but catalytic system of defluorination of aromatic C-F is still rare. The landmark homogeneous, catalytic C-F activation of C_6F_6 with $H_2$to give C_6F_5H by $[Rh(SiR_3)(PMe_3)]$ was discovered Milstein et al in 1994 (eq. 1.17).[38]

$$C_6F_6 + H_2\,(90\ psi) \xrightarrow[2\ mol\%\ [Rh(SiEt_3)(PMe_3)_3]]{95\ ^oC,\ 17h} C_6F_5H \quad 50\% \qquad (1.17)$$

Scheme 9 illustrates the proposed mechanism of the catalysis. The cycle begins with the oxidative addition of the triethylsilane Si-H bond to the rhodium(I) complex **19** to give the six-coordinated intermediate **20**. Then, **20** undergoes reductive elimination to give pentafluorobenzene and the rhodium(I) complex **21**. Finally, ligand substitution of

the triethylsilyl group by pentafluorophenyl regenerates **19** with the concomitant production of byproduct Et_3SiF. This substitution is probably driven by the formation of a strong Si-F bond.

With this first homogenous catalytic C-F activation reported, chemists started to not only investigate the improvement of the catalytic systems; but also develop catalytic functionalization of fluoroarenes by cross-coupling approach. More examples were reported in 2000s.

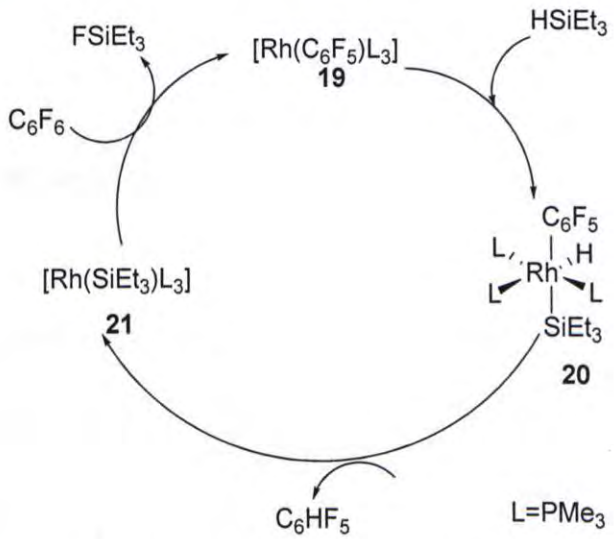

Scheme 9. Catalytic Cycle of C-F Activation by Rhodium Complex

1.4.2.5 Examples of Aromatic C-F Activation in 2000s

Very recently, chemists have successfully developed the catalytic functionalization of strong aromatic C-F bond. Section 1.2 already highlights the key examples. Ackermann et al.[4] reported the Kumada cross coupling of aryl fluoride with ArMgBr at 20 °C catalyzed by $Ni(acac)_2$ with the sterically demanding phosphine oxide ligand (eq. 1.18).[4]

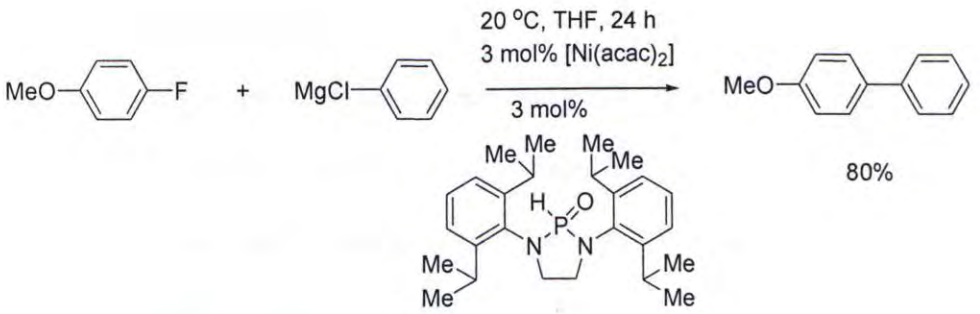

(1.18)

Radius and co-workers[5] illustrated a Suzuki-type bi-aryl coupling reaction from perfluorinated arenes and phenyl boronic acid catalyzed by the nickel N-heterocyclic carbene complex (eq. 1.19).[5]

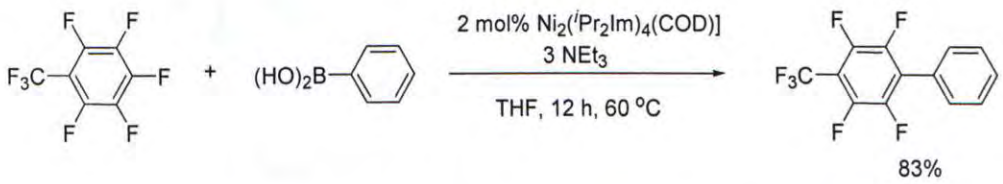

(1.19)

Scheme 10 summarizes the key development of CFA in a timeline.

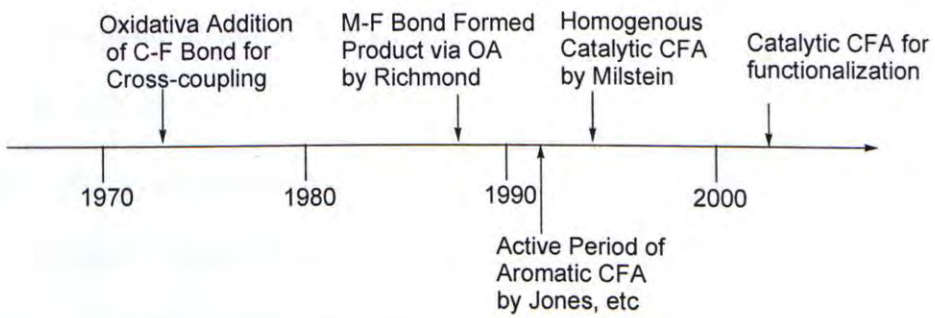

Scheme 10. Timeline of Aromatic C-F Activation

1.4.3 Aromatic Carbon-Hydrogen Bond Activations by Transition Metal Complexes

The key recent reviews of C-H activations by transition metal complexes have been documented by Shul'pin[39] and Bercaw.[20] I will highlight only the representative examples of the varies mechanistic types and catalytic applications in this thesis.

1.4.3.1 Oxidative Addition

In the aromatic C-H activation, oxidatic addition is the most common pathway found. An example has been covered in Section 1.3.1 (eq. 1.5). A similar example was reported by Jones and co-workers[40] in the aromatic C-H bond via oxidative addition with the rhodium(III) complex **22**. The photochemically induced reductive elimination of dihydrogen of **22** lead to the formation of coordinatively unsaturated, reactive intermediate **23** which then undergoes oxidative addition of the aromatic C-D bond to yield the product **24**[40] (Scheme 11).

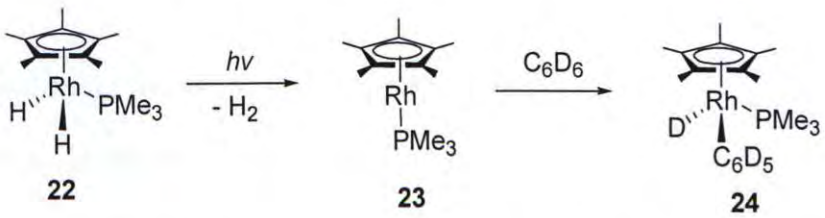

Scheme 11. Oxidative Addition of Aromatic C-H Bond

1.4.3.2 Electrophilic Aromatic Substitution

C-H activation via electrophilic aromatic substitution has been discussed in Scheme 2. The much-related example in this thesis has been reported by Ogoshi in 1986.[41] Rh(oep)Cl reacted with various arenes in the presence of silver salts such as $AgClO_4$ to give aromatic CHA selectively. An electrophilic aromatic substitution (S_EAr) pathway via an arenium ion intermediate was suggested to account the selective formation of the *para*-aryl product [41] (Scheme 12).

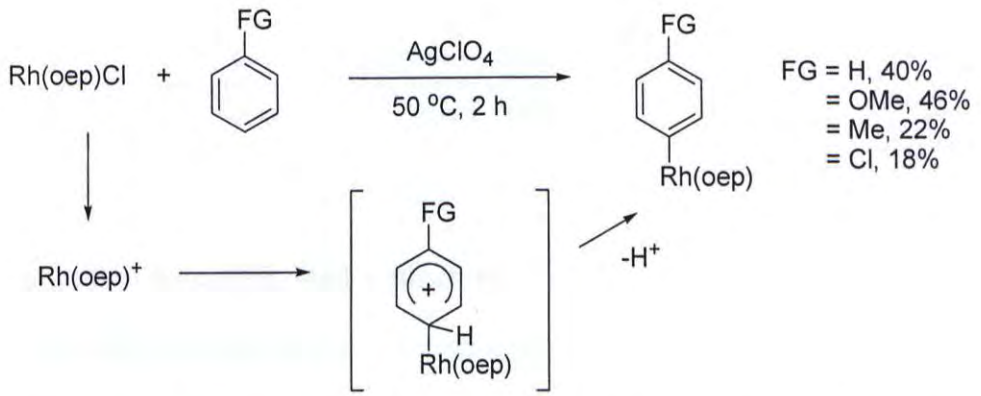

Scheme 12. C-H Activation of Substituted Benzene by Cationic Rhodium Porphyrins

1.4.3.3 1,2-Addition Across M-C Double Bonds

Wolczanski and co-workers[42] reported the activation of the C-H bond of benzene by the zirconium imido complex **26**. The formation of the strong phenyl zirconium bond provides the driving force of the reaction to form the product **27**[42] (Scheme 13).

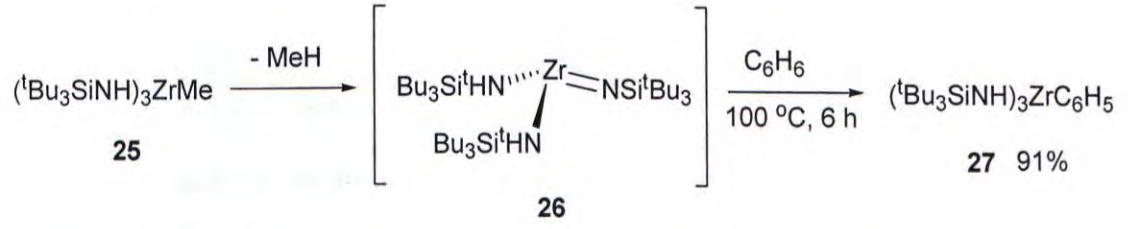

Scheme 13. Addition of Aromatic C-H Bond into Zr=N Linkage

1.4.3.4 Catalytic C-H Activation for Functionalization

Aromatic C-H activation can be applied for the catalytic functionalization of arenes. Murai et al.[43] reported the catalytic C-H activation of acetonephenone by $RuH_2(CO)(PPh_3)_3$ to give the bi-aryl complex **28**(eq. 1.20).[43]

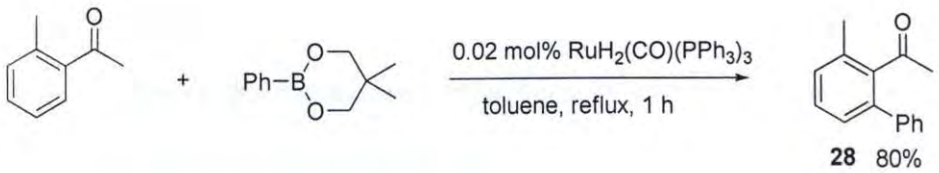

(1.20)

1.5 Competitive Aromatic Bond Activations

Substituted Aromatic haloarenes have at least 2 potential sites for bond activation: the C-X and C-H bonds. In Scheme 14, a halobenzene can in principle undergo either C-X activation to give aryl metal complex **28** or C-H activation to produce substituted aryl metal complex **29** selectively to give *o*-product or non-selectively to give other CHA isomers. The underlying principles for the selectivity of CXA versus CHA and the regioselectivity of CHA are challenging to understand.

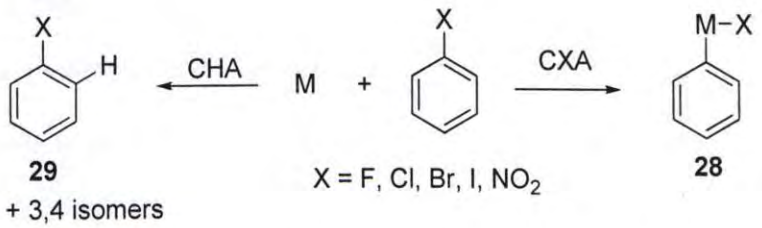

Scheme 14. Competitive Activation Between C-X and C-H Bonds

1.5.1 Competitive Aromatic Carbon-Hydrogen and Carbon-Halogen Bond Activation

In the reaction of haloarenes with transition metal complexes, competitive activation between a C-X bond and a C-H bond exists. Thermodynamic is helpful to understand the selectivity or the lack of it. Table 1.4 lists the BDEs of aromatic carbon-halogen and carbon-hydrogen bonds. An aromatic C-H bond is stronger than a carbon-halogen bond except the C-F bond. It therefore suggests that the reactivity follows the

bond strength: C-I > C-Br > C-Cl > C-H > C-F. Particularly important from a synthetic point of view is the regioselective activation of strong C-H bonds in the presence of a potentially reactive halogen substituent.

Table 1.4 BDE of Aromatic Carbon Bonds

Aromatic C-X Bond	Bond Dissociation Energy[21] / kcal mol^{-1}
C-F	126
C-Cl	95
C-Br	79
C-I	64
C-H	110

However, kinetic factors such as chelation-assistance can direct the selectivity between C-H activation or C-X activation. In C-H activation, there are also various regio-positions to result in *o*-, *m*-, and *p*-isomers.

The chelation-assistance effect has been demonstrated by Milstein and co-workers Scheme 15)[44]. In the reactions of halobenzenes with the iridium(I) complex, for chloro and bromobenzene, the *ortho*-isomer is formed preferentially over *meta*- and *para*-isomers (greater than the statistical ratio). The pre-coordination of the halogens to the iridium metal centers accounts the *ortho* selectivity even though the *ortho* position is a sterically more hindered reaction site. After prolonged heating, the thermodynamically favored carbon-halogen bond activations occurred in bromobenzene and chlorobenzene but not in the fluorobenzene due to the difficulty in cleaving the strong C-F bond[44]

(Scheme 15). Therefore, the C-Cl and C-Br oxidative addition products are the thermodynamic products.

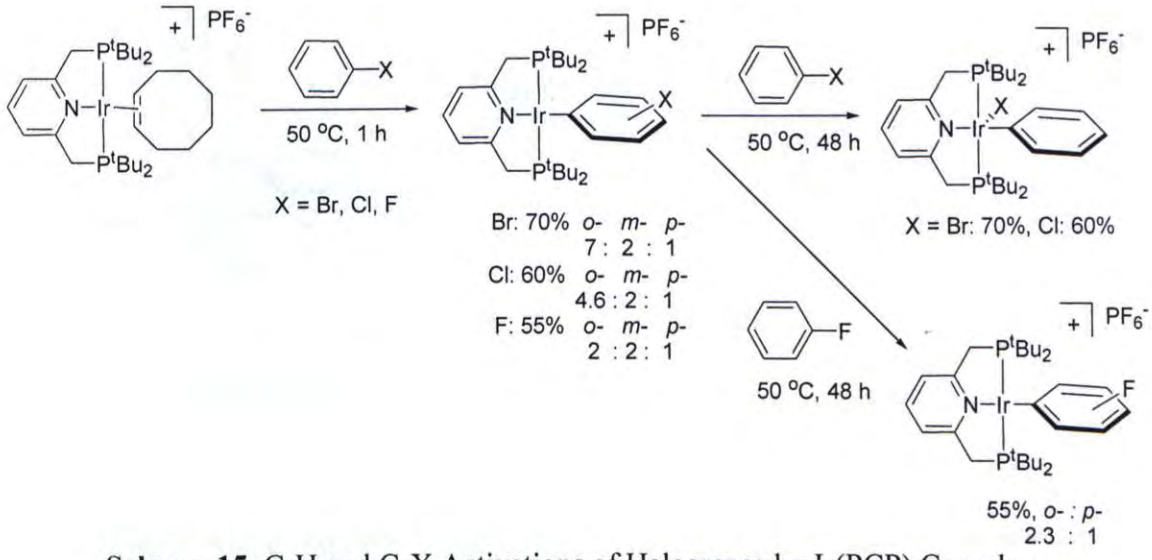

Scheme 15. C-H and C-X Activations of Haloarenes by Ir(PCP) Complex

In 2004, Goldman and co-workers[45] reported a non-chelating-assisted *ortho*-directing C-H activation of nitrobenzene by an iridium complex (Scheme 16). Treatment of the Ir(PCP) complex **30** in nitrobenzene at -10 °C gave the *ortho*-directing product, the *trans*-aryl iridium hydride **31**. The thermodynamic product, the *cis*-aryl iridium hydride **32** was formed in elevated temperature at 135 °C in 95% yield. At the lower temperature of -47 °C, the kinetically favored *para*- and *meta*-substituted products formed. The *ortho*-directing product is kinetically less favored and thermodynamically more stable, probably due to additional 6-O-coordination of the nitro-group[45] (Scheme 16). This raises the concerns on the kinetic origin of the *ortho*-selectivity in the Milstein report.

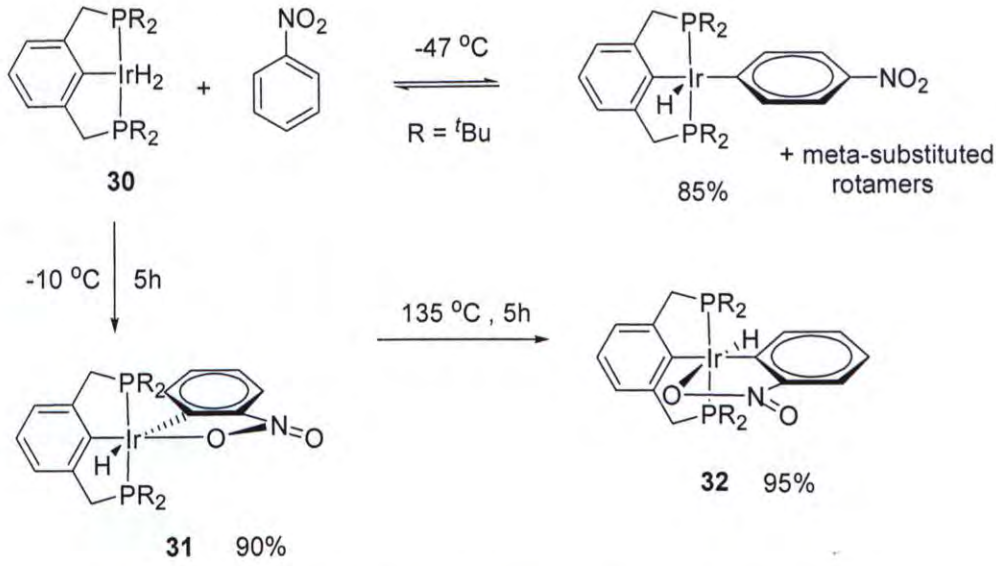

Scheme 16. Activation of Nitrobenzene by Iridium complex.

Ozerov and co-workers[46] explored this kind of reaction by the Ir-PNP pincer complex **33** in 2005 (Scheme 17). The Ir complex **33** reacts with chlorobenzene at room temperature to firstly produce a mixture of C-H oxidative addition products **34**. Thermolysis of the mixtures of product **34** at 70 °C gives the only *ortho* C-H activation isomer. Further heating at 120 °C produces the C-Cl activation product **35.** The solid state structure of the *ortho* C-H activation product indicates that the *ortho* Cl is oriented appropriately for additional Cl→Ir donation which stabilizes the product and this product simply forms the strongest σ-Ir-C bond among the other chlorophenyl isomers. Upon heating up to 120 °C, the interaction is diminished and drives the reaction into the lowest energy state of the thermodynamically favorable C-Cl activation product **35**.[46]

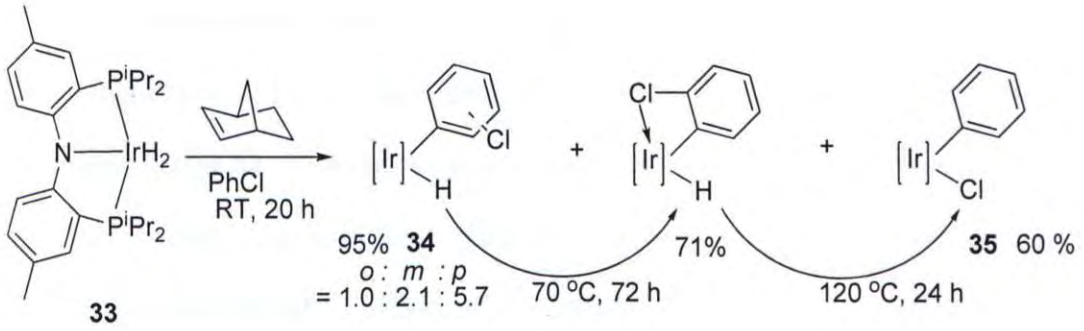

Scheme 17. Competitive C-H and C-Cl Activations of Chlorobenzene by Ir(PNP) Complex **33**

In 2006, Legzdins et al.[47] reported that Cp*W(NO)(CH_2CMe_3)$_2$ underwent CHA with halobenzenes to yield isomeric products, with *ortho*-activated isomer being formed in the greatest amount. There is no coordination of the halogen to tungsten center. The origin of the *ortho*-selectivity may due to thermodynamic reasons impacted by both electronic and steric factors[47] (Scheme 18).

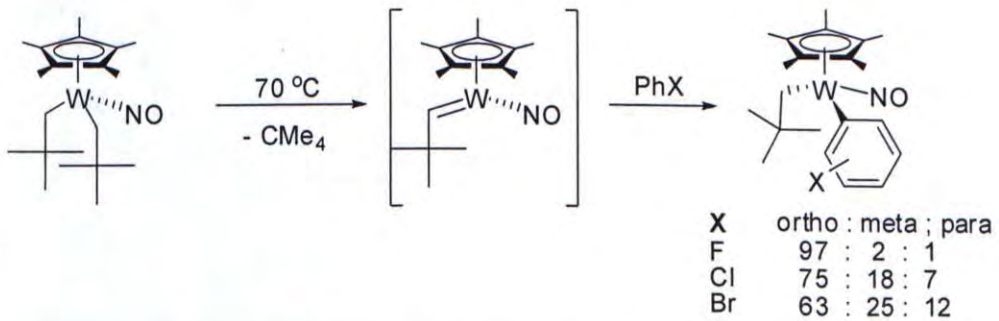

Scheme 18. Selectivity of C-H Activation of Halobenzenes.

1.5.2 Competitive Aromatic Carbon-Hydrogen and Carbon-Fluorine Bond Activations

In fluoroarenes, although C-F bonds are stronger than C-H bonds, competitive CFA can still occur. Tomas and co-workers[48] reported that the preference depends on the substrate. In scheme 19, when the hexahydride-osmium complex **36** reacts with both **37** and **38**, because of the four electrons repulsion of the fluorine and oxygen substituents ,the orientation of both **37** and **38** have C-H bond next to the carbonyl group which favors C-H activation. In the case of substrate **39**, as both phenyl and petafluorophenyl groups are sterically demanding, so C-F and C-H bonds are open for activation. As the more thermodynamically stable co-product HF is produced in the C-F activation than H_2 in the C-H activation, C-F activation occurs exclusively in refluxing toluene.[48]

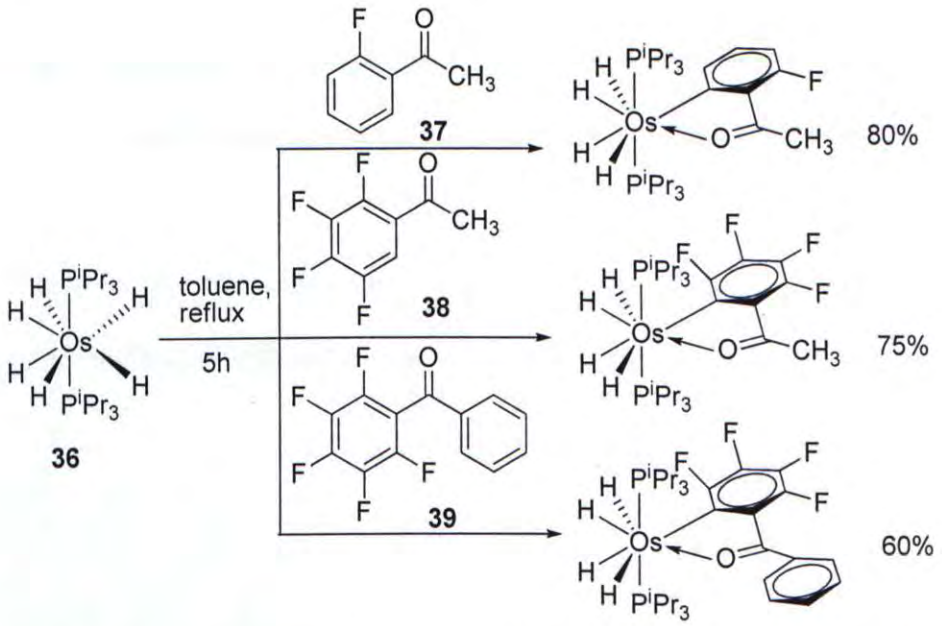

Scheme 19. Competitive C-F and C-H Activations by Osmium Complex **35**

The selectivity issue between CFA and CHA has been addressed thereotically by a recent report by Reinhold et al.[49] They calculated the energetics of C-F and C-H activation products by zerovalent nickel and platinum complexes. It is shown that there is

dπ-pπ M-F repulsion in the larger size platinum but not in the smaller size nickel. As a result, platinum shows the preference to C-H activation over C-F activation and vice versa in nickel complex (Scheme 20).[49]

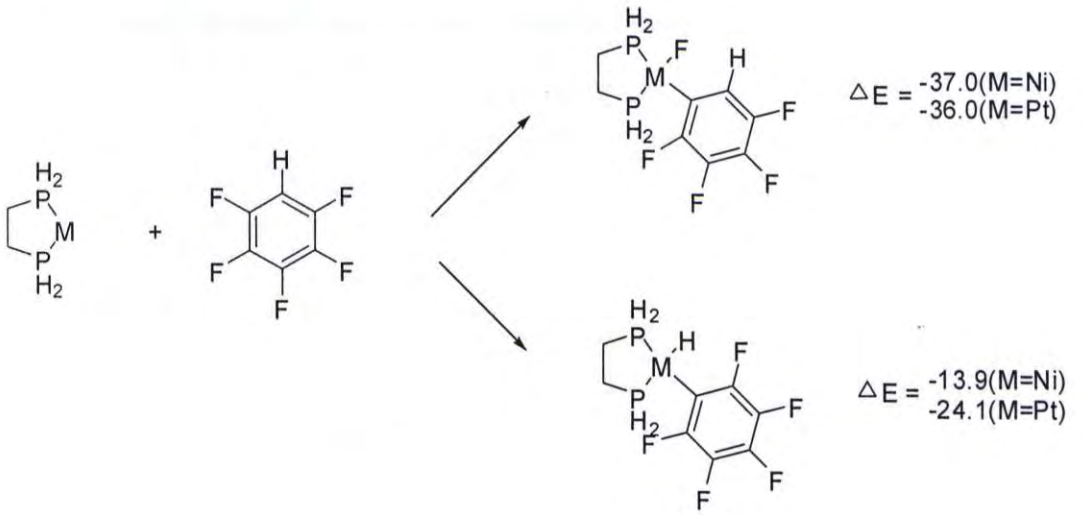

Scheme 20. Comparison of Computed Engergetics of C-F and C-H Activation in Isomeric Products (energies in kcal mol^{-1})

Therefore, for the examples of competitive aromatic CFA and CHA would provide better understandings of the origins of the selectivity.

1.6 Structural Features of Rhodium Porphyrins

Porphyrin ligand is a tetradentate and dianionic ligand with an 18 π conjugated system. It consists of 4 pyrroles with methine linkages (Figure 1). Properties of porphyrins can be modified by substituents at the *meso* (R) and β (X) positions.[50]

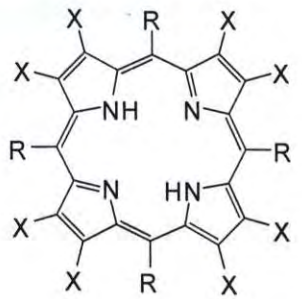

Figure 1. General Structure of Porphyrin.

The modifications of different aryls at the *meso*-position (R) and functional groups at the β-positions (X) give different porphyrins in various electronic and steric properties. Some porphyrins and their abbreviations are listed in Table 1.5.

Table 1.5 Abbreviation of Porphyrins

Abbreviation	Porphyrin	X	R
H_2(oep)	Octaethylporphyrin	Ethyl	H
H_2(ttp)	Tetratolyporphyrin	H	4-$CH_3C_6H_4$
H_2(tpp)	Tetraphenylporphyrin	H	C_6H_5

Metalloporphyrins can be formed from the metalation of porphyrin ligands. The metal occupies the center of the porphyrin hole and is coordinated by the four nitrogen atoms of the pyrroles through the four lone pairs.

Rhodium porphyrins can exist in +1, +2, and +3 oxidation states. The anionic species +1 oxidation state of a rhodium porphyrin has two lone pair electrons in d_z^2 with d_8 electronic configuration in metal and behaves as a strong nucleophile. The +2 oxidation state of a rhodium porphyrin acts as a metalloradical with one electron in the d_z^2 orbital in rhodium. The +3 oxidation state is a cationic species with and hence as a strong Lewis acid and an electrophile.[51]

The CHA reactions of rhodium porphyrins have been reported by Ogoshi[41] as shown in Scheme 12. In 1998, Chan et al.[52] reported that Rh(ttp)Cl reacted with the electron poor benzonitrile in refluxing conditions to give meta-cyano phenyl rhodium porphyrin complex, likely via an electrophilic aromatic substitutution in view of the meta-substituted product (eq. 1.21).[52]

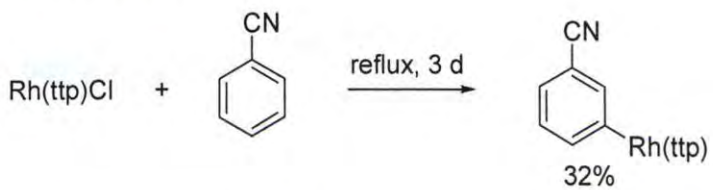

(1.21)

Further systematic studies of the bond activations by rhodium(III) porphyrins are being carried out in the Chan group.

1.7 Objectives of the Work

This thesis concerns the chemistries of rhodium porphyrins complexes in

1. the C-F activation of fluoroarenes;
2. the competitive *ortho* selective CHA of fluoroarenes;
3. the mechanistic studies of the above two processes.

Chapter 2 Competitive C-F and C-H Activation of Fluorobenzenes by Rhodium(III) Porphyrins

2.1 C-F Activation of Fluorobenzene by Rhodium(III) porphyrins

The activation of aromatic C-F bond by rhodium(III) porphyrin chloride was discovered by Mr. P. F. Chiu in our group in 2006.[53] In the course of investigating of the activation of carbon-halogen bonds in aryl halides, he found that Rh(ttp)Cl reacted with fluorobenzene in the presence of 10 equivalents of NaOH to give Rh(ttp)Ph in 48% yield (eq 2.1). The C-F bond in fluorobenzene, the least reactive halobenzene, has been cleaved. This finding has led to the systematic studies of C-F activation of fluoroarenes in this thesis.

$$\text{Rh(ttp)Cl} + \text{C}_6\text{H}_5\text{F} \xrightarrow[\text{10 equiv NaOH}]{\text{120 °C, N}_2\text{, 12 h}} \underset{\textbf{4}\ \ 48\%}{\text{Rh(ttp)Ph}} \qquad (2.1)$$

2.2 Preparation of Starting Materials

2.2.1 Synthesis of Porphyrins

Tetratolylporphyrin (H_2ttp) and tetraphenylporphyrin (H_2tpp) were synthesized directly from the reactions of the corresponding aldehydes and pyrrole in refluxing propanoic acid for 30 minutes (eq. 2.2).[54]

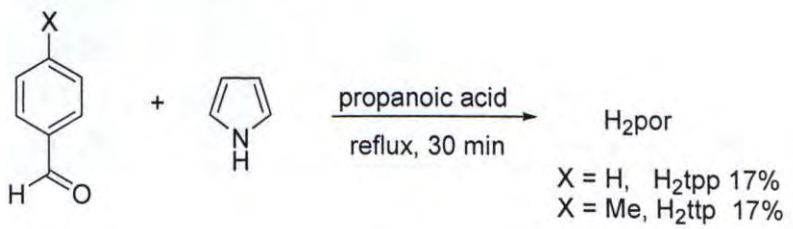

(2.2)

2.2.2 Synthesis of Rhodium(III) Porphyrins

Rh(por)Cl was prepared from the reaction of 1.5 equiv of $RhCl_3.xH_2O$ with 1 equiv of porphyrin in refluxing benzonitrile for 3 hours (eq. 2.3).[52]

$$H_2por + RhCl_3{\cdot}H_2O \xrightarrow[\text{reflux, 3 h}]{\text{PhCN}} Rh(por)Cl \qquad (2.3)$$

por = tpp, 68%
por = ttp, 70%

2.3 Base Effect of CFA

As the successful C-F activation was carried out initially with 10 equivalents of NaOH in fluorobenzene both as the solvent and reagent, so a series of bases was screened to search for the optimized base in the reaction Rh(ttp)Cl with PhF at 120 °C for 1 d. (eq. 2.4, Table 2.1).

$$\underset{(0.018M)}{Rh(ttp)Cl} + \underset{(500\ equiv)}{PhF} \xrightarrow[\text{10 equiv Base}]{\text{120 °C, } N_2\text{, 1 d}} \underset{\mathbf{4}}{Rh(ttp)Ph} + \underset{\mathbf{5a}}{Rh(ttp)\text{-}o\text{-}C_6H_4F} + \underset{\mathbf{7a}}{Rh(ttp)\text{-}p\text{-}C_6H_4F} \qquad (2.4)$$

Table 2.1 Base Effect of the CFA with Rh(ttp)Cl.

Entry	Base	pK_a of the conjugated acid[55]	CFA **4** Yield / %	*o*-CHA **5a** Yield / %	*p*-CHA **7a** Yield / %	Total Yield / %
1	none	N.A.	0	0	18	18
2	Na_2CO_3	10.3		complex mixtures		
3	K_2CO_3	10.3		complex mixtures		
4	Ag_2CO_3	10.3	0	6	13	19
5	NaOH	13.8	40	trace	0	40
6	KOH	13.5	63	trace	0	63
7	KO^{t}Bu	17.0		complex mixtures		

Without any base added, the *p*-CHA product **7a** was obtained in a low yield of 18%. Weaker bases like Na_2CO_3 and K_2CO_3 did not give any product **4**, **5a**, **7a**, Rh(ttp)H or $Rh_2(ttp)_2$ from the analysis of the crude reaction mixture by both TLC and ^1H NMR, but only gave complex reaction mixtures (Table 2.1, entries 2 and 3). Ag_2CO_3 promoted the *o*-CHA and *p*-CHA without any CFA (Table 2.1, entries 4). These results were similar to Ogoshi's report on the electrophilic aromatic substitution of chlorobenzene with Rh(oep)Cl and $AgClO_4$ (Chapter 1, Scheme 12).[41] Likely an electrophilic Rh(ttp) cation is generated by the reaction of Rh(ttp)Cl with Ag cation and then the electrophilic aromatic substitution products result.

On the other hand, the stronger bases such as NaOH and KOH showed a higher selectivity in promoting the CFA with KOH giving a higher product yield in 63% (Table 2.1, entries 5 and 6). Both bases gave a trace amount of the *o*-CHA product **5a**, which was detected by TLC analysis in the crude mixture but was isolated in less than 5% yield. Therefore, KOH was chosen as the optimal base for further CFA reactions.

The effect of KOH loading for CFA reactions has also been examined and Table 2.2 lists the results. A lower loading of KOH of 2 or 5 equivalents gave Rh(ttp)Ph **4** in 30 and 48%, respectively (Table 2.2, entries 1 and 2). 10 equivalents of KOH gave **4** in a higher yield of 63% while 20 equivalents of KOH produced a lower yield of **4** in 42%. Recently a report from our group showed that a higher loading of KOH in high temperature of 200 °C caused the lowering yield in the benzylic CHA of toluene by iridium porphyrins. The decomposition of an iridium porphyrin intermediate is proposed.[56] Such effect likely operates in this CFA by rhodium porphyrins. Therefore 10 equivalents of KOH was found to be the optimal amount.

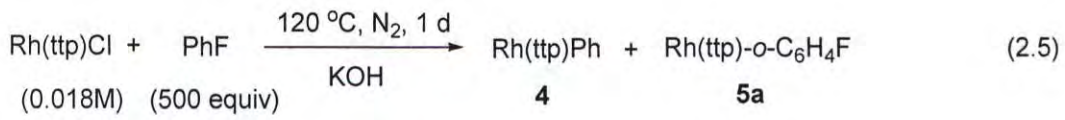

(2.5)

Table 2.2 Effect of Amount of KOH in CFA

Entry	KOH / equiv	CFA **4** Yields / %	*o*-CHA **5a** Yield / %
1	2	30	trace
2	5	48	trace
3	10	63	trace
4	20	42	trace

2.4 Solvent Effect of CFA

Since Rh(ttp)Cl dissolved sparingly in fluorobenzene even at elevated temperature, a suitable solvent was therefore searched to improve the solubility. Benzene was found to enhance the solubility of Rh(ttp)Cl and increase the yield of the CFA reaction (Table 2.3).

To rule out the possibility of direct C-H activation of benzene, fluorobenzene was reacted with Rh(ttp)Cl in benzene-d_6 with 10 equivalents of KOH. Only Rh(ttp)Ph in 50% yield was obtained without any Rh(ttp)Ph-d_5. Since Rh(ttp)Cl in benzene with KOH (10 equiv) at 120 °C in 1 day did not give any Rh(ttp)Ph **4** (Table 2.3, entry 1), and Rh(ttp)C_6H_5 in C_6D_6 with KOH (10 equiv) at 120 °C in 1 day did not exchange to give any Rh(ttp)C_6D_5, so benzene could be used as the solvent as no CHA reaction with benzene occurred (eq. 2.6).

$$\underset{(0.018M)}{Rh(ttp)Cl} + \underset{(1.8M)}{PhF} + \underset{(500\ equiv)}{C_6D_6} \xrightarrow[1\ d,\ 10\ equiv\ KOH]{120\ ^{\circ}C,\ N_2} \underset{\mathbf{4}\ \ 50\ \%}{Rh(ttp)Ph} \qquad (2.6)$$

Though Rh(ttp)Cl dissolved well in THF, complex reaction products formed. Therefore benzene was used as the solvent for subsequent studies (eq. 2.7, Table 2.3).

$$Rh(ttp)Cl + C_6H_5F \xrightarrow[10\ equiv\ KOH]{C_6H_6,\ 120\ ^{\circ}C,\ N_2,\ 1d} \underset{\mathbf{4}}{Rh(ttp)Ph} + \underset{\mathbf{5a}}{Rh(ttp)C_6H_4o\text{-}F} \qquad (2.7)$$

Table 2.3 Solvent Effect of the CFA reactions

Entry	Equivalents of C_6H_5F	$[C_6H_5F]$ / M	CFA **4** Yield / %	*o*-CHA **5a** Yield/ %
1	0	0	0	0
2	25	0.5	55	0
3	50	0.9	61	0
4	100	1.8	77	0
5	100	3.6	72	0
6	500	6	68	0
7	500	11	43	trace

Table 2.3 lists the result of the concentration effect of C_6H_5F in benzene. The product yield increased with the fluorobenzene concentration with the maximum yield of **4** obtained in 1.8 M. Higher concentration proves to be inferior possibly due to poor solubility of Rh(ttp)Cl in the reaction media. In a high concentration of C_6H_5F (11 M) in benzene (Entry 7), trace amount of the *o*-CHA product **5a** was observed in the reaction mixture by TLC analysis only after 6 hours. However, the CFA product formed within 4 hours and the amount appeared to increase slowly with time as observed in the intensity of the TLC analysis of the crude mixture.

2.5 Temperature Effect of CFA Reaction

The temperature effect was investigated by the reaction of 1,4-difluorobenzene with Rh(ttp)Cl added with KOH (10 equiv) (eq 2.8, Table 2.4). Little reaction occurred at 80 °C (Table 2.4, entry 1). The total product yields increased from 100 to 150 °C with its maximum at 120 °C (Table 2.4, entry 3). At 200 °C, the product yield decreased slightly (Table 2.4, entry 5).

At 80 °C, only 8% yield of CFA product **7a** formed (Table 2.4, entry 1). A higher ratio of CHA product **7b** to CFA product **7a** formed at 100 °C in 2 days (Table 2.4, entry 2). At 120 °C, the yield of CFA product **7a** increased and the ratio of CFA product to CHA product **7b** were 3:2. At 150 and 200 °C, CFA product **7a** formed exclusively in around 70% (Table 2.4, entries 4 and 5). The results indicate that CFA is favored by high temperature. CHA product **7b** was formed at 100 and 120 °C together with CFA product.

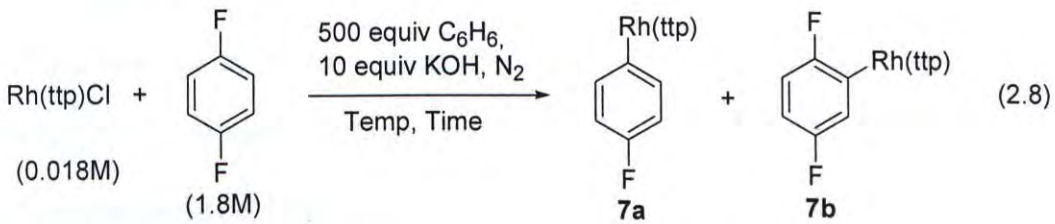

(2.8)

Table 2.4 Temperature of Activation of 1,4-Difluorobenzene by Rh(ttp)Cl

Entry	Temp / °C	Time / h	CFA **7a** Yield / %	CHA **7b** Yield / %	Total Yield / %
1	80	168	8	0	8
2	100	48	15	34	49
3	120	24	48	30	78
4	150	10	76	0	76
5	200	5	69	0	69

2.6 Activations of Fluorobenzenes

The optimized reaction conditions with fluorobenzene at 120 °C in KOH (10 equiv) were successfully applied to the reactions of various fluorobenzenes with Rh(ttp)Cl and eq. 2.9 and Table 2.5 list the results. Aromatic bond activations occurred to give both CFA and *ortho*-selective CHA products. The CFA products are the major products with higher total yields. For the activation reactions of the difluorobenzenes, the CFA products yields were generally the same (42-53%, Table 2.5, entries 2-4). The reactivity of the fluorobenzenes increased with more fluorosubstituted arenes as observed in the faster formation of the CFA products by TLC analysis. For instance, the CFA product **9** formed at about 3 hours in activation of hexafluorobenzene while it took about 4 hours for the CFA product **4** to form in the activation of fluorobenzene.

All the C-H activation products are *ortho*-selective to fluorine substituents. The *o*-CHA products have similar yields in 20% to 31% (Table 2.5, entries 2-5). Exclusive C-H activation was observed in the pentafluorobenzene even when there are 5 C-F bonds compared to 1 C-H bond. This may due to the high acidity of hydrogen resulted from 5 electrowithdrawing fluorine groups.

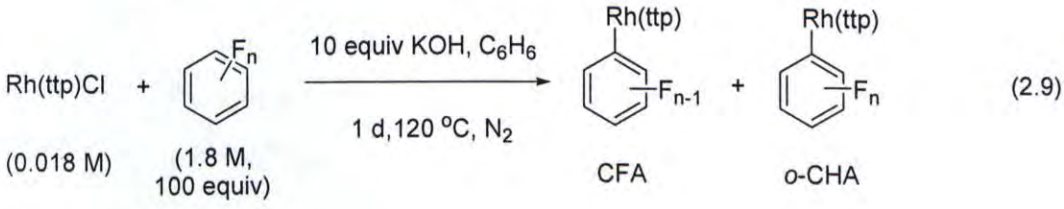

(2.9)

The structures of the products in **5a** to **8a** were ascertained by ^{19}F NMR. There is only 1 fluorine signal in the 4 CFA products in **5a** to **8a**. The fluorine signals in **5a**, **6a** and **7a** resonate at -45.2, -53.4 and -62.5 ppm, respectively. The fluorine signal in **8a** falls

Table 2.5 Activation of Fluorobenzenes by Rh(ttp)Cl

Entry	Fluorobenzene	CFA Yield / %	*Ortho*-CHA Yield / %	Total Yield / %
1	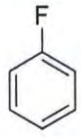	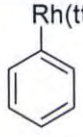 77 **4**	no	77
2	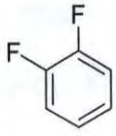	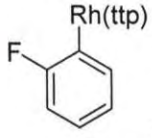 53 **5a**	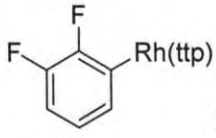 30 **5b**	83
3	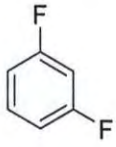	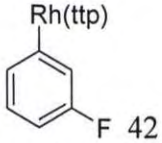 42 **6a**	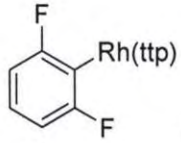 31 **6b**	73
4	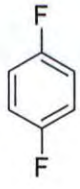	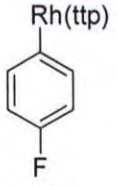 48 **7a**	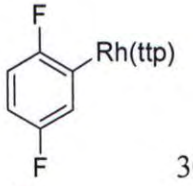 30 **7b**	78
5	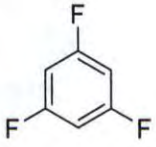	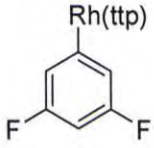 56 **8a**	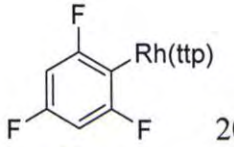 20 **8b**	76
6	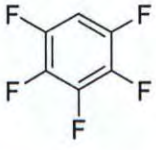	0	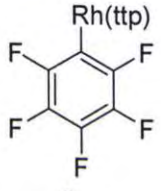 56 **9**	56
7		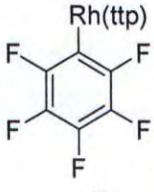 60 **9**	0	60

at -52.9 ppm which agrees that of the *m*-isomer **6a**. **6b** shows a single peak at -37.7 ppm. Likewise, there are two fluorine signals for **7b** and **8b**. The structures of the *o*-CHA products can also be further consistent with observed coupling constant. **5b** shows $^{3}J_{F\text{-}F}$ of 22.2 Hz for the two fluorine substituents in the 1,2 positions. Table 2.6 lists the coupling constants for **6b**. The hydrogen-fluorine coupling constant obtained in ^{1}H NMR are within the range in the literature ($^{3}J_{H\text{-}F}$ = 6 -10 Hz, $^{4}J_{H\text{-}F}$ = 4 – 8 Hz).[57] In an earlier report in our group, the $^{1}J_{C\text{-}Rh}$ and $^{1}J_{C\text{-}F}$ of the 4-FC_6H_5CORh(ttp) values are 20.9 and 21.6 Hz, respectively,[58] which agree with the coupling constant obtained in **6b**.

Table 2.6 Various Coupling Constants of Product **6b**

Type of Coupling	$^{3}J_{H\text{-}H}$	$^{3}J_{H\text{-}F}$	$^{4}J_{H\text{-}F}$	$^{1}J_{C\text{-}Rh}$	$^{1}J_{C\text{-}F}$
Coupling Constant / Hz	8.3	8.9	5.8	25.3	30.2

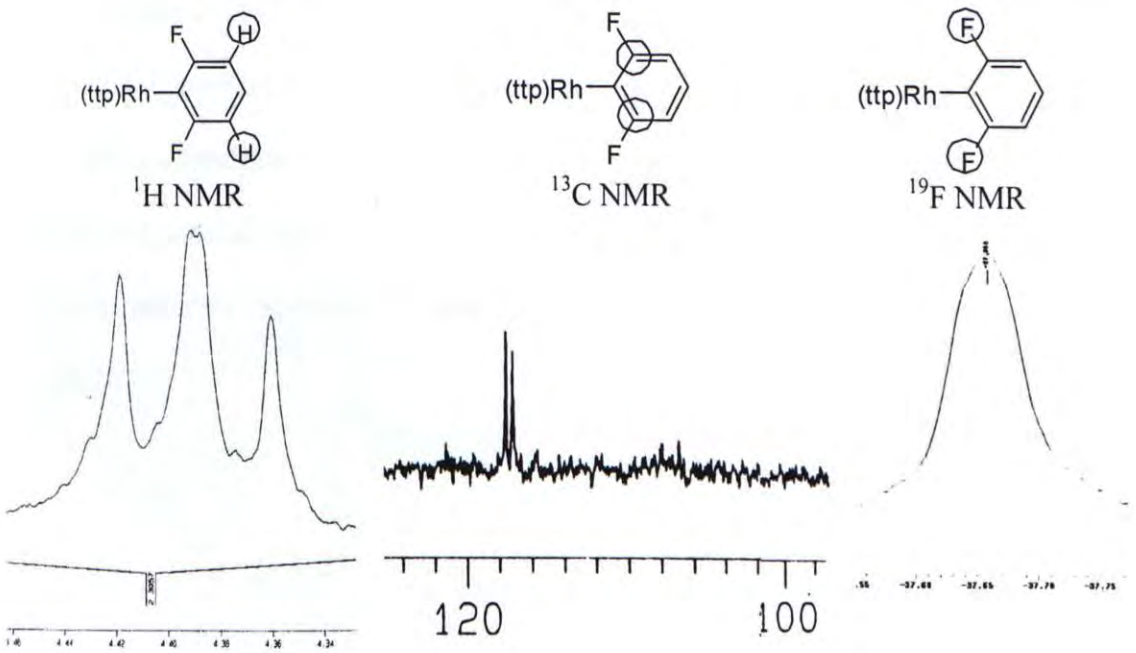

Figure 2a Partial ^{1}H, ^{13}C and ^{19}F NMR spectra of **6b**.

2.7 Electronic Effect of Carbon-Fluorine Bond Activations

To gain further quantitative understanding of the relative reactivities and electronic effect of the carbon-fluorine bond activations of fluorobenzenes, competition experiments were carried out using an equimolar mixture of two fluorobenzenes (eq. 2.10 Table 2.7).

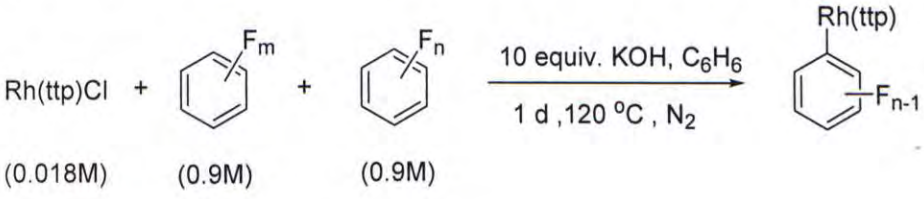

(2.10)

All the competition experiments gave similar yields of CFA products (51-61%) without any CHA products. The more electron-deficient fluoroarenes appeared to be more reactive. Both hexafluorobenzene and 1,2-difluorobenzene are more reactive than fluorobenzene (Table 2.7, entries 1 and 2). Among the difluorobenzenes, the electron-withdrawing effect of fluorine also controls the reactivity. The reactivity order follows: 1,2-difluorobenzene > 1,3-difluorobenzene > 1,4-difluorobenzene in line with the Hammett constant (*m*-fluorine = 0.33, *p*-fluorine = 0.15).[11b] The *o*-substitutent does not have a reported experimental literature value but only a computed theoretical value of 0.26.[59]

Table 2.7 Competition Reactions of Fluorobenzenes

Entry	ArF	Ar'F	CFA Yield / %
1	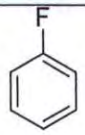	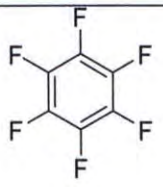	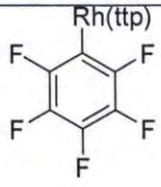 **9** 55
2	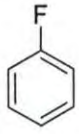	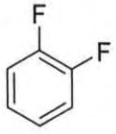	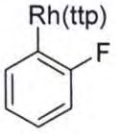 **5a** 58
3	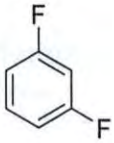	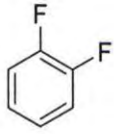	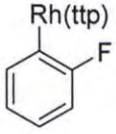 **5a** 51
4	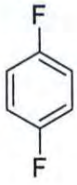	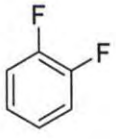	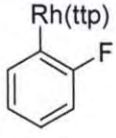 **5a** 61
5	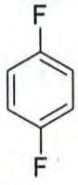	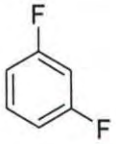	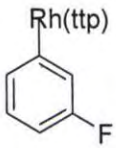 **6a** 51

2.8 Preliminary Mechanistic Studies

2.8.1 Activation of Fluorobenzene

The reaction of Rh(ttp)Cl with 1,4,-difluorobenzene with KOH (10 equiv) in C_6D_6 at 120 °C was carried out in an NMR tube and monitored by ^1H NMR spectroscopy. After 1 hour, Rh(ttp)Cl completely reacted and $Rh_2(ttp)_2$ (pyrrole signal at 8.64 ppm) formed in 68% calibrated with the internal standard residual benzene in C_6D_6. Then after

an hour the $Rh_2(ttp)_2$ was consumed to give $Rh(ttp)^{\cdot}$ (pyrrole signal at 8.47 ppm) in the third hour of reaction. Then CFA product **7a** formed slowly with the consumption of the $Rh(ttp)^{\cdot}$ (Figure 2b).

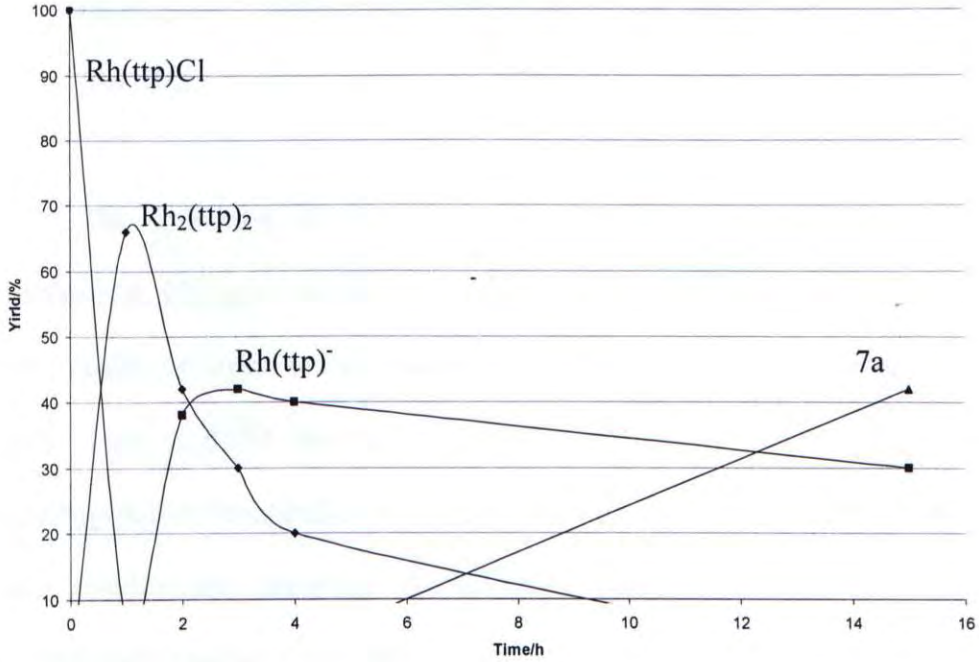

Figure 2b Progress of NMR Tube Reaction of Rh(ttp)Cl with 1,4-Difluorobenzene

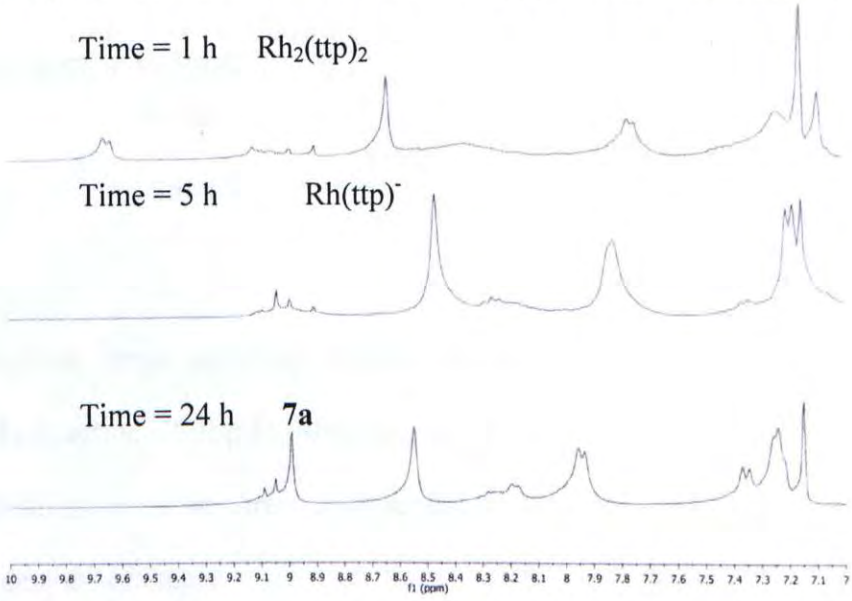

Figure 2c Partial ^1H NMR Spectra of The Activation of 1,4-Difluorobenzene

To gain further insight on the formation of $Rh_2(ttp)_2$, the Rh(ttp)Cl was reacted with KOH (10 equiv) in d_6-benzene. Indeed $Rh_2(ttp)_2$ was formed in 60% yield at a lower temperature of 90 °C in 1 hour (eq. 2.11).

$$\underset{(0.018M)}{Rh(ttp)Cl} + C_6D_6 \xrightarrow[1h,\ 90\ ^oC]{10\ equiv\ KOH} \underset{\mathbf{3}\ 60\%}{Rh_2(ttp)_2} \qquad (2.11)$$

The formation of $Rh_2(ttp)_2$ from Rh(ttp)Cl probably comes from another intermediate, Rh(ttp)H. In fact, Ir(ttp)(CO)Cl is reported to give Ir(ttp)H in the reaction with toluene, a hydride source, with Cs_2CO_3 (20 equivalents) in benzene-d_6 at 150 °C (eq. 2.12). Then Ir(ttp)H slowly yields the $Ir_2(ttp)_2$ in 150 °C in benzene-d_6 via dehydrogenative dimerization (eq. 2.13).[56] So the transformation of Rh(ttp)Cl to $Rh_2(ttp)_2$ likely involves the formation of a Rh(ttp)H intermediate which is not observable in strongly basic media by ^1H NMR.

$$Ir(ttp)Cl(CO) + \underset{50\ equiv}{Ph^{13}CH_3} \xrightarrow[150\ ^oC,\ 30\ min]{Cs_2CO_3\ (20\ equiv),\ C_6D_6} \underset{81\%}{Ir(ttp)H} \qquad (2.12)$$

$$2Ir(ttp)H \xrightarrow[1.5\ h,\ 150\ ^oC]{C_6D_6} Ir_2(ttp)_2 + H_2 \qquad (2.13)$$

Therefore, there are three rhodium porphyrin intermediates generated in the course of the reaction: Rh(ttp)H, $Rh_2(ttp)_2$, and $Rh(ttp)^-$ which are likely in equilibrium. Further identification of the direct involvement of these species in CFA was carried out by independent experiments.

2.8.2 Reactivity of Rh(ttp)H with Fluorobenzene

Rh(ttp)H was synthesized independently in 65% yield according to the literature method via reductive protonation of Rh(ttp)Cl with $NaBH_4$/HCl (eq. 2.14).[60]

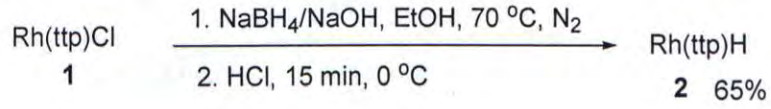

(2.14)

Rh(ttp)H was then reacted with 1,4-difluorobenzene in both neutral or basic as well as in solvent or solventless conditions. The reaction with KOH at 120 °C gave both the C-F activation product **7a** and the C-H activation product **7b** (Table 2.8, entries 1 and 3). However, unidentified complex mixtures formed in the absence of KOH (Table 2.8, entries 2 and 4). Therefore, Rh(ttp)H is not the active intermediate for CFA and CHA. The pK_a of Rh(tpp)H in dimethyl sulfoxide at 25 °C is reported to be around 11,[61] so it is reasonable to estimate the pK_a of the proton in Rh(ttp)H is around 11. Thus Rh(ttp)H is likely deprotoned by KOH to give $Rh(ttp)^-$ responsible for both CFA and CHA.

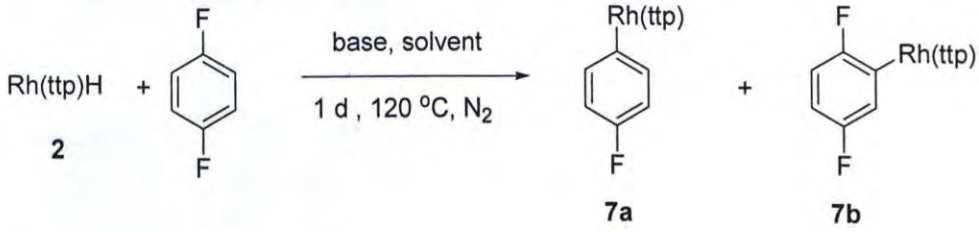

(2.15)

Table 2.8 Reaction of Rh(ttp)H with 1,4-Difluorobenzene

Entry	Base /10 equiv	Solvent	**7a** Yield / %	**7b** Yield / %	Total Yield / %
1	KOH	nil	33	9	42
2	nil	nil	0	0	0
3	KOH	C_6H_6	45	33	78
4	nil	C_6H_6	0	0	0

2.8.3 Reactivity of $Rh_2(ttp)_2$ with Fluorobenzenes

$Rh_2(ttp)_2$ was also independently synthesized by photolysis of Rh(ttp)H according to the procedure by Wayland et al. in 1986.[62] Activation reactions occurred only in the presence of KOH with both **7a** and **7b** formed in 32 and 24%, respectively (eq. 2.16.) No **7a** or **7b** was observed in the absence of KOH (eq 2.17). Therefore $Rh_2(ttp)_2$ is not the intermediate responsible for bond activations. Likely, $Rh_2(ttp)_2$ is converted to $Rh(ttp)^{\cdot}$ and possibly Rh(ttp)OH. Rh(ttp)OH then reacts with PhH to give Rh(ttp)H and $Rh(ttp)^{\cdot}$ upon reaction with KOH. Scheme 21 illustrates this reactions.

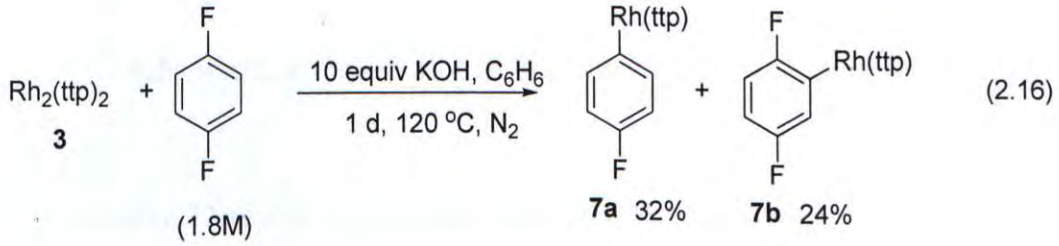

(2.16)

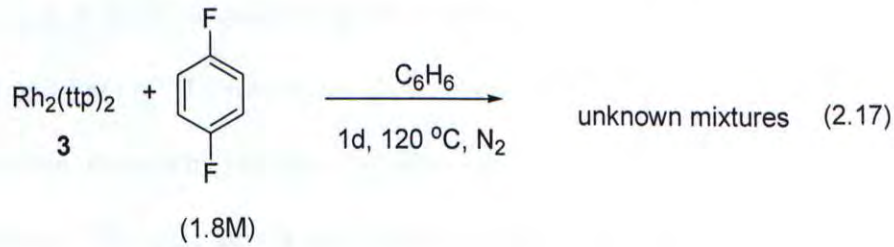

(2.17)

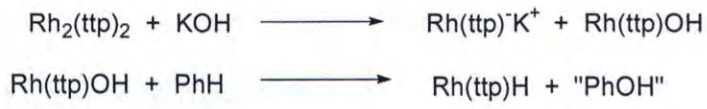

Scheme 21. The Proposed Reactions of $Rh_2(ttp)_2$ with KOH

Since $Rh_2(ttp)_2$ was slowly converted to $Rh(ttp)^-$ anion in the course of the activation reaction as observed by ^1H NMR spectroscopy (Figure 2c), $Rh(ttp)^-$ is likely an active intermediate for the CFA and CHA.

2.9 Proposed C-F Activation Mechanism

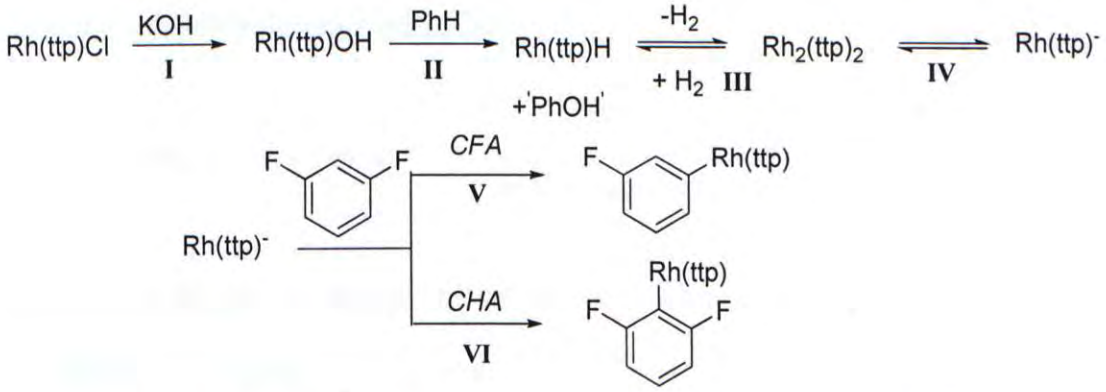

Scheme 22. Proposed Mechanism of Activation of Fluorobenzenes

Scheme 22 depicts the proposed mechanism. Initially, Rh(ttp)Cl undergoes ligand substitution with KOH to give Rh(ttp)OH. Rh(ttp)OH reacts rapidly with PhH to generate Rh(ttp)H and PhO^-K^+. However, the detection of phenol by GC-MS after neutralization of the reaction mixture by HCl was not successful as the amount of them may be too little to be observed. Rh(ttp)H then is equilibrating with $Rh(ttp)^-$ and $Rh_2(ttp)_2$ in basic media at

high temperature. Finally, an aryl fluoride undergoes CFA and CHA reactions with $Rh(ttp)^-$ to give Rh(ttp)Ar via S_NAr pathways.

2.9.1 Attempted Synthesis of Rh(ttp)OR

As the proposed intermediate, Rh(ttp)OH was not directly observed (Scheme 21, step **I**), we attempted to synthesize Rh(ttp)OR independently from the reaction of Rh(ttp)Cl with using sterically bulky alkoxide. However, Rh(ttp)Cl was consumed by RO^- to give undefined complex mixtures (Table 2.9, eq. 2.18). Rh(ttp)OR might have been synthesized but likely is very reactive and reduced by PhH rapidly to yield Rh(ttp)H and $Rh_2(ttp)_2$ in the absence of an electrophile, flouoroarene. Rh(ttp)H or $Rh_2(ttp)_2$ formed are possibly decomposed by base.

$$\text{Rh(ttp)Cl} + \text{MOR} \xrightarrow[120\ ^{o}\text{C, Time}]{N_2} \text{Rh(ttp)OR} \qquad (2.18)$$

Table 2.9 Attempted Synthesize of Rh(ttp)OR

Entry	MOR	Solvent	Time / d	Yield / %
1	NaOPh	PhH	3	Complex mixtures
2	KO^tBu	*t*-BuOH	4	Complex mixtures
3	NaOAr	PhH	2	Complex mixtures

NaOAr = Sodium 3,5-di-*tert*-butylphenoxide

2.9.2 Independent Method of Generation of $Rh(ttp)^-$

$Rh(ttp)^-$ was directly observed by ^1H NMR in the course of CFA reaction (Section 2.8.1) and formed from the reaction of Rh(ttp)H with base (Section 2.8.2). In addition,

independent method of generation of $Rh(ttp)^-$ was carried out to further ascertain the intermediacy. Rh(ttp)R (R = Me, $SiEt_3$) was reacted separately with fluorobenzene in the presence of 10 equivalents of KOH to generate $Rh(ttp)^-$ and examine its reactivity towards fluoroarene.(eq. 2.19, Table 2.10).

$$Rh(ttp)R + C_6H_5X \xrightarrow[\text{time, } 120\ ^\circ C,\ N_2]{\text{solvent, 10 equiv KOH}} Rh(ttp)R + \underset{\mathbf{4}}{Rh(ttp)Ph} + \underset{\mathbf{5a}}{Rh(ttp)\text{-}o\text{-}C_6H_4F} \qquad (2.19)$$

Table 2.10 Reactions of Rh(ttp)R with Fluorobenzene

Entry	R	X	solvent	time	Recovery yield / %	**4** yield / %	**5a** yield / %	Total yield / %
1	Me	F	C_6H_6	4d	66	10	0	76
2	Me	H	none	3d	78	0	0	78
3	$SiEt_3$	F	C_6H_6	2d	0	40	18	58
4	$SiEt_3$	H	none	3d	69	0	0	69

Both Rh(ttp)Me and $Rh(ttp)SiEt_3$ were thermal stable at 120 °C with 10 equivalents of KOH in benzene (Table 2.10, entries 2 and 4). With the addition of fluorobenzene, Rh(ttp)R consumed slowly. Small amounts of Rh(ttp)Me were consumed to generate 10% yield of CFA product **4** via $Rh(ttp)^-$ which then reacts with fluorobenzene (Table 2.10, entry 1). $Rh(ttp)SiEt_3$ was completely consumed in 2 days and gave both CFA product **4** and CHA product **5a** (Table 2.10, entry 3). Complete convertion of $Rh(ttp)^-$ from $Rh(ttp)SiEt_3$ likely occurred to give both CFA and CHA products.

In step **V**, nucleophilic aromatic substitution (S_NAr) can proceed either by (1) addition-elimination (step **Va**) or (2) elimination-addition via a benzyne intermediate (step **Vb**) (Scheme 23). Step **Vb** would likely exhibit a large ^1H kinetic isotope effect.

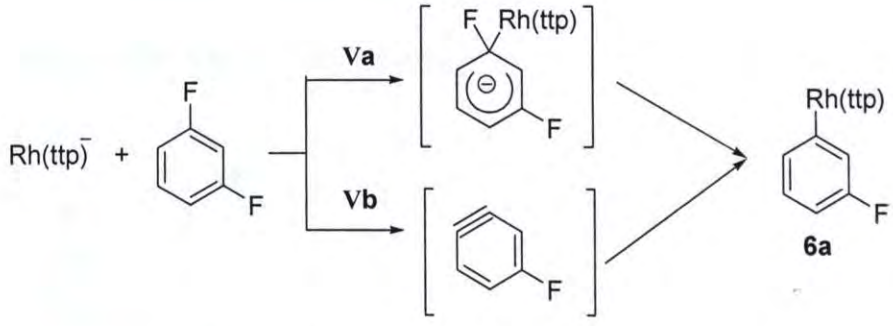

Scheme 23. Two S_NAr Pathways of CFA.

2.9.3 Isotope Effect of C-F and C-H Activations

Measurements of the kinetic isotope effect were carried out by the reaction between Rh(ttp)Cl or Rh(ttp)H and the pre-mixed equimolar mixture of fluorobenzene and fluorobenzene-d_5 at 120 °C with 10 equivalents of KOH. The C-F and C-H activation products were isolated by column chromatography and the ratio of C-F and C-H activation products were determined by the ratio between β-pyrrole signals in ^1H NMR spectroscopy (eq. 2.20).

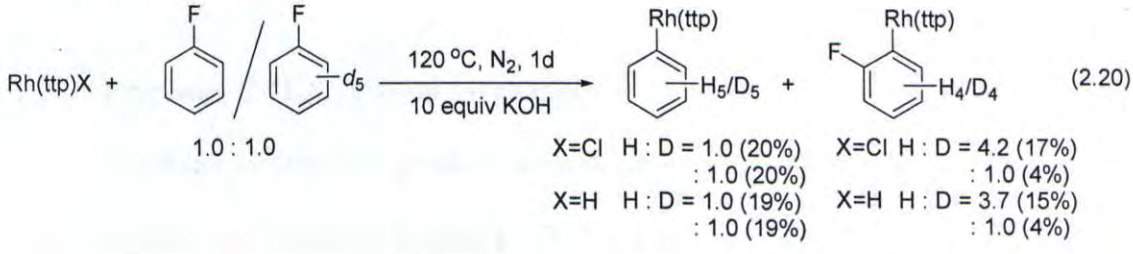

(2.20)

The isotope effect (k_H/k_D) of the C-H activation product was determined to be 4.2 for Rh(ttp)Cl and 3.7 for Rh(ttp)H by ^1H NMR. The values are consistence with the

values obtained in HRMS which determined to be 3.7 for Rh(ttp)Cl and 3.6 for Rh(ttp)H. The KIEs for the CFA products were determined to be 1.0 for both Rh(ttp)Cl and Rh(ttp)H by ^{1}H NMR. Therefore, no CH cleavage step is involved in the rate-determing step. The CFA likely operates through an addition-elimination pathway (**Va**) but not via a benzyne pathway (**Vb**) which would most likely yields non-unity KIEs (Scheme 24).

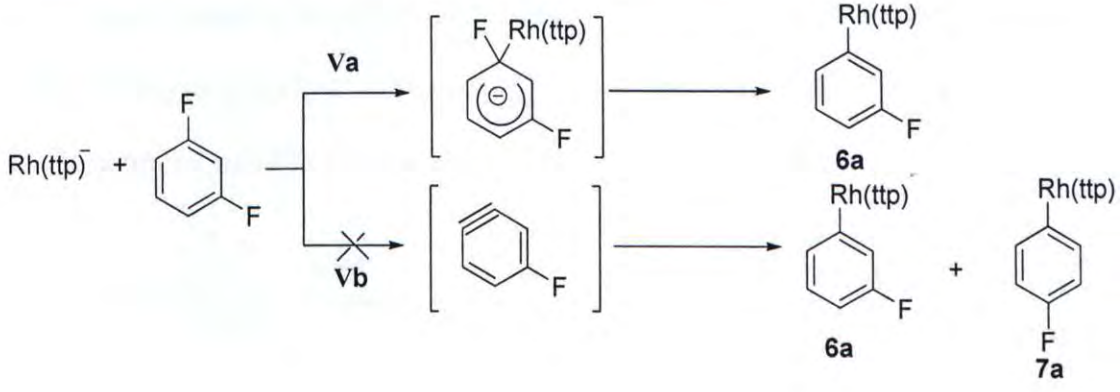

Scheme 24. The Proposed Addition-Elimination S_NAr Pathway.

Further supporting evidence for the addition-elimination process comes from at least the regioselective formation of **6a** and successful CFA of hexafluorobenzene. As no **7a** formed, occurrence of a benzyne, which would give both **6a** and **7a** in activation of 1,3-difluorobenzene, is not likely. And as no CH bond is present in hexafluorobenzene, no CH cleavage is involved.

2.10 Proposed C-H Activation Mechanism

The KIEs for the CHA products were determined to be 4.2 from Rh(ttp)Cl and 3.7 from Rh(ttp)H by ^{1}H NMR. Therefore, CH bond cleavage step is involved in the rate-determing step. As the elimination step of CHA involves the CH bond cleavage, the CHA likely operates through an addition-elimination pathway (**Va**) (Scheme 25).

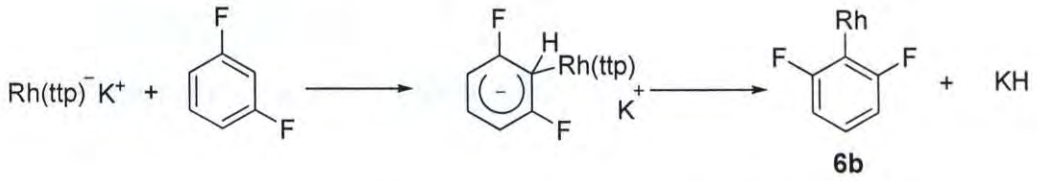

Scheme 25. The Proposed Addition-Elimination S_NAr CHA Pathway.

If the CHA reaction process via the elimination-addition pathway (**Vb**), the intermediate benzyne would result in two isomers. However, the CHA reactions are regioselective and produce only *ipso* products which are unlikely the sole regioselective products from the elimination-addition S_NAr pathway (**Vb**) (Scheme 26).

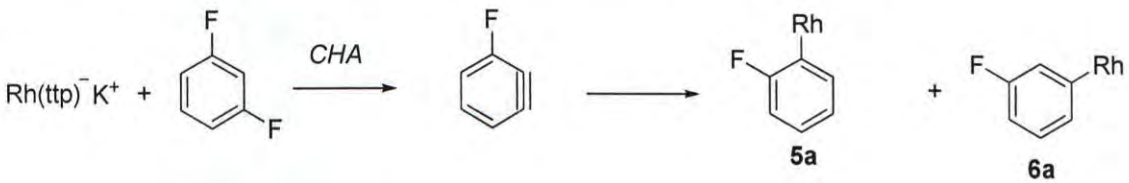

Scheme 26. The Proposed Elimination-Addition S_NAr Pathway.

2.10.1 Kinetic And Thermodynamic Products of CFA and CHA

To gain an idea of the kinetic and thermodynamic stability of the CHA product, the CHA product **7b** was heated at the high temperature of 200 °C for 4 d with or without KOH. (eq. 2.21, Table 2.11) The CHA product **7b** is thermally stable as the majority of **7b** was recovered. However, **7b** was unstable in the presence of KOH and 1,4-difluorobenzene. **7b** was transformed into **7a** in an intermolecular way. **7b** reacts with KOH to give Rh(ttp)⁻ which then reacts with 1,4-difluorobenzene to give **7a**. Therefore the C-F activation product **7a** is the thermodynamic product (Scheme 27). However, the detection of the 2,5-difluorophenol after neutralizing the reaction mixture with HCl was not successful, possibly due to its low concentration. This pathway is the reverse of the

addition-elimination S_NAr pathway for CHA by the principle of microreversibility, the CHA likely operates via an addition-elimination S_NAr pathway.

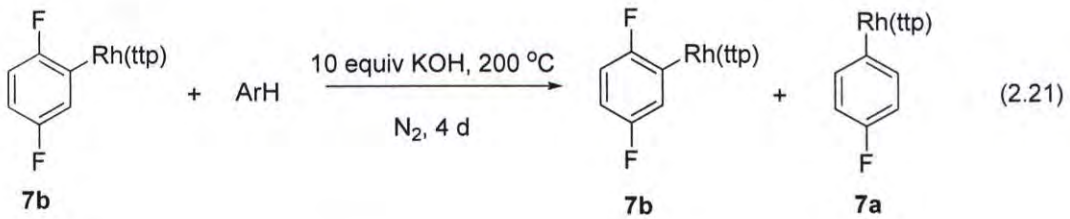

Table 2.11 Thermal Reactions of Selected C-H activated Product

Entry	ArH	Base	**7b** Recovery Yield/%	**7a** Yield/%
1	C_6H_6	KOH	81	0
2	C_6H_6	nil	79	0
3	1,4-difluorobenzene	KOH	61	20
4	1,4-difluorobenzene	nil	82	0

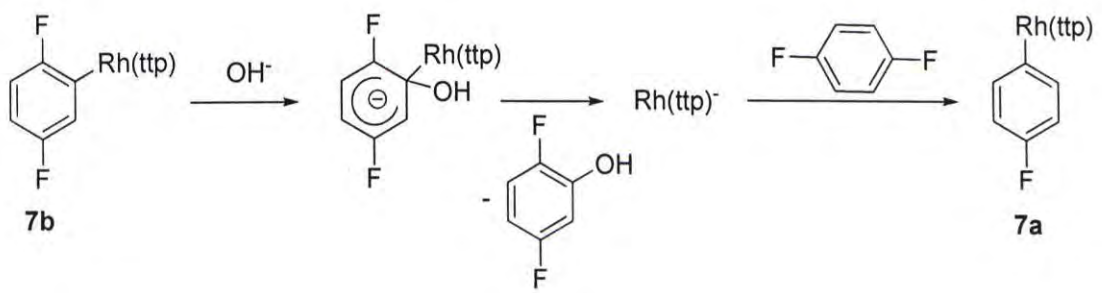

Scheme 27. The Convertion of CHA Product **7b** into CFA Product **7a**

To further confirm the transformation of CHA product **7b** into CHA product **7a** was an intermolecular reaction, hexafluorobenzene was reacted with **7a** in 200 °C with KOH (eq. 2.22). The CFA product **9** was obtained in 23% yield from hexafluorobenzene

with 66% yield of **7b** recovered. Indeed, **7b** was converted to $Rh(ttp)^-$ by KOH to give the CFA product **9**.

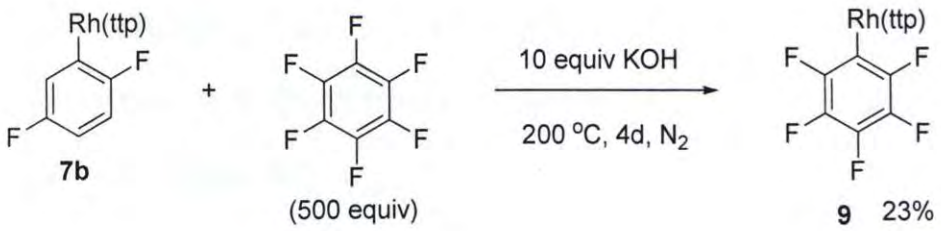

(2.22)

The conversions of C-H activation products into C-F activation products require a higher temperature of 200 °C in at least 4 days. Figure 2d deplicts the energy-level profile of the reaction.

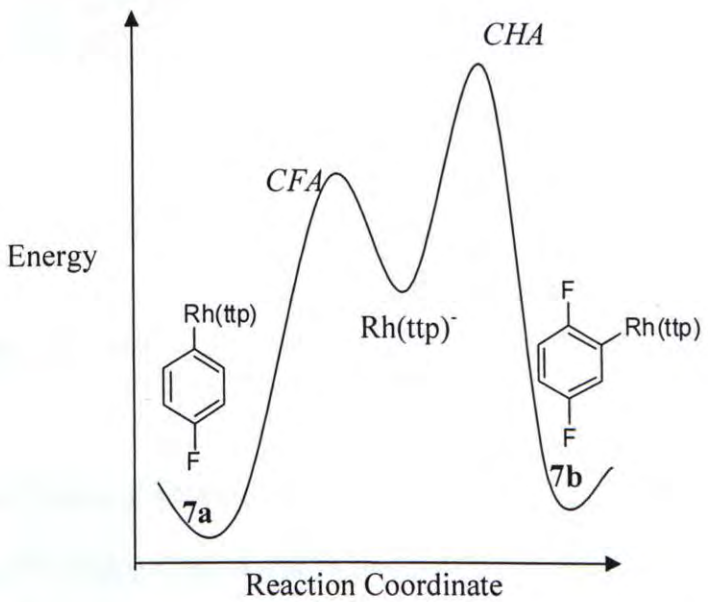

Figure 2d. Potential Energy Level Diagram of **7a** and **7b**

2.10.2 *Ortho* Selectivity of C-H Activation

The *ortho* selective CHA of halobenzene has been proposed to be chelation-assistance (Chapter 1, Scheme 15).[44] To prove whether an *ortho*-aryl fluorine substituent can coordinate to the rhodium atom, single crystal of **4** were grown for gaining structural information (Figure 2e).

Table 2.12 Seclected Bond Distances (Å) and Angles (deg) for Rh(ttp)R

Entry	Rh(ttp)R	Rh-Cα length /Å	Rh-Cα-Cβ bond angle /deg
1[a]	Ph **4**	1.979(7)	120.9(3)
2	C_6H_4(*o*-F) **5a**	2.179(7)	123.5(7)
3[a]	C_6H_4(*p*-F) **7a**	2.072(5)	121.3(5)

a: From Mr. P. F. Chiu's Thesis[53]

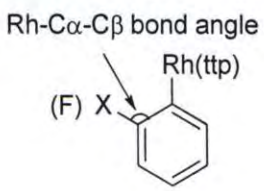

Figure 2f. The Rh-Cα-Cβ Bond Angle of Rhodium Aryl Complexes

Table 2.12 lists the selected bond lengths and angles for **4**, **5a** and **7a**. The Rh-Cα bond distance in **5a** is larger than **4** and **7a** (Figure 2f). The fluorine atom does not appear to coordinate to the rhodium atom. These data clearly indicate that the fluorine atom in the α-carbon of **5a** does not have any attractive interaction with the rhodium centre.[31] Electron repulsion exists between the fluorine and rhodium atoms as indicated by the larger Rh-Cα-Cβ bond angle. Furthermore, the rhodium-fluorine distance is 3.29 Å and is also larger than the sum of the van der Waal radius of the two atoms (3.15 Å).[63]

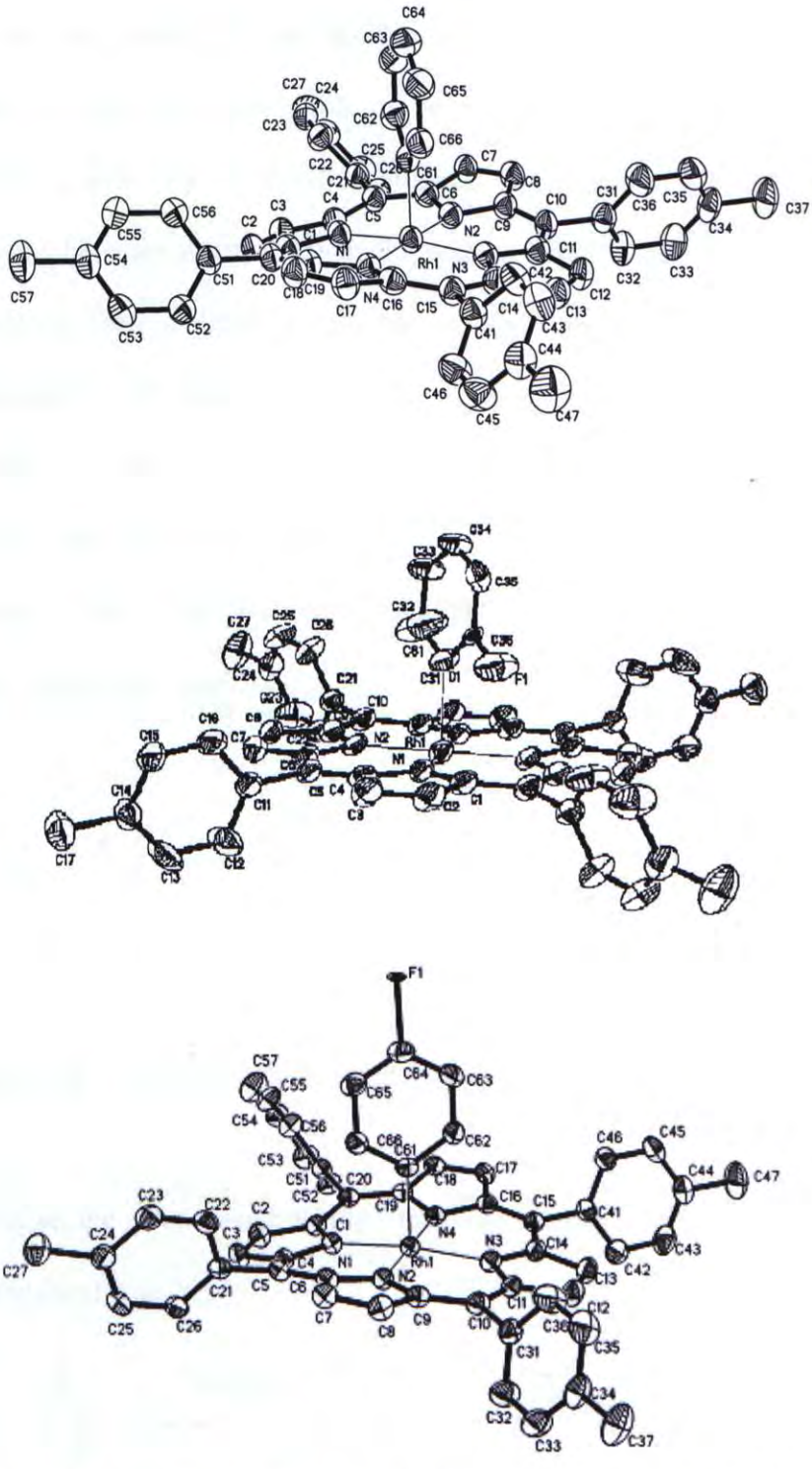

Figure 2e ORTEP of complexes $C_6H_5Rh(ttp)$ **4**, (o-F)$C_6H_4Rh(ttp)$ **5a** and (p-F)$C_6H_4Rh(ttp)$ **7a** showing the atomic labeling scheme and 30 % probability displacement ellipsoids.

Alternatively, the *ortho* C-H activation may involve the pre-coordination of $Rh(ttp)^-$ or less likely Rh(ttp)H with the fluorine atom in fluorobenzene as it was found that the rates of formation and yields of **5a** are dependent on the concentration of flouorobenzene (Table 2.3). All the CHA products formed slower than the CFA products in the reactions between Rh(ttp)Cl with fluoroarenes in the presence of 10 equivalents KOH. Therefore, pre-coordination with the *ortho*-CH bond may exist. The hydrogen *ortho* to fluorine is the most acidic as the influence of strong electron-withdrawing inductive effect of fluorine.[64] Desiraju et al[65] studied the solid state structures of fluorobenzene and found that there are C-H···F interactions in the structures of fluorobenzene (Scheme 28). This weak hydrogen bonding indicated that fluorine can interact in an association complex.

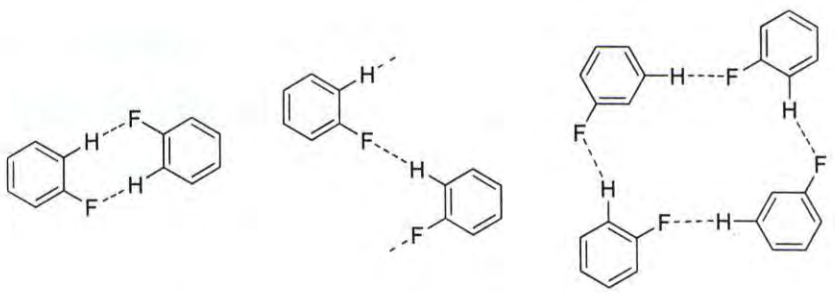

Scheme 28. The Hydrogen Bonding in Various Types of Fluorobenzene

Likewise, the electron-rich $Rh(ttp)^-$ may also interact with the *ortho* C-H bond of fluorobenzene (Secheme 29).

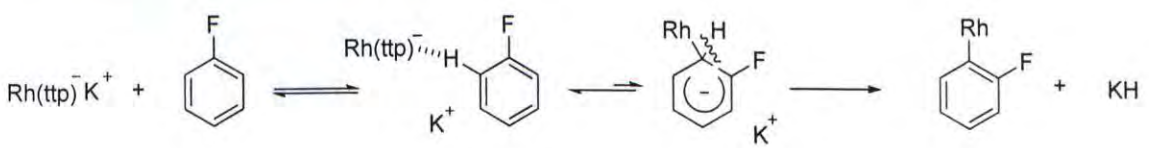

Scheme 29. *o*-CHA of Fluorobenzene by $Rh(ttp)^-$

Indeed, the electron-deficient aromatic, pyridine, is well-known to undergo an S_NAr pathway to give 2-^{t}BuPy and LiH in organic chemistry (eq. 2.23).[66]

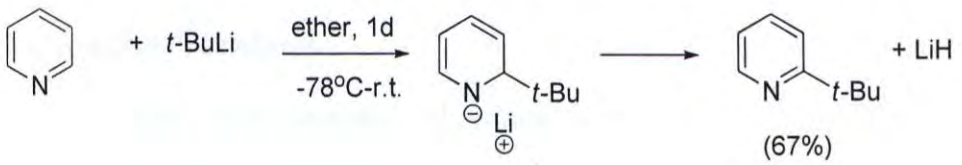

(2.23)

2.11 Summary

Competitive aromatic C-F and C-H activation reactions of fluorobenzenes were successfully carried out with rhodium(III) porphyrins in basic conditions to give the corresponding rhodium(III) porphyrin aryl complexes. Both the CFA and CHA reactions occur via the nucleophilic aromatic substitution S_NAr via the addition-elimination process with Rh(ttp)$^-$ intermediate. The CHA products are *ortho*-selective which are likely due to the pre-coordination effect of Rh(ttp)$^-$ to the hydrogen *ortho* to fluorine atom.

Chapter 3 Experimental Section

3.1 General Procedures

Unless otherwise noted, all reagents were purchased from commercial suppliers and directly used without further purification. Hexane was distilled from anhydrous calcium chloride. Benzene and toluene were distilled from sodium. Thin layer chromatography was performed on pre-coated silica gel 60 F_{254} plates. Silica gel (Merck, 70-230 mesh) were used for column chromatography. All bond activation reactions were carried out inside thich-wall glass tubes equipped with a Rotaflo stopper. The glass tubes were covered by aluminum foil to avoid photochemical reactions.

3.2 Experimental Instrumentation

^{1}H NMR and ^{13}C NMR spectra were recorded on a Bruker DPX-300 at 300 MHz or Bruker DPX-400 spectrometer at 400 MHz and Bruker DPX-300 at 75 MHz or Bruker DPX-400 at 100 MHz respectively. Chemical shifts were referenced to the residual solvent protons in C_6D_6 (δ = 7.15 ppm), $CDCl_3$ (δ = 7.26 ppm) or tetramethylsilane (δ = 0.00 ppm) in ^{1}H NMR spectra and $CDCl_3$ (δ = 77.16 ppm) or THF-d_8 (δ = 67.03 and 25.14 ppm) in ^{13}C NMR spectra as the internal standards. Chemical shifts (δ) were reported as part per million (ppm) in (δ) scale downfield from TMS. ^{19}F NMR spectra were recorded on a Varian XL-400 spectrometer at 376 MHz. Chemical shifts were referenced with the external standard fluorine in $C_6H_5CF_3$ using a sealed melting point tube and put into the NMR tube (δ = 0.00 ppm). Chemical shifts (δ) were reported as part

per million (ppm) in (δ) scale downfield from $C_7H_5F_3$.[67] Coupling constants (J) were reported in Hertz (Hz).

High resolution mass spectra (HRMS) were recorded on a ThermoFinnigan MAT 95 XL mass spectrometer. Fast atom bombardment spectra were performed with 3-nitrobenzyl alcohol (NBA) as the matrix.

3.3 Independent Syntheses of Starting Materials

Preparation of Tetratolylporphyrin (H_2ttp).[54] Pyrrole (23.5 mL, 0.34 mol) was added dropwise to a refluxing solution of tolylaldehyde (40.8 g, 0.34 mol) in propionic acid (1.25 L). The resulting mixture was refluxed for another 30 min. The black solution was then cooled down to room temperature and methanol (1.5 L) was added to precipitate the porphyrin. The purple solid (3.89 g, 0.058 mol, 17%) was collected by filtration and further purified by recrystallization from $CHCl_3$/MeOH. R_f = 0.91 (hexane/CH_2Cl_2 = 1:1). ^{1}H NMR ($CDCl_3$, 300 MHz) δ -2.78 (s, 2 H), 2.71 (s, 12 H), 7.56 (d, 8 H, J = 7.8 Hz), 8.10 (d, 8 H, J = 7.8 Hz), 8.85 (s, 8 H).

Preparation of Tetraphenylporphyrin (H_2tpp).[54] Pyrrole (23.5 mL, 0.34 mol) was added dropwise to a refluxing solution of benzadehyde (35 mL, 0.34 mol) in propionic acid (1.25 L). The resulting mixture was refluxed for another 30 min. The black solution was then cooled down to room temperate and MeOH (1.5 L) was added to precipitate the porphyrin. The purple solid (3.92 g, 0.063 mol, 17%) was collected by filtration and further purified by recrystallization by $CHCl_3$/MeOH. R_f = 0.91 (hexane/CH_2Cl_2 = 1:1).

^{1}H NMR ($CDCl_3$, 300 MHz) δ -2.78 (s, 2H), 7.75 (dd, 8 H, J = 2.0, 7.8 Hz), 8.23 (dd, 8 H, J = 2.0, 7.8 Hz), 8.93 (s, 8 H).

Preparation of Chloro[5,10,15,20-tetratolyllphenylporphyrinato]rhodium (III) Rh(ttp)Cl.[52] $RhCl_3 \cdot xH_2O$ (206 mg, 0.78 mmol) was added to a mixture of 5,10,15,20-tetratolylporphyrin (356.4 mg, 0.53 mmol) in benzonitrile (30 mL) and then was refluxed for 3 h. After removal of the solvent under vacuum, the residue was purified by silica gel column chromatography with CH_2Cl_2 as eluent. The red band was collected to give a red solid which was further recrystallized from CH_2Cl_2/MeOH. A red solid was collected by filtration and vacuum dried for 2 h at 70 °C to give Rh(ttp)Cl (300 mg, 0.372 mmol, 70%). R_f = 0.31 (hexane/CH_2Cl_2 = 1:1). ^{1}H NMR ($CDCl_3$, 300 MHz) δ 2.71 (s, 12 H), 7.55 (d, 8 H, J = 7.8 Hz), 8.08 (d, 4 H, J = 7.2 Hz), 8.13 (d, 4 H, J = 7.2 Hz), 8.94 (s, 8 H).

Preparation of Chloro[5,10,15,20-tetratolylphenylporphyrinato]rhodium (III) Rh(tpp)Cl.[52] $RhCl_3 \cdot xH_2O$ (206 mg, 0.78 mmol) was added to a mixture of 5,10,15,20-tetratolyphenylporphyrin (375.4 mg, 0.533 mmol) in benzonitrile (30 mL). After refluxed for 3 h, the solvent was removed under vacuum. The residue was purified by silica gel column chromatography with CH_2Cl_2 as eluent. The major red band was collected. After removal of CH_2Cl_2 by rotary evaporation, the residue was recrystallized from CH_2Cl_2/MeOH. A red solid was collected by filtration and then vacuum dried for 2 h in 70 °C to give the red solid of Rh(tpp)Cl (300 mg, 0.372 mmol, 68%). R_f = 0.30

(hexane/CH_2Cl_2 = 1:1). ^1H NMR ($CDCl_3$, 300 MHz) δ 7.75 (dd, 8 H, J = 2.0, 7.8 Hz), 8.23 (dd, 8 H, J = 2.0, 7.8 Hz), 8.93 (s, 8 H).

Preparation of (5,10,15,20-tetratolylporphyrinato)hydridorhodium(III), Rh(ttp)H[62]

A suspension of Rh(ttp)Cl (100.0 mg, 0.12 mmol) was dissolved in EtOH (40 mL) and a solution of $NaBH_4$ (16.6 mg, 0.44 mol) in aq. NaOH (0.1 M, 2 mL) were purged with N_2 for 15 min separately. Then the $NaBH_4$ solution was then added to the solution of Rh(ttp)Cl via a cannular under N_2. The mixture was heated at 50 °C for 1 h under N_2 giving a brick red suspension. After cooling to 0 °C under N_2 for 15 min, HCl was added (0.1 M, 30 mL) via a cannular and a bright red suspension resulted. The red solid was filtered and washed with H_2O (2 x 10 mL) under N_2 using a cannular wrapped with filter paper. After vacuum-dried at 70 °C for 1 h, a red solid of Rh(ttp)H (57.0 mg, 0.71 mmol, 58 %) was obtained. ^1H NMR (C_6D_6, 300 MHz) δ -40.19 (d, 1 H, J = 43.5 Hz), 2.42 (s, 12 H), 7.24 (d, 4 H, J = 6.9 Hz), 7.37 (d, 4 H, J = 7.2 Hz), 7.96 (d, 4 H, J = 8.0 Hz), 8.24 (d, 4 H, J = 8.1 Hz), 9.03 (s, 8 H).

General Procedure for Preparation of Rh(ttp)OR.

A. **Rh(ttp)OPh** Rh(ttp)Cl (30.0 mg, 0.037 mmol) and 5 equiv of anhydrous NaOPh (21.5 mg, 0.185 mmol), freshly prepared from the reaction of Na (4.3 mg, 0.185 mmol) and PhOH (18.3 mg, 0.185 mmol), were added into benzene (1.5 mL) and degassed for three freeze-thaw-pump cycles. After heating at 120 °C under N_2 for 3 d, the solvent was removed by vacuum. The residue was redissolved in benzene-d_6 for ^1H NMR spectroscopy, which indicated that unidentifiable porphyrin species.

B. **Rh(ttp)O^{t}Bu** Rh(ttp)Cl (30.0 mg, 0.037 mmol) and 5 equiv of KO^{t}Bu (20.7 mg, 0.185mmol) were added into *tert*-butanol (1.5 mL) and degassed for three freeze-thaw-pump cycles. After heating at 120 °C under N_2 for 3 d, the solvent was then removed in vacuum. The residue was redissolved in benzene-d_6 for ^{1}H NMR spectroscopy, which indicated that unidentifiable porphyrin species.

C. **Rh(ttp)ODBPh** Rh(ttp)Cl (30.0 mg, 0.037 mmol) and 5 equiv of sodium 3,5-di*tert*butylphenoxide (38.2 mg, 0.185 mmol), freshly prepared from the reaction of Na (4.3 mg, 0.185 mmol) and 3,5-di*tert*butylphenol (33.9 mg, 0.185 mmol), were added into benzene (1.5 mL) and degassed for three freeze-thaw-pump cycles. After heating at 120 °C under N_2 for 3 d, the solvent was then removed in vacuum. The residue was redissolved in benzene-d_6 for ^{1}H NMR spectroscopy, which indicated that unidentifiable porphyrin species.

General Procedure for Preparation of Rh(ttp)R.

A. **Rh(ttp)Me**[68] Rh(ttp)Cl (100 mg, 0.124 mmol) and K_2CO_3 (171 mg. 1.24 mmol) was added to methanol (3 mL). The mixture was heated at 150 °C for 1 d, and the solvent was removed under vacuum. The crude mixture was purified by silica gel column chromatography with a mixture of hexane and CH_2Cl_2 (1:1) as eluent. The red solid was recrystallized from CH_2Cl_2/MeOH (1:1) and was collected by filtration and vacuum-dried for 2 h in 70 °C to give the red solid of Rh(ttp)Me (77 mg, 0.098 mmol, 79%). R_f = 0.70 (hexane/CH_2Cl_2 = 1:1). ^{1}H NMR ($CDCl_3$, 300 MHz) δ -5.82 (d, 3 H, J = 3.0 Hz), 2.70 (s, 12 H), 7.53 (d, 8 H, J = 8.1 Hz), 8.01 (dd, 4 H, J = 2.1, 8.4 Hz), 8.07 (dd, 4 H, J = 2.1, 8.4 Hz), 8.73 (s, 8 H).

B. **Rh(ttp)SiEt$_3$**[69] A mixture of Rh(ttp)Cl (100 mg, 0.124 mmol) in triethylsilane (5 mL) was heated at 200 °C for 3 h. Then the solvent was removed by vacuum. The residue was purified by silica gel column chromatography eluting with a mixture of hexane and CH_2Cl_2 (1:1) to give Rh(ttp)SiEt$_3$ (97 mg, 0.109 mmol, 88%) which was further recrystallized from CH_2Cl_2/MeOH. R_f = 0.31. ^{1}H NMR ($CDCl_3$, 300 MHz) δ -3.41 (q, 6 H, J = 7.2, 8.7 Hz), -1.35 (t, 9 H, J = 8.7 Hz), 2.68 (s, 12 H), 7.55 (d, 8 H, J = 8.1 Hz), 8.04 (t, 8 H, J = 7.8 Hz), 8.65 (s, 8 H).

General Procedure for Reactions of Rh(ttp)Cl with Fluorobenzene and Various Bases

A. **Addition of NaOH.** A mixture of Rh(ttp)Cl (30.0 mg, 0.037 mmol), 10 equiv of NaOH (14.9 mg, 0.37 mmol) and fluorobenzene (1.5 mL, 0.16 mmol) was degassed for three freeze-thaw-pump cycles and heated at 120 °C under N_2 for 1 d. The solvent was then removed in vacuum and the residue was purified by silica gel column chromatography eluting with a solvent mixture of hexane:CH_2Cl_2 (1:1) to give Rh(ttp)Ph **4** (15.2 mg, 0.018 mmol, 48%). R_f = 0.50 (hexane/CH_2Cl_2 = 1:1). ^{1}H NMR ($CDCl_3$, 300 MHz) δ 0.26 (d, 2 H, J = 8.1 Hz), 2.69 (s, 12 H), 4.76 (dt, 2 H, J = 1.2, 7.8 Hz), 5.23 (t, 1 H, J = 7.8 Hz), 7.52 (dd, 8 H, J = 2.0, 7.3 Hz), 8.00 (dd, 4 H, J = 2.1, 8.9 Hz), 8.06 (dd, 4 H, J = 2.2, 8.7 Hz), 8.76 (s, 8 H).

B. **Addition of KOH.** A mixture of Rh(ttp)Cl (30.0 mg, 0.037 mmol), 10 equiv of KOH (20.8 mg, 0.37 mmol) and fluorobenzene (1.5 mL) was degassed for three freeze-thaw-pump cycles and heated at 120 °C under N_2 for 1 d. The solvent was then removed in vacuum and the residue was purified by silica gel column

chromatography eluting with a solvent mixture of hexane:CH_2Cl_2 (1:1) to give Rh(ttp)Ph **4** (15.2 mg, 0.018 mmol, 48%) and a trace amount of (*o*-F)(C_6H_4)Rh(ttp) **5a**, R_f = 0.58 (hexane:CH_2Cl_2 = 1:1). ^{1}H NMR ($CDCl_3$, 300 MHz) δ 0.01 (m, 1 H), 2.69 (s, 12 H), 4.48 (t, 1 H, J = 7.3 Hz), 4.68 (dd, 1 H, J = 7.3, $^1J_{H\text{-}F}$ = 8.3 Hz), 5.28 (dd, 1 H, J = 7.3, 7.5 Hz) 7.53 (dd, 8 H, J = 2.2, 8.3 Hz), 8.02 (dd, 4 H, J = 2.2, 8.6 Hz), 8.07 (dd, 4 H, J = 2.2, 8.6 Hz), 8.79 (s, 8 H). ^{13}C NMR ($CDCl_3$, 75 MHz) δ 21.76, 107.43 (d, $^1J_{C\text{-}F}$ = 25.2 Hz), 112.10, (d, $^1J_{C\text{-}Rh}$ = 27.8 Hz), 119.43, 122.09, 122.87, 127.52, 131.75, 132.30, 133.75, 134.25, 137.38, 139.18, 143.55. ^{19}F NMR ($CDCl_3$, 376 MHz) δ -45.15 (s, 1F, *o*-F). Calcd for $(C_{54}H_{40}N_4FRh)^+$: m/z 866.2238. Found: m/z 866.2287. Crystal structures were grown from slow diffusion of solvent mixture of methanol and dichloromethane.

C. **Addition of Ag_2CO_3.** A mixture of Rh(ttp)Cl (30.0 mg, 0.037 mmol), 10 equiv of Ag_2CO_3 (106.8 mg, 0.37 mmol) and fluorobenzene (1.5 mL) was degassed for three freeze-thaw-pump cycles and heated at 120 °C under N_2 for 1 d. The solvent was then removed in vacuum and the residue was purified by silica gel column chromatography eluting with a solvent mixture of hexane:CH_2Cl_2 (1:1) to give (*o*-F)(C_6H_4)Rh(ttp) **5a** (2.1 mg, 2.4 μmol, 6%) and (*p*-F)C_6H_4Rh(ttp) **7a** (3.2 mg, 3.7 μmol, 13%).

D. **Addition of K_2CO_3.** A mixture of Rh(ttp)Cl (30.0 mg, 0.037 mmol), 10 equiv of K_2CO_3 (53.1 mg, 0.37 mmol) and fluorobenzene (1.5 mL) was degassed for three freeze-thaw-pump cycles and heated at 120 °C under N_2 for 1 d. The solvent was then removed in vacuum and the residue was purified by column chromatography on silica

gel eluting with a solvent mixture of hexane:CH_2Cl_2 (1:1) to give a mixture of unidentified complexes.

E. **Addition of Na_2CO_3.** A mixture of Rh(ttp)Cl (30.0 mg, 0.037 mmol), 10 equiv of Na_2CO_3 (38.2 mg, 0.37 mmol) and fluorobenzene (1.5 mL) was degassed for three freeze-thaw-pump cycles and heated at 120 °C under N_2 for 1 d. The solvent was then removed in vacuum and the residue was purified by silica gel column chromatography eluting with a solvent mixture of hexane:CH_2Cl_2 (1:1) to give a mixture of unidentified complexes.

General Procedure for Reactions of Rh(ttp)Cl with Fluorobenzenes and Various Amount of Bases.

Reaction of Fluorobenzenes with Rh(ttp)Cl with 10 equivalents of KOH. A mixture of Rh(ttp)Cl (30.0 mg, 0.037 mmol) , 10 equiv of KOH (20.8 mg, 0.37 mmol) and fluorobenzene (1.50 mL, 18.5 mmol) were degassed for three freeze-thaw-pump cycles and heated at 120 °C under N_2 for 1 d. The solvent was then removed in vacuum and the red crude mixture was isolated by silica gel column chromatography eluting with a solvent mixture of hexane:CH_2Cl_2 (1:1) to give Rh(ttp)Ph **4** (24.1 mg, 0.028 mmol, 77%).

General Procedure for Reactions of Rh(ttp)Cl with Fluorobenzenes and Various Concentration of Fluorobenzene.

Reaction of Fluorobenzenes with Rh(ttp)Cl in Benzene. A mixture of Rh(ttp)Cl (30.0 mg, 0.037 mmol), 10 equiv of KOH (20.8 mg, 0.37 mmol) and fluorobenzene (1.50 mL, 18.5 mmol) with benzene (0.16 mL, 1.9 mmol) were degassed for three freeze-thaw-

pump cycles and heated at 120 °C under N_2 for 1 d. The solvent was then removed in vacuum and the red crude mixture was purified by silica gel column chromatography eluting with a solvent mixture of hexane:CH_2Cl_2 (1:1) to give Rh(ttp)Ph **4** (13.2 mg, 0.016 mmol, 43%) and a trace amount of (*o*-F)(C_6H_4)Rh(ttp) **5a**.

3.4 Activation Reactions of Fluorobenzenes by Rhodium Porphyrin

General Procedure for Reactions of Rh(ttp)Cl with Various Fluorobenzenes.

A. **Reaction of 1,2-Difluorobenzene with Rh(ttp)Cl.** A suspension of Rh(ttp)Cl (20.0 mg, 0.025 mmol), 10 equiv of KOH (13.7 mg, 0.25 mmol) and 1,2-difluorobenzene (0.31 mL, 2.5 mmol) with benzene (1.1 mL, 12.5 mmol) were degassed for three freeze-thaw-pump cycles and heated at 120 °C under N_2 for 1 d. The solvent was then removed by vacuum and the red crude mixture was purified by silica gel column chromatography on eluting with a solvent mixture of hexane:CH_2Cl_2 (3:1) to give (*o*-F)C_6H_4Rh(ttp) **5a** (11.5 mg, 0.013 mmol, 53%) as a red solid and (1,2-F_2)C_6H_3Rh(ttp) **5b**. (6.6 mg, 7.5 μmol, 30%) as a red solid. R_f = 0.45 (hexane:CH_2Cl_2 = 1:1). ^{1}H NMR ($CDCl_3$, 300 MHz) δ –0.27 (m, 1H) 2.69 (s, 12 H), 4.56 (t, 1 H, J = 8.0 Hz), 5.14 (ddd, 1 H, $^4J_{H\text{-}F}$ = 1.6, J = 8.0, $^3J_{H\text{-}F}$ = 8.1 Hz), 7.54 (d, 8 H, J = 9.0 Hz), 8.03 (dd, 4 H, J = 2.0, 8.8 Hz), 8.08 (dd, 4 H, J = 2.2, 8.7 Hz), 8.79 (s, 8 H) ^{13}C NMR ($CDCl_3$, 75 MHz) δ 21.08, 96.21 (d, $^1J_{C\text{-}F}$ = 24.8 Hz), 96.25 (d, $^1J_{C\text{-}F}$ = 24.8 Hz), 111.11, (d, $^1J_{C\text{-}Rh}$ = 22.6 Hz), 123.06, 127.60, 127.67, 131.80, 131.99, 133.79, 134.33, 137.60, 138.95, 143.05. ^{19}F NMR ($CDCl_3$, 376 MHz) δ -71.35 (d, 1 F, J = 22.2 Hz, *o*-F), δ -77.14 (d, J = 22.2 Hz, 1 F, *m*-F). Calcd for $(C_{54}H_{40}N_4FRh)^+$: m/z 866.2238. Calcd for $(C_{54}H_{39}N_4F_2Rh)^+$: m/z 884.2145. Found: m/z 884.2192.

B. Reaction of 1,3-Difluorobenzene with Rh(ttp)Cl. A suspension of Rh(ttp)Cl (20.0 mg, 0.025 mmol) and 10 equiv of KOH (13.7 mg, 0.25 mmol) and 1,3-difluorobenzene (0.25 mL, 2.5 mmol) with benzene (1.1 mL, 12.5 mmol) was degassed for three freeze-thaw-pump cycles and heated at 120 °C under N_2 for 1 d. The solvent was then removed in vacuum and the residue was purified by silica gel column chromatography eluting with a solvent mixture of hexane:CH_2Cl_2 (2:1) to give (*m*-F)C_6H_4Rh(ttp) **6a** (9.1 mg, 0.011 mmol, 42%) as a red solid. R_f = 0.58 (hexane:CH_2Cl_2 = 1:1). ^{1}H NMR ($CDCl_3$, 300 MHz) δ 0.00 (d, 1 H, $^3J_{H\text{-}F}$ = 8.0 Hz), 0.06 (d, 1 H, J = 7.3 Hz,), 2.69 (s, 12 H), 4.67 (dd, 1 H, J = 7.3, $^3J_{H\text{-}F}$ = 8.0 Hz), 4.69 (dt, 1 H, $^4J_{H\text{-}F}$ 2.4, J = 8.3 Hz), 7.53 (dd, 1 H, J = 2.1, 7.3 Hz), 8.02 (dd, 4 H, J = 2.2, 8.6 Hz), 8.07 (dd, 4 H, J = 2.2, 8.6 Hz), 8.78 (s, 8 H). ^{13}C NMR ($CDCl_3$, 100 MHz) δ 21.74, 107.27 (d, $^1J_{Rh\text{-}C}$ = 21.3 Hz) 115.33 (d, $^1J_{C\text{-}F}$ = 20.5 Hz), 115.33, 123.11, 123.48, 124.50, 127.64, 131.94, 133.89, 134.37, 137.57, 139.61, 143.21. ^{19}F NMR ($CDCl_3$, 376 MHz) δ -52.85 (s, 1 F, *m*-F). Calcd for $(C_{54}H_{40}N_4FRh)^+$: m/z 876.2238. Found: m/z 866.2287. and (2,6-F_2)C_6H_3Rh(ttp) **6b** (6.8 mg, 7.6 μmol, 31%) as a red solid. R_f = 0.48 (hexane:CH_2Cl_2 = 1:1). ^{1}H NMR ($CDCl_3$, 300 MHz) 2.67 (s, 12 H), 4.40 (dd, 2 H, J = 8.3, $^3J_{H\text{-}F}$ = 8.9 Hz), 5.3 (dd, 1 H, $^4J_{H\text{-}F}$ = 5.8, J = 8.0 Hz), 7.50 (dd, 8 H, J = 2.0, 8.4 Hz), 7.96 (dd, 4 H, J = 2.1, 8.6 Hz), 7.98 (dd, 4 H, J = 2.1, 8.5 Hz), 8.78 (s, 8 H). ^{13}C NMR ($CDCl_3$, 75 MHz) δ 13.01, 117.58 (d, $J_{C\text{-}F}$ = 30.2 Hz), 126.05, 129.13, 129.58 (d, $J_{C\text{-}Rh}$ = 25.3 Hz), 130.26, 135.41, 140.30, 140.76, 142.61, 143.17, 146.82, 148.86, 153.43. ^{19}F NMR ($CDCl_3$, 376 MHz) δ -37.66 (s, 2 F, *o*-F). Calcd for $(C_{54}H_{39}N_4F_2Rh)^+$: m/z 884.2145. Found: m/z 884.2192.

C. **Reaction of 1,4-Difluorobenzene with Rh(ttp)Cl** . A mixture of Rh(ttp)Cl (20.0 mg, 0.025 mmol), 10 equiv of KOH (13.7 mg, 0.25 mmol) and 1,4-difluorobenzene (0.25 mL, 2.5 mmol) with benzene (1.1 mL, 12.5 mmol) was degassed for three freeze-thaw-pump cycles and heated at 120 °C under N_2 for 1 d. The solvent was then removed in vacuum and the residue was purified by silica gel column chromatography eluting with a solvent mixture of hexane: CH_2Cl_2 (2:1) to give (*p*-F)C_6H_4Rh(ttp) **7a** (10.4 mg, 0.012 mmol, 48%) as a red solid. R_f = 0.58 (hexane:CH_2Cl_2 = 1:1). ^{1}H NMR ($CDCl_3$, 300 MHz) δ 0.16 (dd, 2 H, $^4J_{H\text{-}F}$ = 1.8, J = 8.9 Hz), 2.69 (s, 12 H), 4.55 (dd, 1 H, $^3J_{H\text{-}F}$ = 8.6, J = 8.9 Hz), 7.54 (d, 8 H, J = 8.3 Hz), 7.99 (dd, 4 H, J = 2.2, 8.5 Hz), 8.02 (dd, 4 H, J = 2.2, 8.7 Hz), 8.74 (s, 8 H). ^{19}F NMR ($C_6H_5CF_3$, 376 MHz) δ -62.84 (s, 1F). Calcd for $(C_{54}H_{40}N_4FRh)^+$: m/z 876.2238. Found: m/z 866.2287. and (2,5-F_2)C_6H_3Rh(ttp) **7b** (6.5 mg, 5.6 μmol, 30%) as a red solid. R_f = 0.43 (hexane:CH_2Cl_2 = 1:1). ^{1}H NMR ($CDCl_3$, 300 MHz) δ -0.27 (m, 1 H), 2.69 (s, 12 H), 4.35 (ddd, 1 H, J = 5.2, 9.0, 9.2 Hz), 4.96 (m, 1 H), 7.52 (dd, 8 H, J = 2.1, 8.5 Hz), 8.02 (dd, 8 H, J = 2.1, 8.6 Hz), 8.81 (s, 8 H). ^{13}C NMR ($CDCl_3$, 75 MHz) δ 21.69, 108.35 (d, $^1J_{C\text{-}F}$ = 23.5 Hz) 111.42 (d, $^1J_{C\text{-}Rh}$ = 31.4 Hz), 118.11 (d, $^1J_{C\text{-}F}$ = 24.1 Hz), 122.91, 127.59, 131.87, 133.68, 134.27, 137.48, 139.06, 143.50. ^{19}F NMR ($CDCl_3$, 376 MHz) δ -52.69 (s, 1 F, *o*-F), -60.67, (s. 1F, *m*-F). Calcd for $(C_{54}H_{39}N_4F_2Rh)^+$: m/z 884.2145. Found: m/z 884.2192.

D. **Reaction of 1,3,5-Trifluorobenzene with Rh(ttp)Cl** A mixture of Rh(ttp)Cl (20.0 mg, 0.025 mmol), 10 equiv of KOH (13.7 mg, 0.25 mmol) and 1,3,5-trifluorobenzene (0.26 mL, 2.5 mmol) with benzene (1.1 mL, 12.5 mmol) was degassed for three freeze-thaw-pump cycles and heated at 120 °C under N_2 for 1 d. The solvent was then

removed by vacuum and the red crude mixture was purified by silica gel column chromatography eluting with a solvent mixture of hexane:CH_2Cl_2 (2:1) to give (3,5-F_2)C_6H_3Rh(ttp) **8a** (12.4 mg, 0.014 mmol, 56%) as a red solid. R_f = 0.35 (hexane:CH_2Cl_2 = 1:1). ^{1}H NMR ($CDCl_3$, 300 MHz) δ –0.19 (d, 2 H, $^3J_{H\text{-}F}$ = 9.3 Hz), 2.70 (s, 12 H), 4.74 (t, 1 H, $^3J_{H\text{-}F}$ = 9.3 Hz), 7.56 (dd, 8 H, J = 2.1, 8.3 Hz), 8.00 (dd, 4 H, J = 2.1, 8.9 Hz), 8.06 (dd, 4 H, J = 2.1, 8.7 Hz), 8.80 (s, 8 H). ^{13}C NMR ($CDCl_3$, 75 MHz) δ 30.25, 94.82 (d, $^1J_{C\text{-}F}$ = 26.3 Hz) 95.15 (d, $^1J_{C\text{-}F}$= 26.3 Hz), 111.78 (d, $^1J_{C\text{-}Rh}$ = 21.8 Hz), 122.48, 127.62, 127.85, 131.70, 131.85, 134.20, 134.89, 137.80, 139.82, 143.20. ^{19}F NMR ($CDCl_3$, 376 MHz) δ - 52.86 (s, 2 F, *m*-F). Calcd for $(C_{54}H_{39}N_4F_2Rh)^+$: m/z 884.2145. Found: m/z 884.2192. And (2,4,6-F_3)C_6H_2Rh(ttp) **8b** (5.8 mg, 6.5 μmol, 26%) as a red solid. R_f = 0.31 (hexane:CH_2Cl_2 = 1:1). ^{1}H NMR ($CDCl_3$, 300 MHz) δ 2.67 (s, 12 H), 4.24 (t, 2 H, $^3J_{H\text{-}F}$ = 9.3 Hz,), 7.96 (d, 8 H, J = 7.5 Hz), 8.23 (dd, 4 H, J = 2.1, 8.9 Hz), 8.26 (dd, 4 H, J = 2.1, 8.8 Hz), 8.78 (s, 8 H). ^{13}C NMR ($CDCl_3$, 100 MHz) δ 21.53, 95.82 (d, $^1J_{C\text{-}F}$ = 26.3 Hz) 95.99 (d, $^1J_{C\text{-}F}$ = 26.3 Hz), 96.32 (d, $^1J_{C\text{-}Rh}$ = 21.8 Hz), 122.31, 127.40, 131.66, 133.46, 134.01, 137.25, 138.80, 143.62. ^{19}F NMR ($CDCl_3$, 376 MHz) δ -34.53 (s, 2 F, *o*-F), -56.93 (s, 1 F, *p*-F). Calcd for $(C_{54}H_{38}N_4F_3Rh)^+$: m/z 902.2145.Found: m/z 902.2192.

E. **Reaction of Pentafluorobenzene with Rh(ttp)Cl** A mixture of Rh(ttp)Cl (20.0 mg, 0.025 mmol), 10 equiv of KOH (13.7 mg, 0.25 mmol) and pentafluorobenzene (0.28 mL, 2.5 mmol) with benzene (1.1 mL, 12.5 mmol) was degassed for three freeze-thaw-pump cycles and heated at 120 °C under N_2 for 1 d. The solvent was then removed by vacuum and the residue was purified by silica gel column chromatography eluting with a solvent mixture of hexane:CH_2Cl_2 (1:1) to give

$C_6F_5Rh(ttp)$ **9** (13.2 mg, 0.014 mmol, 56%) as a red solid. R_f = 0.28 (hexane:CH_2Cl_2 = 1:1). ^1H NMR ($CDCl_3$, 300 MHz) δ 2.69 (s, 12 H), 7.51 (d, 8 H, J = 7.6 Hz), 7.99 (s, 8 H) 8.82 (s, 8 H). ^{13}C NMR ($CDCl_3$, 100 MHz) δ 21.68, 122.32, 127.61, 132.03, 133.67, 134.32, 137.51, 138.82, 143.69. ^{19}F NMR ($CDCl_3$, 376 MHz) δ -71.36 (d, 2 F, J = 22.0 Hz, *o*-F), -102.16 (t, 2 F, J = 22.8 Hz, *m*-F) -105.80 (t, 1 F, J = 22.8 Hz, *p*-F). Calcd for $(C_{54}H_{36}N_4F_5Rh)^+$: m/z 938.1868. Found: m/z 938.1910.

F. Reaction of Hexafluorobenzene with Rh(ttp)Cl in Benzene A mixture of Rh(ttp)Cl (20.0 mg, 0.025 mmol), 10 equiv of KOH (13.7 mg, 0.25 mmol) and hexafluorobenzene (0.29 mL, 2.5 mmol) with benzene (1.1mL, 12.5 mmol) were degassed for three freeze-thaw-pump cycles and heated at 120 °C under N_2 for 1 d. The solvent was then removed in vacuum and the residue was purified by silica gel column chromatography eluting with a solvent mixture of hexane:CH_2Cl_2 (1:1) to give $C_6F_5Rh(ttp)$ **9** (14.0 mg, 0.015 mmol, 60%) as a red solid. R_f = 0.28 (hexane:CH_2Cl_2 = 1:1).

General Procedure for Competition Reactions of Rh(ttp)Cl with Various Fluorobenzenes.

A. Competiton Reaction between Fluorobenzene and Hexafluorobenzene with Rh(ttp)Cl. A mixture of Rh(ttp)Cl (20.0 mg, 0.025 mmol), 10 equiv of KOH (13.7 mg, 0.25 mmol), fluorobenzene (0.12 mL, 1.3 mmol) and hexafluorobenzene (0.15 mL, 1.3 mmol) with benzene (1.1 mL, 12.5 mmol) was degassed for three freeze-thaw-pump cycles and heated at 120 °C under N_2 for 1 d. The solvent was then removed by vacuum and the red crude mixture was purified by silica gel column chromatography eluting with a solvent mixture of hexane:CH_2Cl_2 (1:1) to give

$C_6F_5Rh(ttp)$ **9** (12.9 mg, 0.014 mmol, 55%) as a red solid. R_f = 0.28 (hexane:CH_2Cl_2 = 1:1).

B. Competiton Reaction between Fluorobenzene and 1,2-Difluorobenzene with Rh(ttp)Cl. A mixture of Rh(ttp)Cl (20.0 mg, 0.025 mmol), 10 equiv of KOH (13.7 mg, 0.25 mmol), fluorobenzene (0.12 mL, 1.3 mmol) and 1,2-difluorobenzene (0.13mL, 1.3 mmol) with benzene (1.1 mL, 12.5 mmol) was degassed for three freeze-thaw-pump cycles and heated at 120 °C under N_2 for 1 d. The solvent was then removed by vacuum and the red crude mixture was isolated by column chromatography on silica gel eluting with a solvent mixture of hexane:CH_2Cl_2 (1:1) to give (*o*-F)$C_6H_4Rh(ttp)$ **5a** (12.6 mg, 0.015 mmol, 58%) as a red solid. R_f = 0.58 (hexane:CH_2Cl_2 = 1:1).

C. Competiton Reaction between 1,3-Difluorobenzene and 1,2-Difluorobenzene with Rh(ttp)Cl. Rh(ttp)Cl (20.0 mg, 0.025 mmol) and 10 equiv of KOH (13.7 mg, 0.25 mmol), 1,3-difluorobenzene (0.13 mL, 1.3 mmol) and 1,2-difluorobenzene (0.13 mL, 1.3 mmol) with benzene (1.1 mL, 12.5 mmol) were degassed for three freeze-thaw-pump cycles and heated at 120 °C under N_2 for 1 d. The solvent was then removed by vacuum and the residue was purified by silica gel column chromatography eluting with a solvent mixture of hexane: CH_2Cl_2 (1:1) to give (*o*-F)$C_6H_4Rh(ttp)$ **5a** (12.6 mg, 0.015 mmol, 58%) as a red solid. R_f = 0.58 (hexane:CH_2Cl_2 = 1:1).

D. Competiton Reaction between 1,4-Difluorobenzene and 1,2-Difluorobenzene with Rh(ttp)Cl. A mixture of Rh(ttp)Cl (20.0 mg, 0.025 mmol), 10 equiv of KOH (13.7 mg, 0.25 mmol), 1,4-fluorobenzene (0.12 mL, 1.3 mmol) and 1,2-

difluorobenzene (0.13 mL, 1.3 mmol) with benzene (1.1 mL, 12.5 mmol) was degassed for three freeze-thaw-pump cycles and heated at 120 °C under N_2 for 1 d. The solvent was then removed by vacuum and the red crude mixture was purified by silica gel column chromatography eluting with a solvent mixture of hexane:CH_2Cl_2 (1:1) to give (*o*-F)C_6H_4Rh(ttp) **5a** (11.6 mg, 0.013 mmol, 61%) as a red solid. R_f = 0.58 (hexane:CH_2Cl_2 = 1:1).

E. **Competiton Reaction between 1,4-Difluorobenzene and 1,3-Difluorobenzene with Rh(ttp)Cl.** A mixture of Rh(ttp)Cl (20.0 mg, 0.025 mmol), 10 equiv of KOH (13.7 mg, 0.25 mmol), 1,4-difluorobenzene (0.13 mL, 1.3mmol) and 1,3-difluorobenzene (0.13 mL, 1.3 mmol) with benzene (1.1mL, 12.5 mmol) was degassed for three freeze-thaw-pump cycles and heated at 120 °C under N_2 for 1 d. The solvent was then removed by vacuum and the red crude mixture was purified by silica gel column chromatography eluting with a solvent mixture of hexane:CH_2Cl_2 (1:1) to give (*m*-F)C_6H_4Rh(ttp) **6a** (11.5 mg, 0.013 mmol, 51%) as a red solid. R_f = 0.55 (hexane:CH_2Cl_2 = 1:1).

Reaction of 1,4-Difluorobenzene with Rh(ttp)Cl in Sealed NMR Tube Rh(ttp)Cl (7.0 mg, 8 μmol) and 10 equiv of KOH (4.9 mg, 0.08 mmol) and 1,4-fluorobenzene (0.091 mL, 0.8 mmol) and C_6D_6 (0.5 ml) were added to an NMR tube with rotaflo stopper and degassed for three freeze-thaw-pump cycles. The mixtures were frozen under liquid nitrogen and then flame-sealed under vacuum. The sealed tube was heated at 120 °C for 3 d. The reaction was monitored by ^{1}H NMR spectroscopy and the amount of product was calibrated with the internal standard residual benzene in C_6D_6.

Table 3.1. The Amount of Species Involved in the Course of Reaction

Time / h	Rh(ttp)Cl Yield / %	$Rh_2(ttp)_2$ Yield / %	Rh(ttp)˙ Yield / %	**7a** Yield / %
0	100	0	0	0
1	5	66	0	0
2	0	42	38	0
3	0	30	42	0
4	0	20	40	3
15	0	0	30	42
24	0	0	22	45
48	0	0	15	50
72	0	0	5	53

General Procedure for Reactions of Rh(ttp)H with Fluorobenzenes.

A. **Reaction of Fluorobenzene with Rh(ttp)H with KOH.** A suspension of Rh(ttp)H (15.0 mg, 0.019 mmol), 10 equiv of KOH (10.7 mg, 0.19 mmol), fluorobenzene (0.18 mL, 1.9 mmol) in benzene (0.93 mL, 8.5 mmol) was degassed for three freeze-thaw-pump cycles and heated at 120 °C under N_2 for 1 d. The solvent was then removed in vacuum and the red crude mixture was purified by silica gel column chromatography eluting with a solvent of hexane:CH_2Cl_2 (1:1) to give Rh(ttp)Ph **4** (6.9 mg, 8.2 μmol, 43%).

B. **Reaction of Fluorobenzene with Rh(ttp)H.** A suspension of Rh(ttp)H (15.0 mg, 0.019 mmol), fluorobenzene (0.18 mL, 1.9 mmol) in benzene (0.93 mL, 8.5 mmol)

was degassed for three freeze-thaw-pump cycles and heated at 120 °C under N_2 for 1 d. The solvent was then removed in vacuum and the red crude mixture was purified by silica gel column chromatography eluting with a solvent mixture of hexane:CH_2Cl_2 (1:1) to give an unidentified mixture of complexes.

C. **Reaction of 1,4-Difluorobenzene with Rh(ttp)H with KOH.** A solution of Rh(ttp)H (15.0 mg, 0.019 mmol), 10 equiv of KOH (10.7 mg, 0.19 mmol), 1,4-fluorobenzene (0.19 mL, 1.9 mmol) in benzene (0.93 mL, 8.5 mmol) was degassed for three freeze-thaw-pump cycles and heated at 120 °C under N_2 for 1 d. The solvent was then removed in vacuum and the red crude mixture was purified by silica gel column chromatography eluting with a solvent mixture of hexane:CH_2Cl_2 (2:1) to give (*p*-F)C_6H_4Rh(ttp) **7a** (7.1 mg, 6.3 μmol, 33%) as a red solid. R_f = 0.58 (hexane:CH_2Cl_2 = 1:1) and (2,4-F_2)C_6H_3Rh(ttp) **7b** (1.6 mg, 1.7 μmol, 9%) as a red solid. R_f = 0.43 (hexane:CH_2Cl_2 = 1:1).

D. **Reaction of 1,4-Difluorobenzene with Rh(ttp)H.** A solution of Rh(ttp)H (15.0 mg, 0.019 mmol), 1,4-difluorobenzene (0.19 mL, 1.9 mmol) in benzene (0.93 mL, 8.5 mmol) was degassed for three freeze-thaw-pump cycles and heated at 120 °C under N_2 for 1 d. The solvent was then removed in vacuum and the red crude mixture was purified by silica gel column chromatography eluting with a mixture of hexane: CH_2Cl_2 (1:1) to give an unidentified mixture of complexes..

General Procedure for Reactions of Rh(ttp)R with Fluorobenzene.

A. **Reaction of benzene with Rh(ttp)Me with KOH.** A suspension of Rh(ttp)Me (15.0 mg, 0.019 mmol), 10 equiv of KOH (10.7 mg, 0.19 mmol) and benzene (1 mL) was degassed for three freeze-thaw-pump cycles and heated at 120 °C under N_2 for 4 d.

The solvent was then removed in vacuum and the red crude mixture was purified by silica gel column chromatography eluting with a mixture of hexane:CH_2Cl_2 (1:1) to recover Rh(ttp)Me (11.6 mg, 0.015 mmol, 78%).

B. **Reaction of Fluorobenzene with Rh(ttp)Me with KOH.** A suspension of Rh(ttp)Me (15.0 mg, 0.019 mmol) and 10 equiv of KOH (10.7 mg, 0.19 mmol) and fluorobenzene (0.18 mL, 1.9 mmol) in benzene (1 mL) was degassed for three freeze-thaw-pump cycles and heated at 120 °C under N_2 for 4 d. The solvent was then removed by vacuum and the red crude mixture was purified by silica gel column chromatography eluting with a mixture of hexane:CH_2Cl_2 (1:1) to recover Rh(ttp)Me (9.9 mg, 0.013 mmol, 66%) and give Rh(ttp)Ph **4** (1.5 mg, 0.001 mmol, 10%).

C. **Reaction of Benzene with Rh(ttp)$SiEt_3$ with KOH.** A mixture of Rh(ttp)$SiEt_3$ (15.0 mg, 0.017 mmol), 10 equiv of KOH (9.6 mg, 0.17 mmol) and benzene (1 mL) was degassed for three freeze-thaw-pump cycles and heated at 120 °C under N_2 for 4 d. The solvent was then removed by vacuum and the red crude mixture was purified by silica gel column chromatography eluting with a mixture of hexane:CH_2Cl_2 (1:1) to give unreacted Rh(ttp)$SiEt_3$ (10.4 mg, 0.012 mmol, 69%).

D. **Reaction of Fluorobenzene with Rh(ttp)$SiEt_3$ with KOH** A mixture of Rh(ttp)$SiEt_3$ (15.0 mg, 0.017 mmol) and 10 equiv of KOH (9.6 mg, 0.17 mmol) and fluorobenzene (0.17 mL, 1.7 mmol) in benzene (1 mL) were degassed for three freeze-thaw-pump cycles and heated at 120 °C under N_2 for 4 d. The solvent was then removed by vacuum and the red crude mixture was purified by silica gel column chromatography eluting with a mixture of hexane:CH_2Cl_2 (1:1) to give Rh(ttp)Ph **4** (6.0 mg, 7 μmol, 40%) and (*o*-F)C_6H_4Rh(ttp) **5a** (2.7 mg, 3 μmol, 18%).

Reactions of Rh(ttp)Cl with Fluorobenzene/Fluorobenzene-d_5 (1:1 molar ratio).

Rh(ttp)Cl (20.0 mg, 0.025 mmol) and KOH (14.0 mg, 0.25 mmol) were added to a premixed equimolar solvent mixture of fluorobenzene/ fluorobenzene-d_5 (1.0 mL) and then the suspension was degassed for three freeze-thaw-pump cycles in the rotaflo tube. The reaction mixture was heated to 120 °C under N_2 for 1 d and two red solids were purified by chromatography on silica gel eluting with a solvent mixture of hexane: CH_2Cl_2 (1:1) to give the mixtures of CFA products, R_f = 0.63 (hexane:CH_2Cl_2 = 1:1), $C_6H_5Rh(ttp)$ **4** (6.3 mg, 7 μmol, 20% NMR yield) and $C_6D_5Rh(ttp)$ **4-d_5** (6.3 mg, 7 μmol, 20% NMR yield) were collected in one portion. Two CHA products, (*o*-F)$C_6H_4Rh(ttp)$ **5a** (3.7 mg, 4 μmol, 17% NMR yield) and (*o*-F)$C_6H_4Rh(ttp)$ **5a-d_5** (0.9 mg, 1 μmol, 4% NMR yield) were collected in another portion.

The isotope effect was calculated as follow:

Integration of the aromatic protons (observed = 0.81) were used to calculate the ratio with the integration of pyrrole signal (δ = 8.78) was taken as 8.00. Let the integration of aromatic deuterium to be y.

y = Integration of aromatic proton without deuterium incorporation

– Observed integration of aromatic proton with deuterium incorporation

= 1 – 0.81

k_H/k_D = Integration of aromatic proton/ Integration of aromatic deuterium

= 0.81 / (1 - 0.81)

= 4.26

Reactions of Rh(ttp)H with Fluorobenzene/Fluorobenzene-d_5 (1:1 molar ratio).

The same procedure was followed to the case of Rh(ttp)Cl. The mixtures of CFA products, R_f = 0.63 (hexane:CH_2Cl_2 = 1:1), $C_6H_5Rh(ttp)$ **4** (4.2 mg, 5 μmol, 19% NMR yield) and R $C_6D_5Rh(ttp)$ **4-d_5** (4.2 mg, 5 μmol, 19% NMR yield) were collected in one portion. Two CHA products, (*o*-F)$C_6H_4Rh(ttp)$ **5a** (3.3 mg, 4 μmol, 15% NMR yield) and (*o*-F)$C_6H_4Rh(ttp)$ **5a-d_5** (0.9 mg, 1 μmol, 4% NMR yield) were collected in another portion.

The isotope effect was calculated as follow:

Integration of aromatic protons (observed = 0.79) were used to calculate the ratio with the integration of pyrrole signal (δ = 8.78) was taken as 8.00. Let the integration of aromatic deuterium to be y.

y = Integration of aromatic proton without deuterium incorporation

– Observed integration of aromatic proton with deuterium incorporation

= 1 – 0.79

k_H/k_D = Integration of aromatic proton/ Integration of aromatic deuterium

= 0.79 / (1-0.79)

= 3.76

General Procedure for Reactions of Rh(ttp)R with Fluorobenzene.

A. Reaction of (2,5-F_2)$C_6H_3Rh(ttp)$ 7b with KOH in Benzene A mixture of (2,4-F_2)$C_6H_3Rh(ttp)$ **7b** (15.0 mg, 0.017 mmol), 10 equiv of KOH (9.5 mg, 0.17 mmol) and benzene (1 mL) was degassed for three freeze-thaw-pump cycles and heated at 200 °C under N_2 for 4 d . The solvent was then removed by vacuum and the red crude

mixture was purified by silica gel column chromatography eluting with a mixture of hexane: CH_2Cl_2 (1:1) to recover $(2,5\text{-}F_2)C_6H_3Rh(ttp)$ **7b** (12.2 mg, 0.014 mmol, 81%).

B. **Reaction of Benzene with $(2,5\text{-}F_2)C_6H_3Rh(ttp)$ 7b** A mixture of $(2,4\text{-}F_2)C_6H_3Rh(ttp)$ **7b** (15.0 mg, 0.017 mmol) in benzene (1 mL) was degassed for three freeze-thaw-pump cycles and heated at 200 °C under N_2 for 3 d. The solvent was then removed by vacuum and the red crude mixture was purified by silica gel column chromatography eluting with a mixture of hexane: CH_2Cl_2 (1:1) to recover $(2,5\text{-}F_2)C_6H_3Rh(ttp)$ **7b** (11.9 mg, 0.013 mmol, 79%).

C. **Reaction of Fluorobenzene with $(2,5\text{-}F_2)C_6H_3Rh(ttp)$ 7b with KOH** A solution of $(2,5\text{-}F_2)C_6H_3Rh(ttp)$ **7b** (15.0 mg, 0.017 mmol) and 10 equiv of KOH (9.5 mg, 0.17 mmol0 and 1,4-difluorobenzene (0.19 mL, 1.7 mmol) in benzene (1 mL) was degassed for three freeze-thaw-pump cycles and heated at 200 °C under N_2 for 4 d. The solvent was then removed by vacuum and the red crude mixture was purified by silica gel column chromatography eluting with a mixture of hexane: CH_2Cl_2 (1:1) to recover $(2,5\text{-}F_2)C_6H_3Rh(ttp)$ **7b** (9.2 mg, 0.010 mmol, 61%) and $(p\text{-}F)C_6H_4Rh(ttp)$ **7a** (2.9 mg, 3 μmol, 20%).

D. **Reaction of Fluorobenzene with $(2,5\text{-}F_2)C_6H_3Rh(ttp)$ 7b** $(2,5\text{-}F_2)C_6H_3Rh(ttp)$ **7b** (15.0 mg, 0.017 mmol) and 1,4-difluorobenzene (0.19 mL, 1.7 mmol) in benzene(1 mL) was degassed for three freeze-thaw-pump cycles and heated at 200 °C under N_2 for 4 d. The solvent was then removed by vacuum and the red crude mixture was purified by silica gel column chromatography eluting with a solvent mixture of hexane: CH_2Cl_2 (1:1) to recover $(2,4\text{-}F_2)C_6H_3Rh(ttp)$ **7b** (8.3 mg, 0.014 mmol, 82%).

Reaction of (2,4-F_2)C_6H_3Rh(ttp) 7b with Hexafluorobenzene with KOH. A mixture of (2,4-$F_2C_6H_3$)Rh(ttp) **7b** (15.0 mg, 0.017 mmol), 10 equiv of KOH (9.5 mg, 0.17 mmol) and hexafluorobenzene (0.97 mL, 8.5 mmol) was degassed for three freeze-thaw-pump cycles and heated at 200 °C under N_2 for 4 d. The solvent was then removed by vacuum and the red crude mixture was purified by silica gel column chromatography eluting with a mixture of hexane:CH_2Cl_2 (1:1) to give C_6F_5Rh(ttp)C_6F_5 **9** (3.7 mg, 40 μmol, 23%) and recovered (2,4-F_2)C_6H_3Rh(ttp) **7b** (9.9 mg, 0.011 mmol, 66%).

References:

1. Campeau, L. C.; Parisien, M.; Jean, A.; Fagnou, K. *J. Am. Chem. Soc.* **2006**, *128*, 581-590.
2. Terao, J.; Nii, S.: Chowdhury, F. A.; Nakamura, A.; Kambe, N. *Adv. Synth. Catal.* **2004**, *346*, 905-908.
3. Mongin, F.; Mojovic, L.; Guillamet, B.; Trécourt, F.; Quéguiner, G. *J. Org. Chem.* **2002**, *67*, 8991-8994.
4. Ackermann, L.; Born, R.; Spatz, J. H.; Meyer, D. *Angew. Chem., Int. Ed.* **2005**, *44*, 7216-7219
5. Schaub, T.; Backes, M.; Radius, U. *J. Am. Chem. Soc*, **2006**, *128*, 15964-15965.
6. (a) Jaonwicz, A. H.; Bergman, R. G. *J. Am. Chem. Soc.* **1983**, *105*, 3929-3939. (b) Hoyano, J. K.; Graham, W. A. G. *J. Am. Chem. Soc.* **1982**, *104*, 3723-3725.
7. Janowicz, A. H.; Bergman, R. G. *J. Am. Chem. Soc.* **1982**, *104*, 352-354.
8. Edelbach, B. L.; Fazlur Rahman, A. K.; Lachicotte, R. J.; Jones, W. D. *Organometallics* **1999**, *18*, 3170-3177.
9. Olah, G. A. *Acc. Chem. Res.* **1971**, *4*, 240-248.
10. Li, Z.; Capretto, D. A.; Rahaman, R. O.; He, C. *J. Am. Chem. Soc.* **2007**, *129*, 12058-12059.
11. (a) Kochi, J. *Organometallics Mechanisms and Catalysis*; Academic press, New York, 1978, Chapter 7.

    (b) Anslyn, E. V.; Dougherty, D. A. *Modern Physical Organic Chemistry*; University Science Books, 2006.

12. Kim, Y. M.; Yu, S. *J. Am. Chem. Soc.* **2003**, *125*, 1696-1697.

13. Chan, P. K.; Leong, W. K. *Organometallics* **2008**, *27*, 1247-1253.

14. Halpern, J.; Maher, J. P. *J. Am. Chem. Soc.* **1965**, *87*, 5361-5366.

15. Alonso, F.; Beletskaya, I. P.; Yus, M. *Chem. Rev.* **2002**, *102*, 4009-4092.

16. Adams, C. S.; Legzdins, P.; Tran, E. *J. Am. Chem. Soc.* **2001**, *123*, 612-624.

17. Doherty, N. M; Hoffman, N. W. *Chem. Rev.* **1991**, *91*, 553-573.

18. Crabtree, R. H. *J. Chem. Soc., Dalton Trans.* **2001**, 2427-2440.

19. Mann, J. B.; Meek, T. L.; Allen, L. C. *J. Am. Chem. Soc.* **2000**, *122*, 2780-2786.

20. Kilawiec, R. J.; Crabtree, R. H. *Chem. Rev.* **1990**, *99*, 89-115.

21. Strauss, S. H. *Chem. Rev.* **1993**, *93*, 927-942.

22. Labinger, J. A.; Bercaw, J. E. *Nature* **2002**, *417*, 507-514.

23. (a) Smart, B. E. *Mol. Struct. Energ.* **1986**, *3*, 141-191. (b) Luo, Y. R. *Handbook of Bond Dissociation Energies in Organic Compounds*; CRC press: Boca Raton, Florida, **2003**.

24. Simóes, J. A. M.; Beauchamp, J. L. *Chem Rev.* **1990**, *90*, 629-688.

25. Maron, L.; Werkema, E. L.; Perrin, L.; Eisenstein, O.; Andersen, R. A. *J. Am. Chem. Soc.* **2005**, *127*, 279-292.

26. Büker, H. H.; Nibbering, N. M. M.; Espinosa, D.; Schlosser, M. *Tetrahedron Lett.* **1997**, *38*, 8519-8522.

27. Collman, J. P.; Hegedus, L. S. *Principles and Applications of Organotransition Metal Chemistry*; 2nd Ed.; University Science Books: Mill Valley, CA, 1987, Chapter 5.

28. Kiplinger, J. L.; Richmond, T. G.; Osterberg, C. E. *Chem. Rev.* **1994**, *94*, 373-431.

29. Torrens, H. *Coord. Chem. Rev.* **2005**, *249*, 1957-1985.

30. Kiso, Y.; Tamo, K.; Kumada, M. *J. Organomet. Chem.* **1973**, *50*, 12-14.

31. Bruce, M. L.; Gardner, R. C. F.; Stone, F. G. A. *J. Chem. Soc., Dalton Trans.* **1976**, 81-89.

32. Richmond, T. G.; Osterberg, C. E.; Arif, A. M. *J. Am. Chem. Soc.* **1987**, *109*, 8091-8092.

33. Kulawiec, R. J.; Holt, E. M.; Lavin, M.; Crabtree, R. H. *Inorg. Chem.* **1987**, *26*, 2559-2561.

34. Blum, O.; Frolow, F.; Milstein, D. *J. Chem. Soc. Chem. Commun.* **1991**, 258-259.

35. (a) Edelbach, B. L.; Jones, W. D. *J. Am. Chem. Soc.* **1997**, *179*, 7734-7740. (b) Edelbach, B. L.; Kraft, B. M.; Jones, W. D. *J. Am. Chem. Soc.* **1999**, *121*, 10327-10331

36. Braun, T.; Noveski, D.; Neumann, B.; Stammler, H. G. *Angew. Chem., Int. Ed.* **2002**, *41*, 2745-2748.

37. Peterson, A. A.; McNeill, K. *Organometallics* **2006**, *25*, 4938-4940.

38. Aizenberg, M.; Milstein, D. *Science* **1994**, *265*, 359-361.

39. Shilov, A. E.; Shul'pin, G. B. *Chem. Rev.* **1997**, *97*, 2879-2932.

40. Jones, W. D.; Feher, F. J. *J. Am. Chem. Soc.* **1984**, *106*, 1650-1663.

41. Aoyama, Y.; Yoshida, T.; Sakurai, K. I.; Ogoshi, H. *Organometallics* **1986**, *5*, 168-173.

42. Schaller, C. P.; Cummins, C. C.; Wolczanski, P. T. *J. Am. Chem. Soc.* **1996**, *118*, 591-611.

43. Kakiuchi, F.; Kan, S.; Igi, K.; Chatani, N.; Murai, S. *J. Am. Chem. Soc.* **2003**, *125*, 1698-1699.

44. Ben-Ari, E.; Gandelman, M.; Rozenberg, H.; Shimon, L. J. W.; Milstein, D. *J. Am. Chem. Soc.* **2003**, *125*, 4714-4715.

45. Zhang, X.; Kanzelberger, M.; Emge, T. J.; Goldman, A. S. *J. Am. Chem. Soc.* **2004**, *126*, 13192-13193.

46. Fan, L.; Parlin, S.; Ozerov, O. V. *J. Am. Chem. Soc.* **2005**, *127*, 16772-16773.

47. Tsang, J. Y. K.; Buschhaus, M. S. A.; Legzdins, P.; Patrick, B. O. *Organometallics* **2006**, *25*, 4215-4225.

48. Barrio, P.; Castarlenas, R.; Esteruelas, M. A.; Lledos, A.; Maseras, F.; Onate, E.; Tomas, J. *Organometallics* **2001**, *20*, 442-452.

49. Reinhold, M; McGrady, J. E.; Perutz, R. N. *J. Am. Chem. Soc.* **2004**, *126*, 5268-5276.

50. (a) Fleischer, E. B. *Acc. Chem. Res.* **1970**, *3*, 105-112. (b) *The Porphyrin Handbook Volume 3*; Kadish, K. M., Smith, K. M., Guilard, R., Eds.; Academic Press: Boston, **2000**. (c) *Porphyrin and Metalloporphyrins*; Smith, K. M., Ed.; Elsevier Scienticfic Pub. Co.: New York, **1975**. (d) Ogoshi, H.; Mizutani, A. *Acc. Chem. Res.* **1998**, *31*, 81-89.

51. Wayland, B. B.; Balkus, K. J. J.; Farnos,M. D. *Organometallics* **1989**, *8*, 950-953.

52. (a) Zhou, X.; Li, Q.; Mak, T. C. W.; Chan, K. S. *Inorg. Chim. Acta* **1998**, *270*, 551-554. (b) Zhou, X.; Wang, R-J.; Xue, F.; Mak, T. C. W.; Chan, K. S. *J. Organomet. Chem.* **1999**, *580*, 22-25. (c) Zhou, X.; Tse, M. K.; Wu, D-D.; Mak, T. C. W.; Chan, K. S. *J. Organomet. Chem.* **2000**, *598*, 80-86.

53. Chui, P. F. *M. Phil. Thesis* **2006**, The Chinese University of Hong Kong.

54. Chan. K. S.; Chen, X. M.; Mak, T. C. W. *Polyhedron* **1992**, *11*, 2703-2716.

55. Borwell, F. G. *Acc. Chem. Res.* **1988**, *21*, 456-463.

56. Cheung, C. W.; Chan, K. S. *Organometallics* **2008**, 27, 3043-3055.

57. Pretsch, E.; Seibl, J.; Clerc, T.; Biemann, K.; *Tables of Spectral Data for Structure Determination of Organic Compounds*, 2nd Ed; Springer-Verlag, **1989**.

58. Chan, K. S.; Lau, C. M.; Yeung, S. K.; Lai, T. H. *Organometallics* **2007**, *26*, 1981-1985.

59. Segura, P.; *J. Org. Chem.* **1985**, *50*, 1045-1053.

60. (a) Crabtree, R. H. *Chem. Rev.* **1985,** *85*, 245-269. (b) Crabtree, R. H. *J. Chem. Soc. Dalton Trans.* **2001**, 2437-2450.

61. Nelson, A. P.; DiMagno, S. G. *J. Am. Chem. Soc.* **2000**, *122*, 8569-8570.

62. Wayland, B. B.; Van Voorhees, S. L.; Wilker, C. *Inorg. Chem.* **1986**, *25*, 4039-4042.

63. Bondi, A. *J. Phys. Chem.* **1964**, *68*, 441-451.

64. Belkova, N. V.; Gutsul, E. I.; Filippov, O. A.; Levina, V. A.; Valyaev, D. A.; Epstein, L. M.; Lledos, A.; Shubina, E. S. *J. Am. Chem. Soc.* **2006**, 128, 3486-3487.

65. Thalladi, V. R.; Weiss, H.-C.; Blaser, D.; Boese, R.; Nangia, A.; Desiraju, G. R. *J. Am. Chem. Soc.* **1998**, *120*, 8702-8710.

66. Brown, H. C.; Kanner, B. *J. Am. Chem. Soc*, **1966**, *88*, 986-992.

67. Mooney, E. F. *An introduction to ^{19}F NMR spectroscopy*; Heyden, in co-operation with Sadtler Research Laboratories, **1970**.

68. Fung, H. S. *Undergraduate Thesis* **2007**, The Chinese University of Hong Kong.

69. Zhang, L.; Chan, K. S. *Organometallics* **2006**, 25, 4822-4829.

Table of Content of Appendix

Appendix I

Crystal Data Collection and Processing Parameters of Complex 5a

(*o*-F)C_6H_4Rh(ttp) 5a

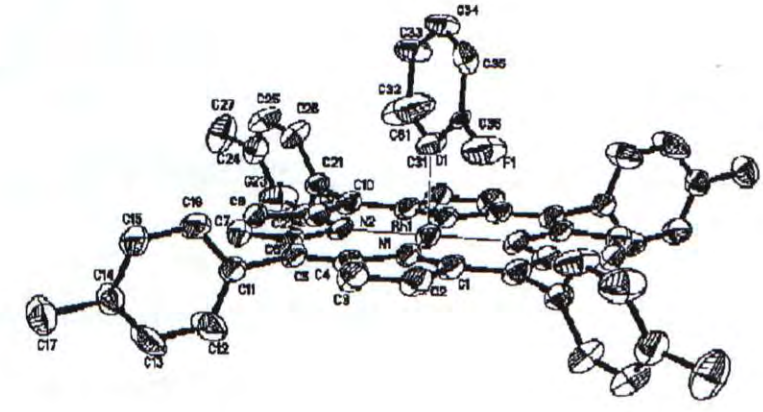

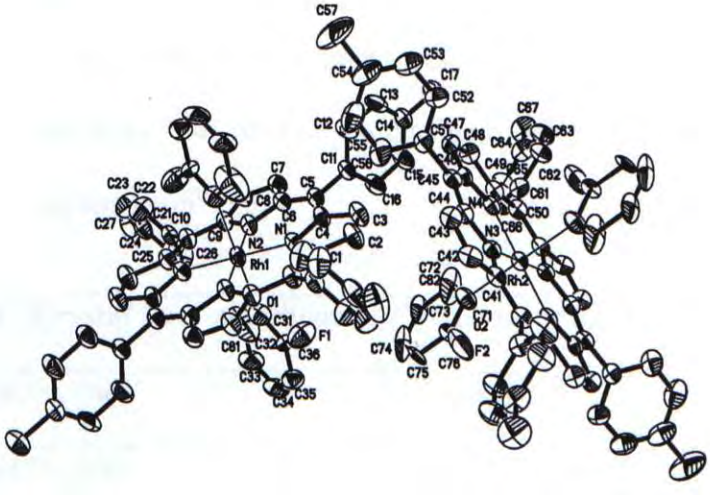

Figure 3a. ORTEP of complex Rh(ttp)(C_6H_4)(*o*-F) **5a**, showing the atomic labeling scheme and 30 % probability displacement ellipsoids.

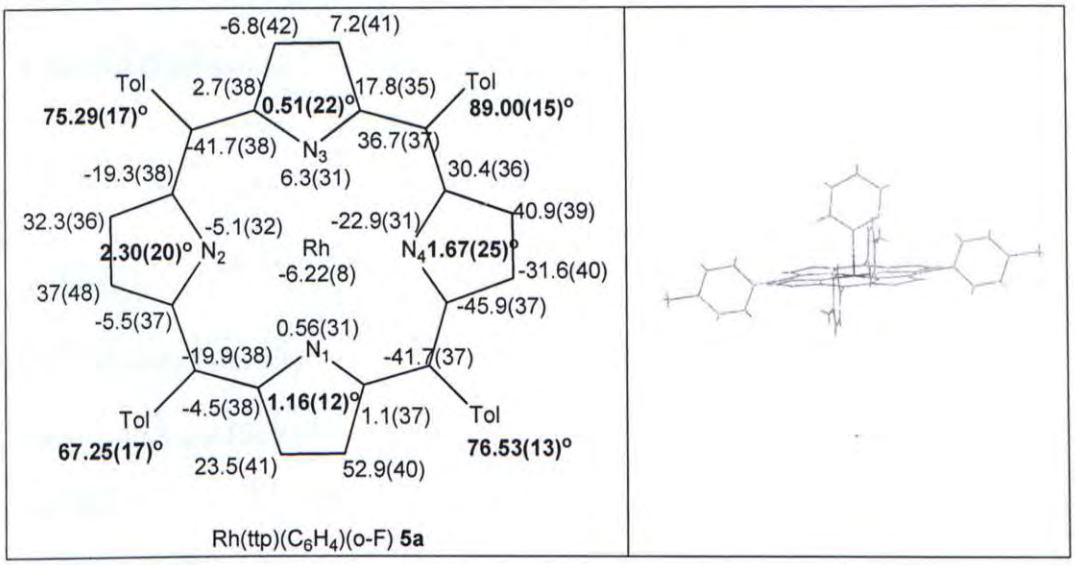

Figure 3b. The conformations of porphyrins in, **5a,** showing the displacement of the core atoms and of Rh from the 24-atom least squares plane of porphyrin core (in pm; negative values correspond to displacement towards the benzyl or phenyl ligands). Absolute values of the angles between pyrrole rings and least-squares plane and angles between tolyl substituents and the least-squares plane are shown in bold.

Table 3.1. Crystal Data and Structure Refinement for 5a	
Identification code	MHL168a
Empirical formula	C_{55} H_{44} F N_4 Rh
Formula weight	898.85
Temperature	293(2) K

Wavelength	0.71073 Å
Crystal system, space group	Triclinic, P1
Unit cell dimensions	a = 11.294(4) Å alpha = 112.69 (3)° b = 12.184(4) Å beta = 94.35(3)° c = 18.827(6) Å gamma = 107.37 (3)°
Volume	2310 (13) $Å^3$
Z, Calculated density	2, 1.292 Mg/m^3
Absorption coefficient	0.417 mm^{-1}
F(000)	928
Crystal size	0.40 x 0.30 x 0.30 mm
Theta range for data collection	1.79 to 25.00°
Limiting indices	-13<=h<=13, 14<=k<=11, -22<=l<=22
Reflections collected / unique	12564 / 8099 [R(int) = 0.0431]
Completeness to theta	99.4.9 %
Absorption correction	ABSCOR
Max. and min. transmission	1.000 and 0.097552
Refinement method	Full-matrix least-squares on F^2
Data / restraints / parameters	8099 / 15 / 607
Goodness-of-fit on F^2	1.129
Final R indices [I>2sigma(I)]	R1 = 0.0826, wR2 = 0.2095
R indices (all data)	R1 = 0.11921, wR2 = 0.2332
Largest diff. peak and hole	0.961 and -0.786 $e.Å^{-3}$

Table 3.2. Bond Lengths [Å] and Angles [deg] for 5a

Rh(1)-N(2)	2.012(7)	C(24)-C(25)	1.358(15)
Rh(1)-N(1)	2.023(7)	C(24)-C(27)	1.525(15)
Rh(1)-C(31)	2.179(7)	C(25)-C(26)	1.322(14)
Rh(2)-N(4)	2.022(6)	C(31)-C(36)	1.346(9)
Rh(2)-N(3)	2.026(6)	C(31)-C(32)	1.401(10)
Rh(2)-C(71)	2.180(7)	C(32)-C(33)	1.375(10)
N(1)-C(1)	1.365(12)	C(33)-C(34)	1.366(10)
N(1)-C(4)	1.382(10)	C(34)-C(35)	1.367(10)
N(2)-C(9)	1.381(11)	C(35)-C(36)	1.363(9)
N(2)-C(6)	1.382(10)	C(36)-F(1)	1.280(17)
N(3)-C(44)	1.360(10)	C(41)-C(42)	1.420(11)
N(3)-C(41)	1.372(9)	C(42)-C(43)	1.319(12)
N(4)-C(46)	1.364(9)	C(43)-C(44)	1.443(10)
N(4)-C(49)	1.397(9)	C(44)-C(45)	1.382(11)
C(1)-C(2)	1.475(12)	C(45)-C(46)	1.393(10)
C(2)-C(3)	1.336(13)	C(45)-C(51)	1.492(11)
C(3)-C(4)	1.454(12)	C(46)-C(47)	1.429(11)
C(4)-C(5)	1.384(12)	C(47)-C(48)	1.359(11)
C(5)-C(6)	1.387(12)	C(48)-C(49)	1.424(12)
C(5)-C(11)	1.482(11)	C(49)-C(50)	1.377(11)
C(6)-C(7)	1.415(13)	C(50)-C(61)	1.504(11)
C(7)-C(8)	1.361(12)	C(51)-C(52)	1.366(12)
C(8)-C(9)	1.443(12)	C(51)-C(56)	1.408(13)
C(9)-C(10)	1.405(11)	C(52)-C(53)	1.372(14)
C(10)-C(21)	1.475(12)	C(53)-C(54)	1.364(18)
C(11)-C(12)	1.339(13)	C(54)-C(55)	1.342(18)
C(11)-C(16)	1.351(12)	C(54)-C(57)	1.552(15)
C(12)-C(13)	1.401(14)	C(55)-C(56)	1.400(14)
C(13)-C(14)	1.320(15)	C(61)-C(62)	1.364(12)
C(14)-C(15)	1.325(13)	C(61)-C(66)	1.399(12)
C(14)-C(17)	1.499(13)	C(62)-C(63)	1.393(13)
C(15)-C(16)	1.396(13)	C(63)-C(64)	1.372(15)
C(21)-C(22)	1.353(14)	C(64)-C(65)	1.351(14)
C(21)-C(26)	1.383(12)	C(64)-C(67)	1.495(13)
C(22)-C(23)	1.368(16)	C(65)-C(66)	1.368(13)
C(23)-C(24)	1.390(16)	C(71)-C(76)	1.360(8)
C(71)-C(72)	1.407(9)	C(74)-C(75)	1.361(10)
C(72)-C(73)	1.371(9)	C(75)-C(76)	1.363(9)
C(73)-C(74)	1.359(10)	C(76)-F(2)	1.16(2)
N(2)-Rh(1)-N(1)	90.3(3)	N(2)-C(9)-C(8)	109.7(7)

N(2)-Rh(1)-C(31)	90.2(3)	C(10)-C(9)-C(8)	124.1(8)
N(1)-Rh(1)-C(31)	91.7(3)	C(9)-C(10)-C(21)	117.6(8)
N(4)-Rh(2)-N(3)	89.1(2)	C(12)-C(11)-C(16)	116.3(9)
N(4)-Rh(2)-C(71)	89.2(3)	C(12)-C(11)-C(5)	121.1(8)
N(3)-Rh(2)-C(71)	91.0(2)	C(16)-C(11)-C(5)	122.5(8)
C(1)-N(1)-C(4)	107.3(7)	C(11)-C(12)-C(13)	120.8(10)
C(1)-N(1)-Rh(1)	126.4(6)	C(14)-C(13)-C(12)	122.9(10)
C(4)-N(1)-Rh(1)	126.2(6)	C(13)-C(14)-C(15)	116.5(9)
C(9)-N(2)-C(6)	106.3(7)	C(13)-C(14)-C(17)	122.3(10)
C(9)-N(2)-Rh(1)	127.2(5)	C(15)-C(14)-C(17)	121.1(10)
C(6)-N(2)-Rh(1)	126.4(6)	C(14)-C(15)-C(16)	122.1(10)
C(44)-N(3)-C(41)	106.9(6)	C(11)-C(16)-C(15)	121.4(9)
C(44)-N(3)-Rh(2)	127.0(5)	C(22)-C(21)-C(26)	116.0(9)
C(41)-N(3)-Rh(2)	126.1(5)	C(22)-C(21)-C(10)	123.3(8)
C(46)-N(4)-C(49)	106.7(7)	C(26)-C(21)-C(10)	120.7(9)
C(46)-N(4)-Rh(2)	127.6(5)	C(21)-C(22)-C(23)	122.2(11)
C(49)-N(4)-Rh(2)	125.6(5)	C(22)-C(23)-C(24)	121.0(12)
N(1)-C(1)-C(2)	109.0(8)	C(25)-C(24)-C(23)	115.1(10)
C(3)-C(2)-C(1)	106.8(9)	C(25)-C(24)-C(27)	124.2(11)
C(2)-C(3)-C(4)	108.0(8)	C(23)-C(24)-C(27)	120.6(13)
N(1)-C(4)-C(5)	126.1(8)	C(26)-C(25)-C(24)	123.9(10)
N(1)-C(4)-C(3)	108.8(8)	C(25)-C(26)-C(21)	121.6(11)
C(5)-C(4)-C(3)	125.1(8)	C(36)-C(31)-C(32)	118.8(11)
C(4)-C(5)-C(6)	124.8(8)	C(36)-C(31)-Rh(1)	123.5(7)
C(4)-C(5)-C(11)	117.5(8)	C(32)-C(31)-Rh(1)	117.2(8)
C(6)-C(5)-C(11)	117.7(8)	C(33)-C(32)-C(31)	122.9(16)
N(2)-C(6)-C(5)	126.0(8)	C(34)-C(33)-C(32)	116.3(19)
N(2)-C(6)-C(7)	109.4(8)	C(33)-C(34)-C(35)	120.8(18)
C(5)-C(6)-C(7)	124.6(8)	C(36)-C(35)-C(34)	122.4(16)
C(8)-C(7)-C(6)	108.6(8)	F(1)-C(36)-C(31)	120.6(11)
C(7)-C(8)-C(9)	106.0(8)	F(1)-C(36)-C(35)	120.7(13)
N(2)-C(9)-C(10)	126.2(8)	C(31)-C(36)-C(35)	118.7(12)
N(3)-C(41)-C(42)	108.9(7)	C(55)-C(54)-C(57)	120.2(15)
C(43)-C(42)-C(41)	108.2(8)	C(53)-C(54)-C(57)	121.2(14)
C(42)-C(43)-C(44)	107.4(8)	C(54)-C(55)-C(56)	121.3(12)
N(3)-C(44)-C(45)	126.5(7)	C(55)-C(56)-C(51)	119.3(11)
N(3)-C(44)-C(43)	108.6(7)	C(62)-C(61)-C(66)	117.9(8)
C(45)-C(44)-C(43)	124.9(7)	C(62)-C(61)-C(50)	120.4(8)
C(44)-C(45)-C(46)	124.3(7)	C(66)-C(61)-C(50)	121.7(8)
C(44)-C(45)-C(51)	117.2(7)	C(61)-C(62)-C(63)	120.6(9)
C(46)-C(45)-C(51)	118.5(8)	C(64)-C(63)-C(62)	121.5(9)
N(4)-C(46)-C(45)	125.5(7)	C(65)-C(64)-C(63)	117.1(9)
N(4)-C(46)-C(47)	109.5(7)	C(65)-C(64)-C(67)	123.0(11)
C(45)-C(46)-C(47)	125.0(7)	C(63)-C(64)-C(67)	119.8(11)
C(48)-C(47)-C(46)	107.5(7)	C(64)-C(65)-C(66)	123.2(10)

C(47)-C(48)-C(49)	107.4(7)	C(65)-C(66)-C(61)	119.7(9)
C(50)-C(49)-N(4)	125.6(8)	C(76)-C(71)-C(72)	119.9(9)
C(50)-C(49)-C(48)	125.7(8)	C(76)-C(71)-Rh(2)	123.9(7)
N(4)-C(49)-C(48)	108.8(7)	C(72)-C(71)-Rh(2)	116.2(6)
C(49)-C(50)-C(61)	118.1(8)	C(73)-C(72)-C(71)	116.7(15)
C(52)-C(51)-C(56)	118.5(9)	C(74)-C(73)-C(72)	123(2)
C(52)-C(51)-C(45)	121.6(8)	C(73)-C(74)-C(75)	119(2)
C(56)-C(51)-C(45)	119.9(8)	C(74)-C(75)-C(76)	119.6(16)
C(51)-C(52)-C(53)	119.8(11)	F(2)-C(76)-C(71)	121.9(12)
C(54)-C(53)-C(52)	122.6(12)	F(2)-C(76)-C(75)	116.6(13)
C(55)-C(54)-C(53)	118.6(11)	C(71)-C(76)-C(75)	121.5(11)

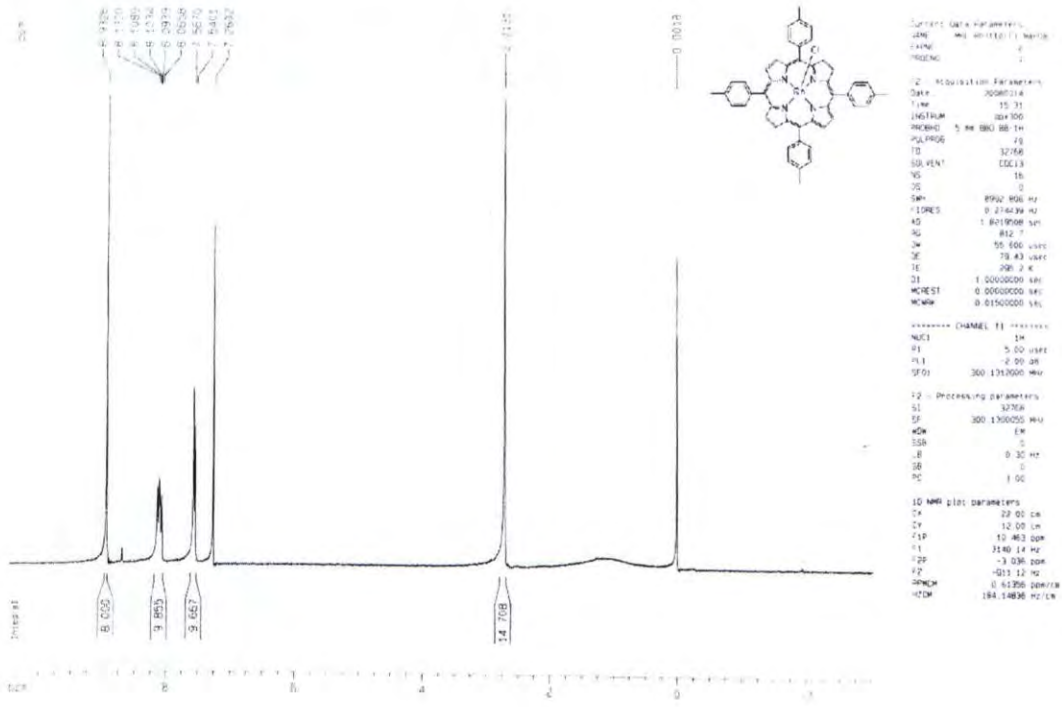

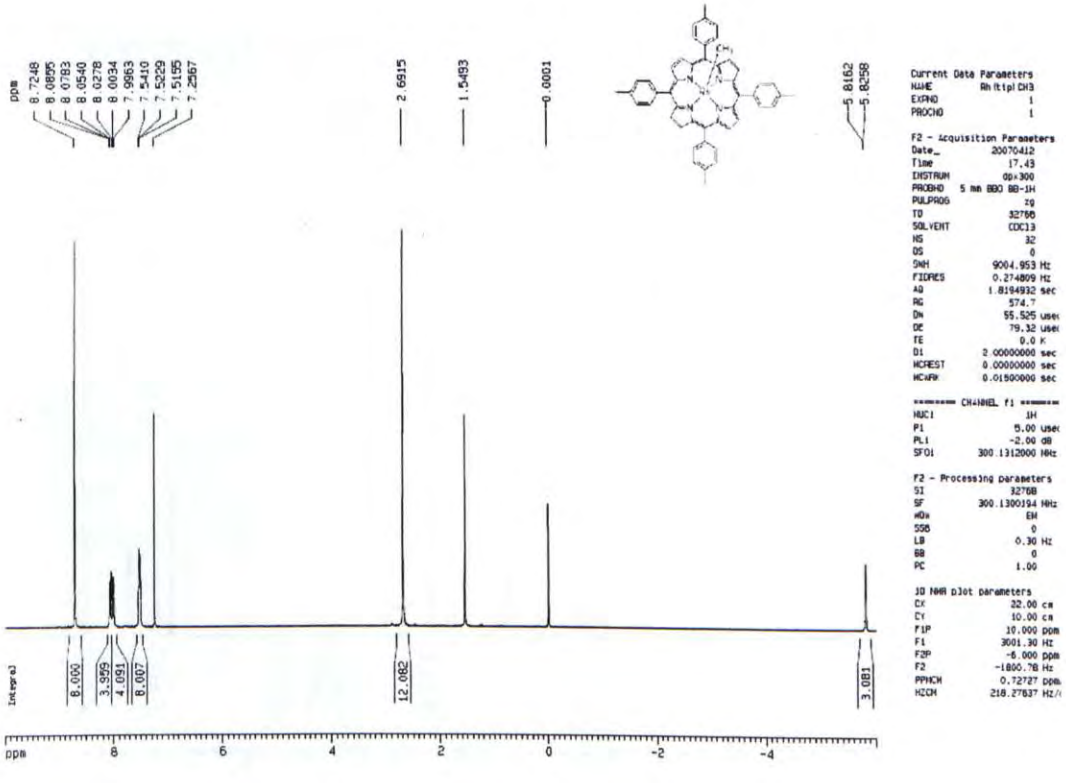

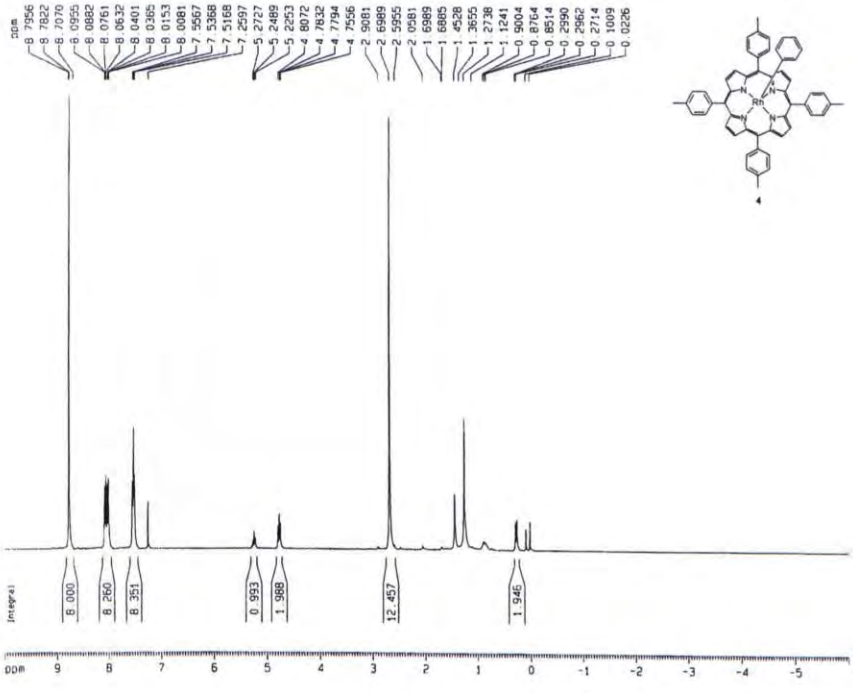


```
Current Data Parameters
NAME                  MHL 51 a
EXPNO                        1
PROCNO                       1

F2 - Acquisition Parameters
Date_               20060905
Time                   13.38
INSTRUM                dpx300
PROBHD  5 mm BBO BB-1H
PULPROG                   zg
TD                       32768
SOLVENT                CDCl3
NS                          32
DS                           0
SWH                 8992.806 Hz
FIDRES              0.274439 Hz
AQ                  1.8219508 sec
RG                       90.5
DW                    55.600 usec
DE                    79.43 usec
TE                       0.0 K
D1                  1.00000000 sec
MCREST              0.00000000 sec
MCWRK               0.01500000 sec

======== CHANNEL f1 ========
NUC1                       1H
P1                      5.00 usec
PL1                     -2.00 dB
SFO1              300.1312000 MHz

F2 - Processing parameters
SI                       32768
SF                300.1300068 MHz
WDW                        EM
SSB                         0
LB                       0.30 Hz
GB                          0
PC                       1.00

1D NMR plot parameters
CX                      22.00 cm
CY                      12.00 cm
F1P                   10.000 ppm
F1                   3001.30 Hz
F2P                   -6.000 ppm
F2                  -1800.78 Hz
PPMCM                0.72727 ppm/cm
HZCM                218.27637 Hz/cm
```

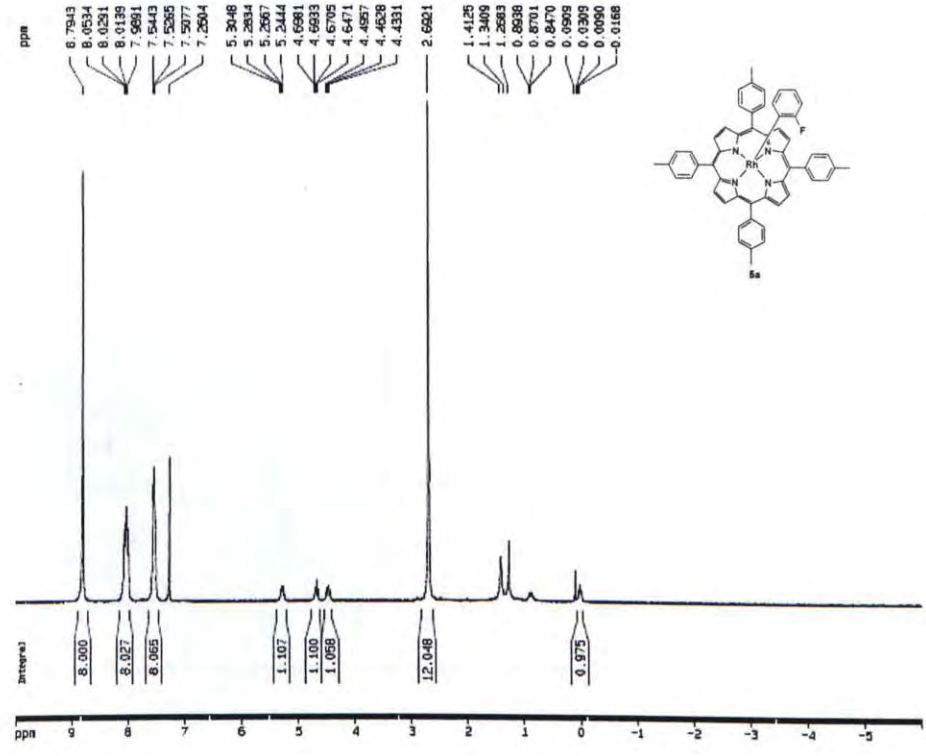


```
Current Data Parameters
NAME                  MHL 27l
EXPNO                        2
PROCNO                       1

F2 - Acquisition Parameters
Date_               20070820
Time                   14.22
INSTRUM                dpx300
PROBHD  5 mm BBO BB-1H
PULPROG                   zg
TD                       32768
SOLVENT                CDCl3
NS                          32
DS                           0
SWH                 9004.953 Hz
FIDRES              0.274809 Hz
AQ                  1.8194932 sec
RG                       287.4
DW                    55.525 usec
DE                    79.32 usec
TE                       0.0 K
D1                  1.00000000 sec
MCREST              0.00000000 sec
MCWRK               0.01500000 sec

======== CHANNEL f1 ========
NUC1                       1H
P1                      5.00 usec
PL1                     -2.00 dB
SFO1              300.1312000 MHz

F2 - Processing parameters
SI                       32768
SF                300.1300051 MHz
WDW                        EM
SSB                         0
LB                       0.30 Hz
GB                          0
PC                       1.00

1D NMR plot parameters
CX                      22.00 cm
CY                      12.00 cm
F1P                   10.000 ppm
F1                   3001.30 Hz
F2P                   -6.000 ppm
F2                  -1800.78 Hz
PPMCM                0.72727 ppm/
HZCM                218.27637 Hz/
```

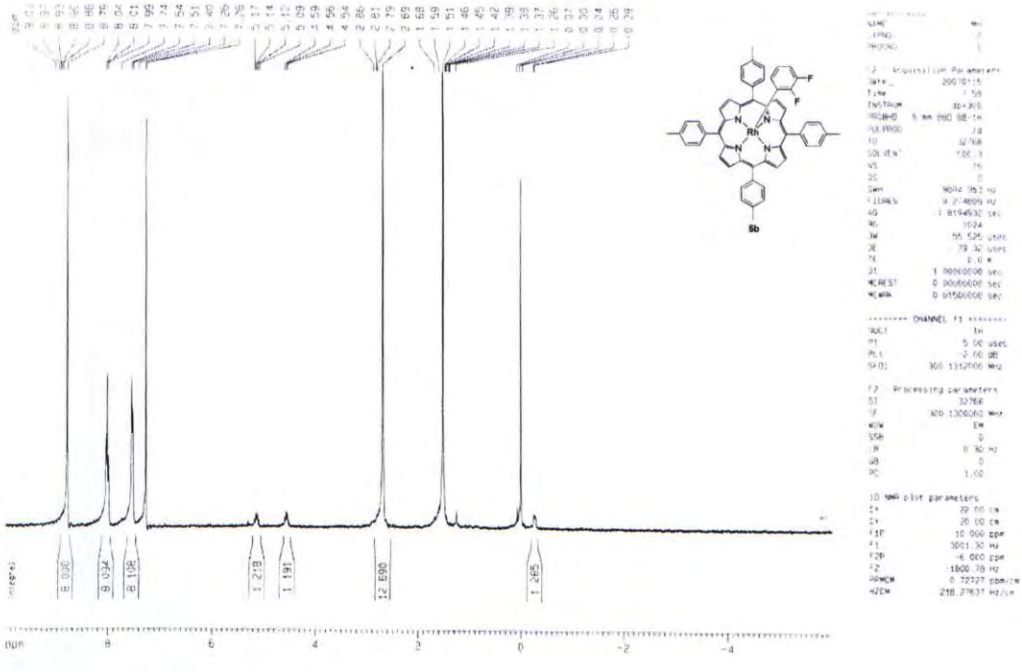

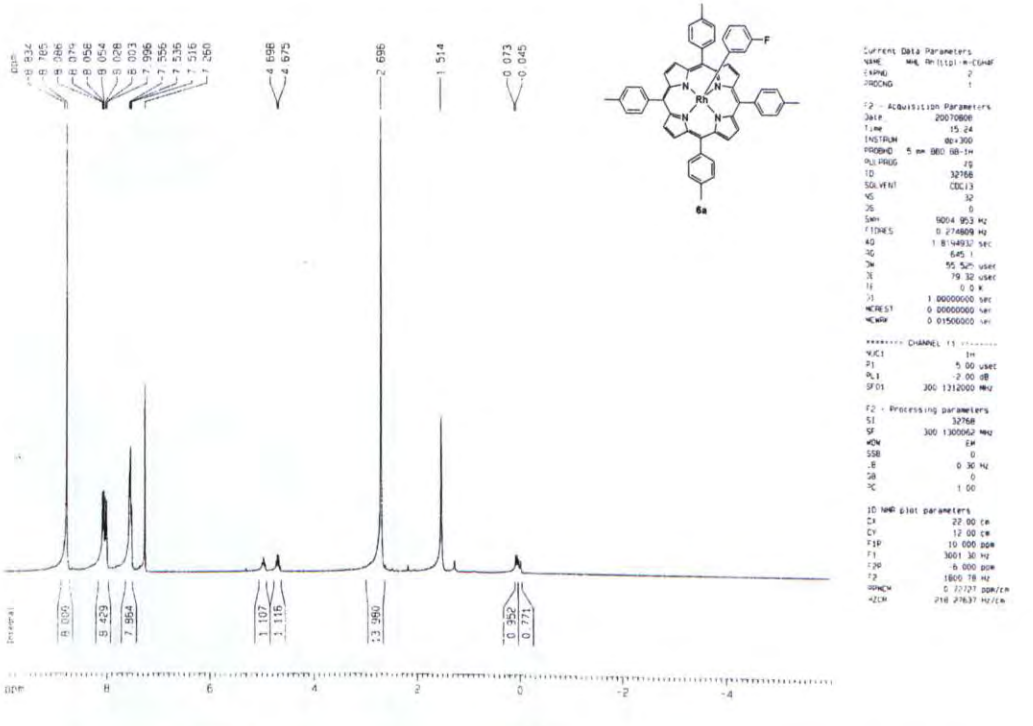

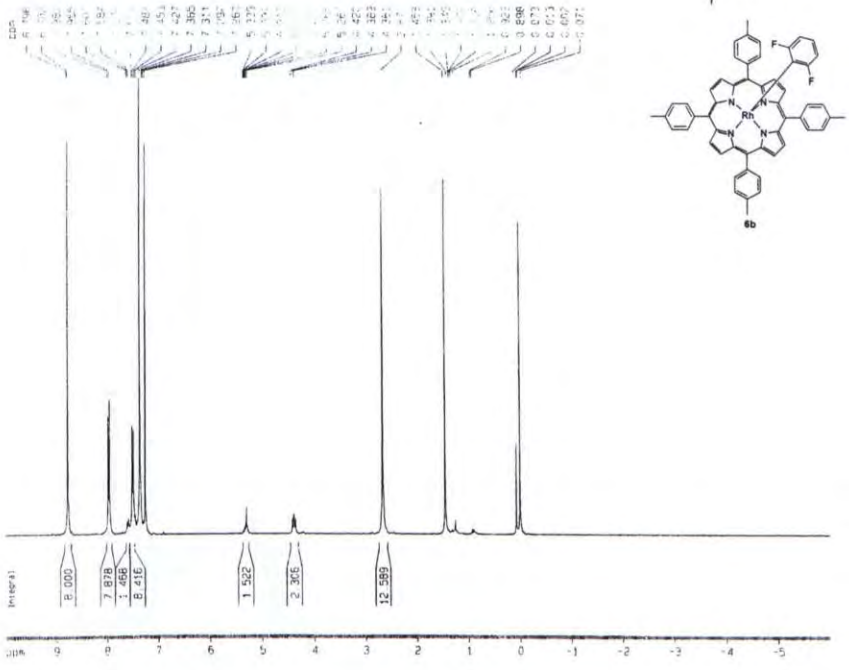


```
Current Data Parameters
NAME          MHL 193 crude
EXPNO                    1
PROCNO                   1

F2 - Acquisition Parameters
Date_              20070320
Time                  13.58
INSTRUM             dpx300
PROBHD  5 mm BBO BB-1H
PULPROG                 zg
TD                   32768
SOLVENT              CDCl3
NS                      32
DS                       0
SWH              8992.806 Hz
FIDRES           0.274498 Hz
AQ               1.8219508 sec
RG                   812.7
DW                55.600 usec
DE                79.43 usec
TE                   0.0 K
D1                1.00000000 sec
MCREST            0.00000000 sec
MCWRK             0.01500000 sec

======== CHANNEL f1 ========
NUC1                    1H
P1                   5.00 usec
PL1                -2.00 dB
SFO1          300.1312000 MHz

F2 - Processing parameters
SI                   32768
SF          300.1300063 MHz
WDW                     EM
SSB                      0
LB                    0.30 Hz
GB                       0
PC                    1.00

1D NMR plot parameters
CX                   22.00 cm
CY                   30.00 cm
F1P                10.000 ppm
F1                 3001.30 Hz
F2P                -6.000 ppm
F2                -1800.78 Hz
PPMCM             0.72727 ppm/cm
HZCM              218.27637 Hz/cm
```

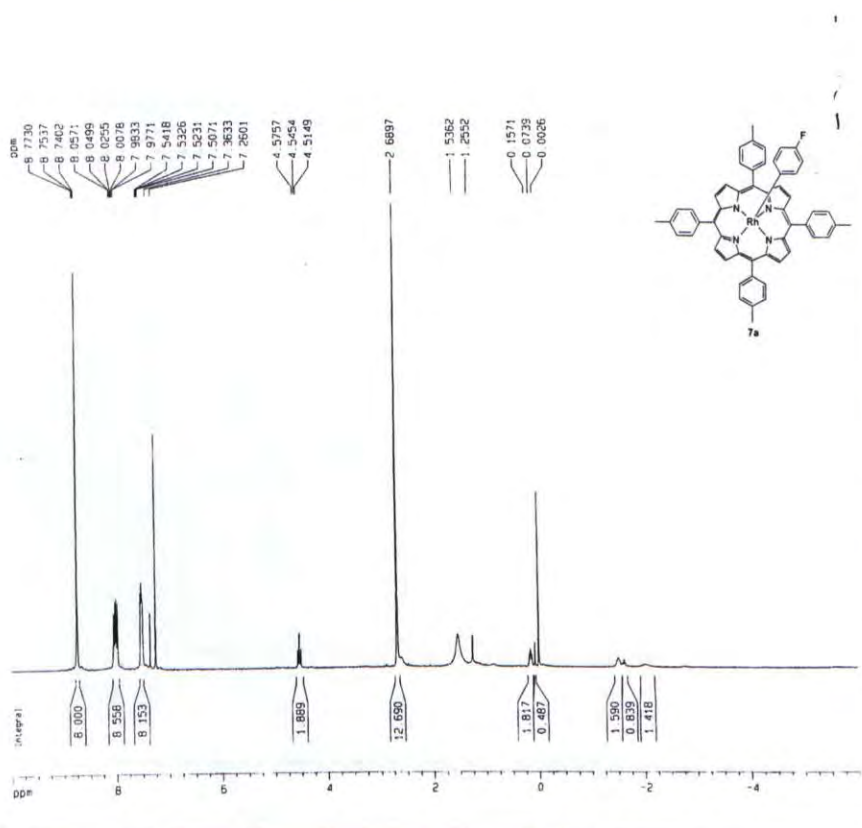


```
Current Data Parameters
NAME          MHL 307
EXPNO                    1
PROCNO                   1

F2 - Acquisition Parameters
Date_              20070926
Time                  1.26
INSTRUM             dpx300
PROBHD  5 mm BBO BB-1H
PULPROG                 zg
TD                   32768
SOLVENT              CDCl3
NS                      32
DS                       0
SWH              9004.953 Hz
FIDRES           0.274805 Hz
AQ               1.8194932 sec
RG                   724.1
DW                55.520 usec
DE                79.32 usec
TE                   0.0 K
D1                1.0000000 sec
MCREST            0.0000000 sec
MCWRK             0.0150000 sec

======== CHANNEL f1 ========
NUC1                    1H
P1                   5.00 usec
PL1                -2.00 dB
SFO1          300.1312000 MHz

F2 - Processing parameters
SI                   32768
SF          300.1300057 MHz
WDW                     EM
SSB                      0
LB                    0.30 Hz
GB                       0
PC                    1.00

1D NMR plot parameters
CX                   22.00 cm
CY                   12.00 cm
F1P                10.000 ppm
F1                 3001.30 Hz
F2P                -6.000 ppm
F2                -1800.78 Hz
PPMCM             0.72727 ppm/cm
HZCM              218.27637 Hz/cm
```

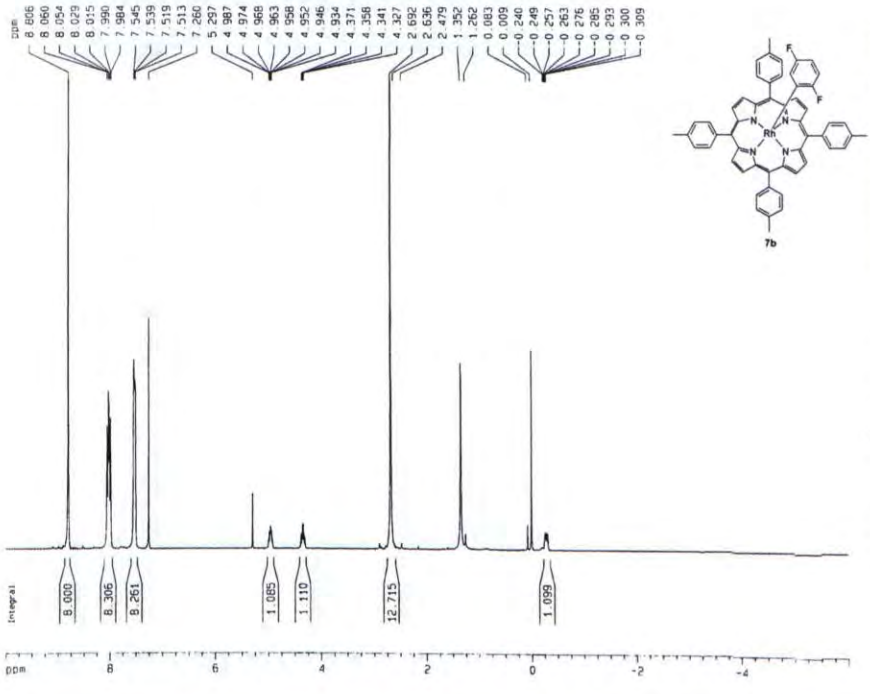

Current Data Parameters
NAME re-cry Rh(tfpp)Ms.esp
EXPNO 1
PROCNO 1

F2 - Acquisition Parameters
Date_ 20070104
Time 17.29
INSTRUM dpx300
PROBHD 5 mm BBO BB-1H
PULPROG zg
TD 32768
SOLVENT CDCl3
NS 32
DS 0
SWH 8992.806 Hz
FIDRES 0.274439 Hz
AQ 1.8219508 sec
RG 128
DW 55.600 usec
DE 79.43 usec
TE 0.0 K
D1 1.00000000 sec
MCREST 0.00000000 sec
MCWRK 0.01500000 sec

======== CHANNEL f1 ========
NUC1 1H
P1 5.00 usec
PL1 -2.00 dB
SFO1 300.1312000 MHz

F2 - Processing parameters
SI 32768
SF 300.1300066 MHz
WDW EM
SSB 0
LB 0.30 Hz
GB 0
PC 1.00

1D NMR plot parameters
CX 22.00 cm
CY 30.00 cm
F1P 10.000 ppm
F1 3001.30 Hz
F2P -6.000 ppm
F2 -1800.78 Hz
PPMCM 0.72727 ppm/cm
HZCM 218.27637 Hz/cm

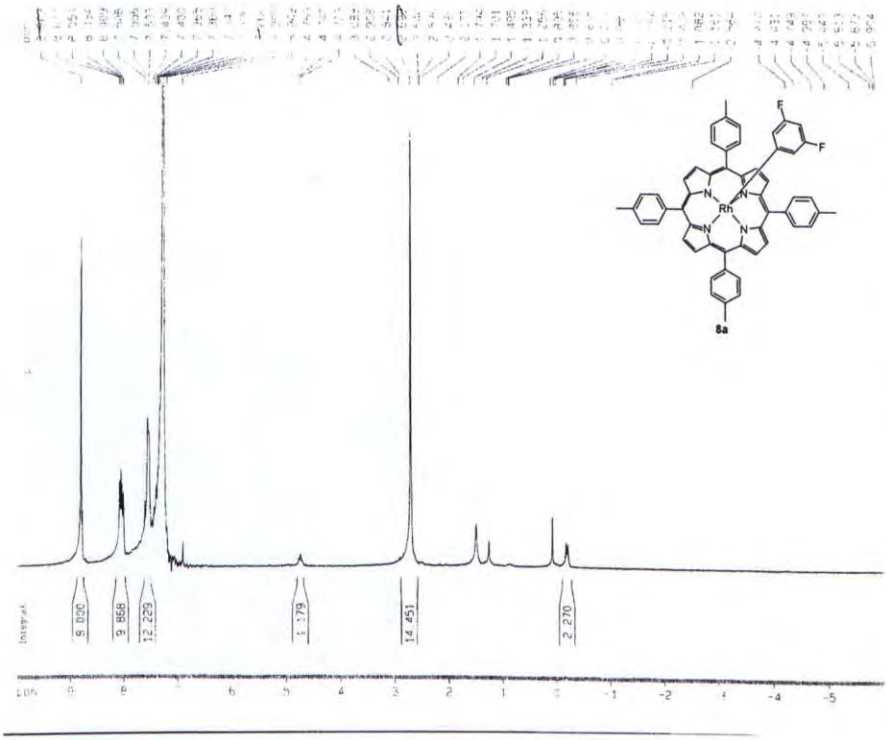

Current Data Parameters
NAME ms_15_a3
EXPNO 1
PROCNO 1

F2 - Acquisition Parameters
Date_ 20070119
Time 11.26
INSTRUM dpx300
PROBHD 5 mm BBO BB-1H
PULPROG zg
TD 32768
SOLVENT CDCl3
NS 32
DS 0
SWH 8992.806 Hz
FIDRES 0.274439 Hz
AQ 1.8219508 sec
RG 362
DW 55.600 usec
DE 79.43 usec
TE 0.0 K
D1 1.00000000 sec
MCREST 0.00000000 sec
MCWRK 0.01500000 sec

======== CHANNEL f1 ========
NUC1 1H
P1 5.00 usec
PL1 -2.00 dB
SFO1 300.1312000 MHz

F2 - Processing parameters
SI 32768
SF 300.1300060 MHz
WDW EM
SSB 0
LB 0.30 Hz
GB 0
PC 1.00

1D NMR plot parameters
CX 22.00 cm
CY 30.00 cm
F1P 10.000 ppm
F1 3001.30 Hz
F2P -6.000 ppm
F2 -1800.78 Hz
PPMCM 0.72727 ppm/cm
HZCM 218.27637 Hz/cm

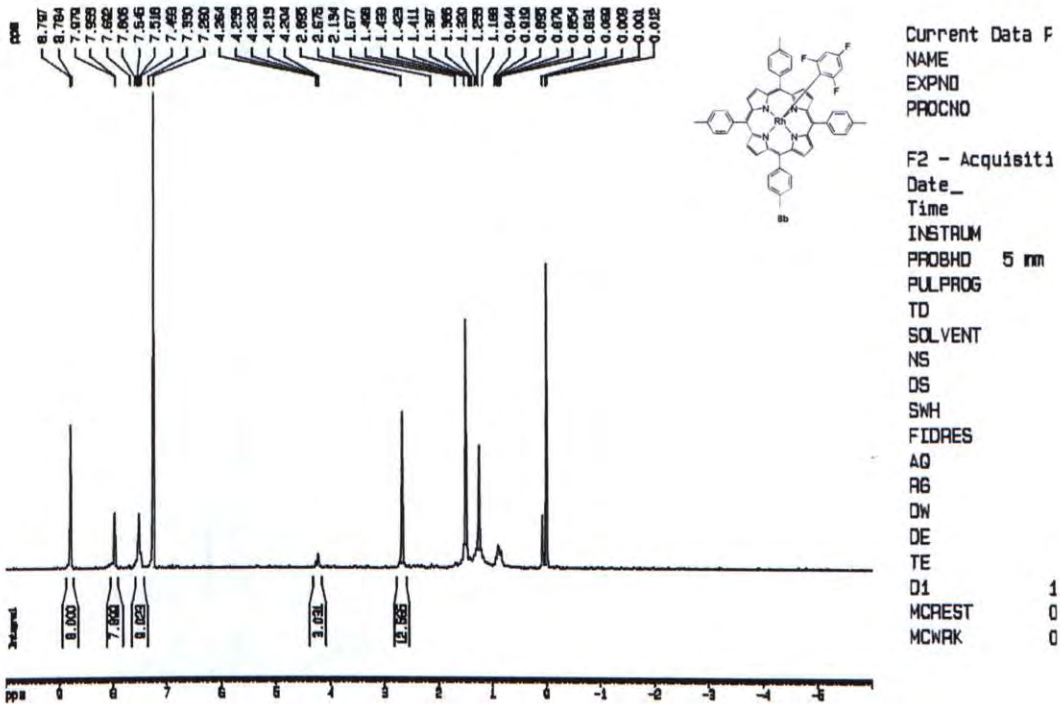
8.000
7.960
8.029
3.624
12.965
Current Data P
NAME
EXPNO
PROCNO
F2 - Acquisiti
Date_
Time
INSTRUM
PROBHD 5 mm
PULPROG
TD
SOLVENT
NS
DS
SWH
FIDRES
AQ
RG
DW
DE
TE
D1 1
MCREST 0
MCWRK 0

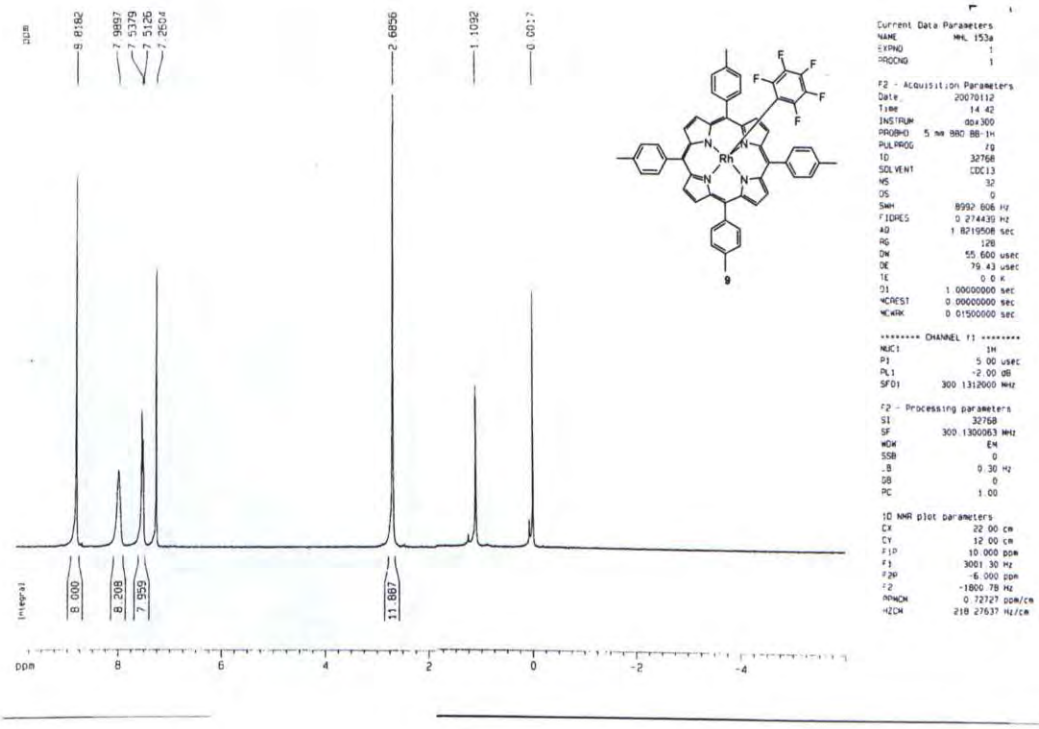
8.000
8.208
7.959
11.867
Current Data Parameters
NAME mHL 153a
EXPNO 1
PROCNO 1
F2 - Acquisition Parameters
Date_ 20070112
Time 14.42
INSTRUM dpx300
PROBHD 5 mm BBO BB-1H
PULPROG zg
TD 32768
SOLVENT CDCl3
NS 32
DS 0
SWH 8992.806 Hz
FIDRES 0.274439 Hz
AQ 1.8219508 sec
RG 128
DW 55.600 usec
DE 79.43 usec
TE 0.0 K
D1 1.00000000 sec
MCREST 0.00000000 sec
MCWRK 0.01500000 sec
******** CHANNEL f1 ********
NUC1 1H
P1 5.00 usec
PL1 -2.00 dB
SFO1 300.1312000 MHz
F2 - Processing parameters
SI 32768
SF 300.1300063 MHz
WDW EM
SSB 0
LB 0.30 Hz
GB 0
PC 1.00
1D NMR plot parameters
CX 22.00 cm
CY 12.00 cm
F1P 10.000 ppm
F1 3001.30 Hz
F2P -6.000 ppm
F2 -1800.78 Hz
PPMCM 0.72727 ppm/cm
HZCM 218.27637 Hz/cm

CFA product mixtures from K.I.E. experiment by Rh(ttp)Cl

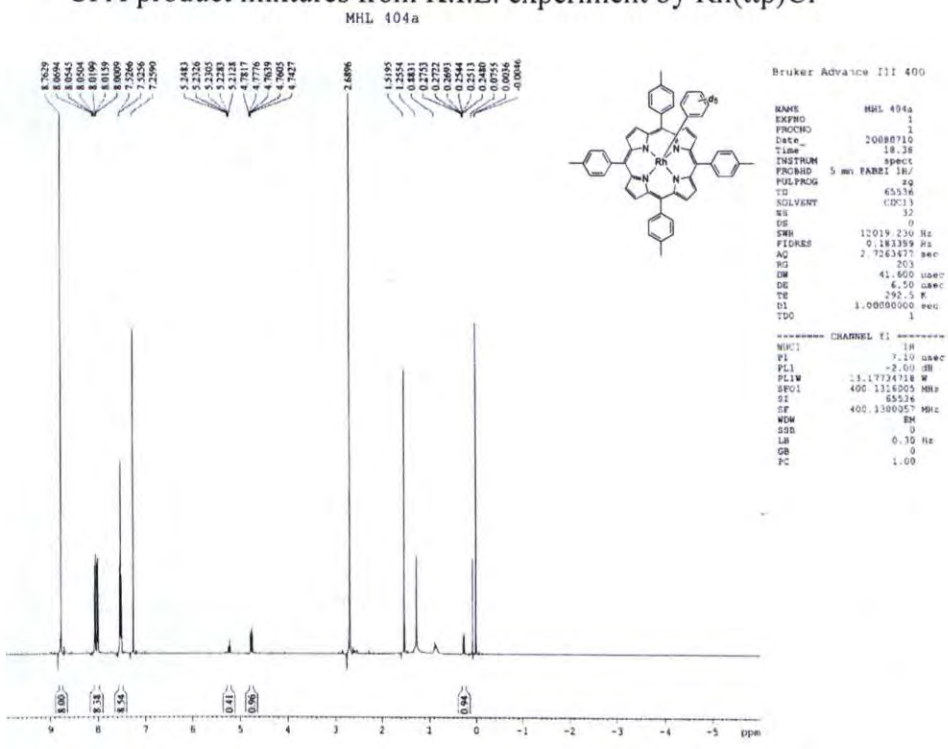

CHA product mixtures from K.I.E. experiment by Rh(ttp)Cl

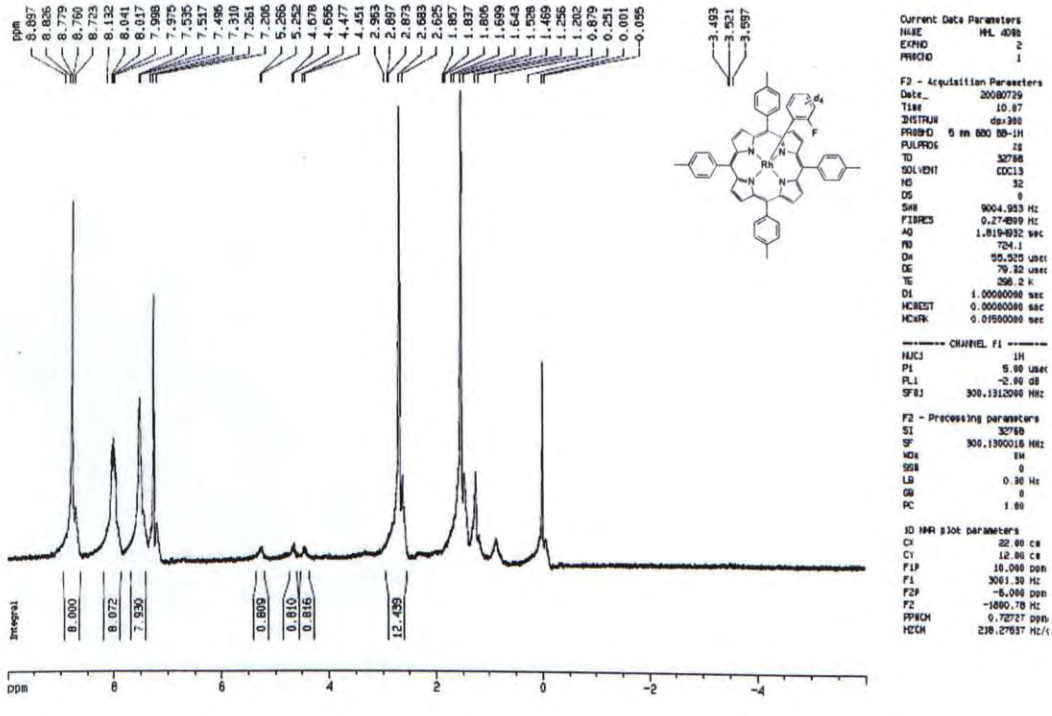

CFA product mixtures from K.I.E. experiment by Rh(ttp)H

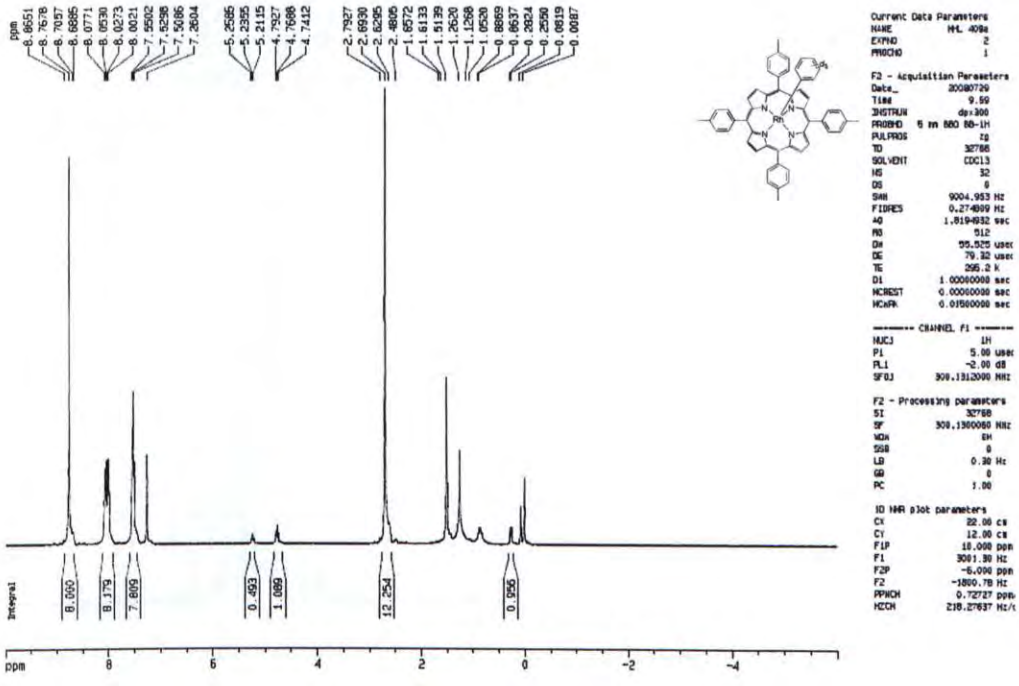

CHA product mixtures from K.I.E. experiment by Rh(ttp)H

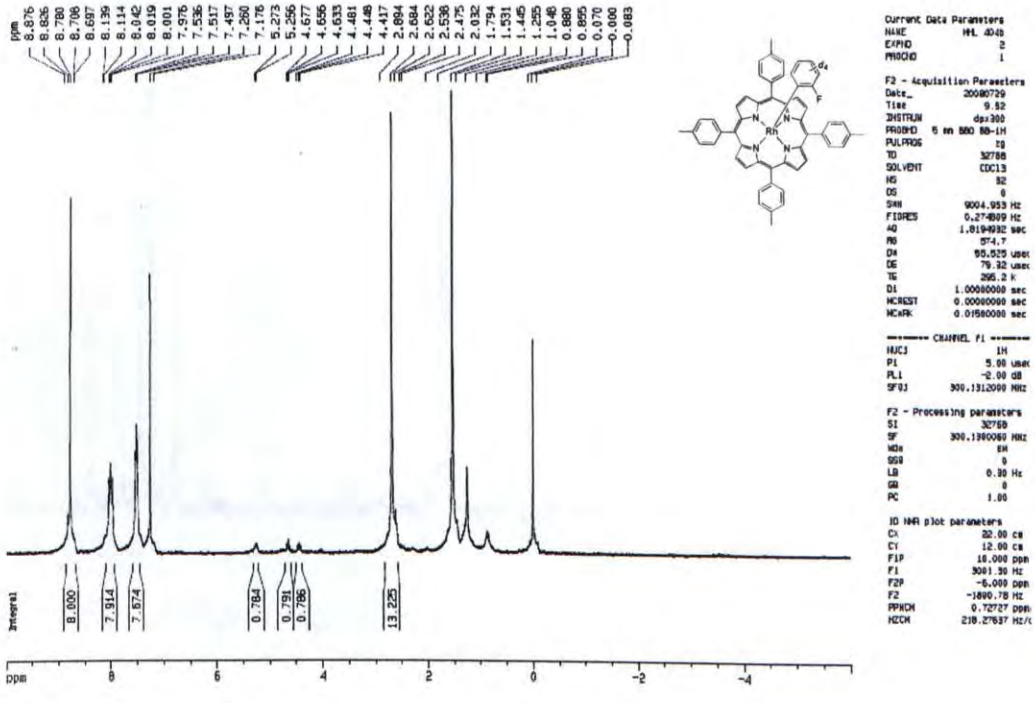

C13

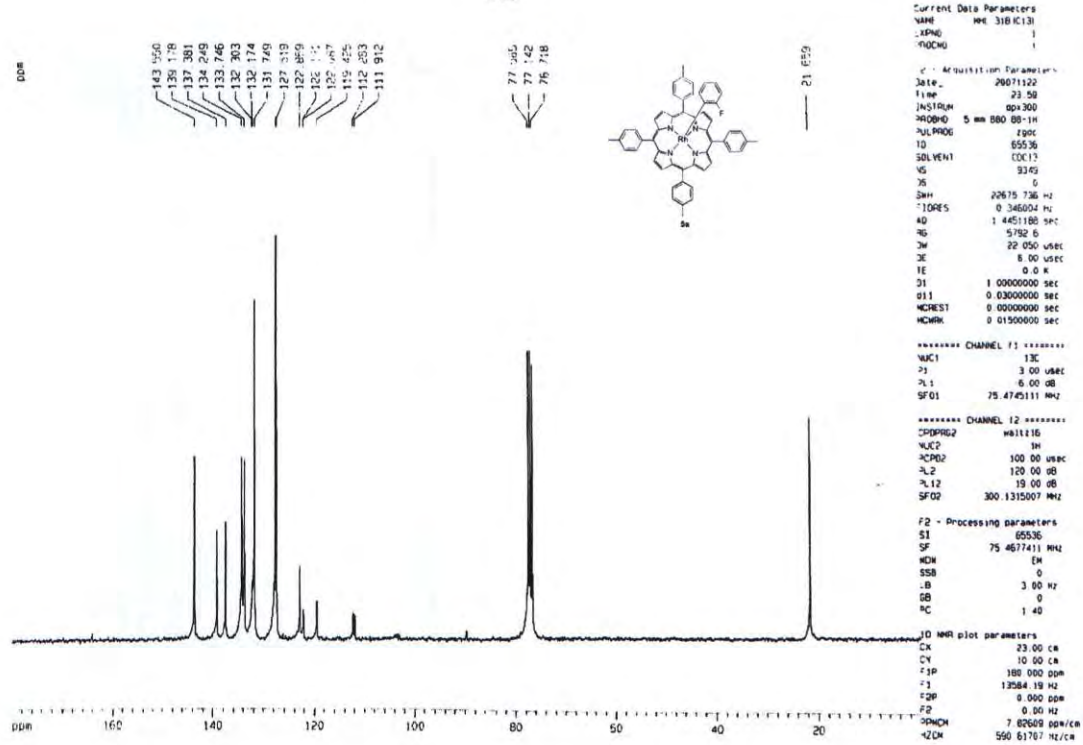

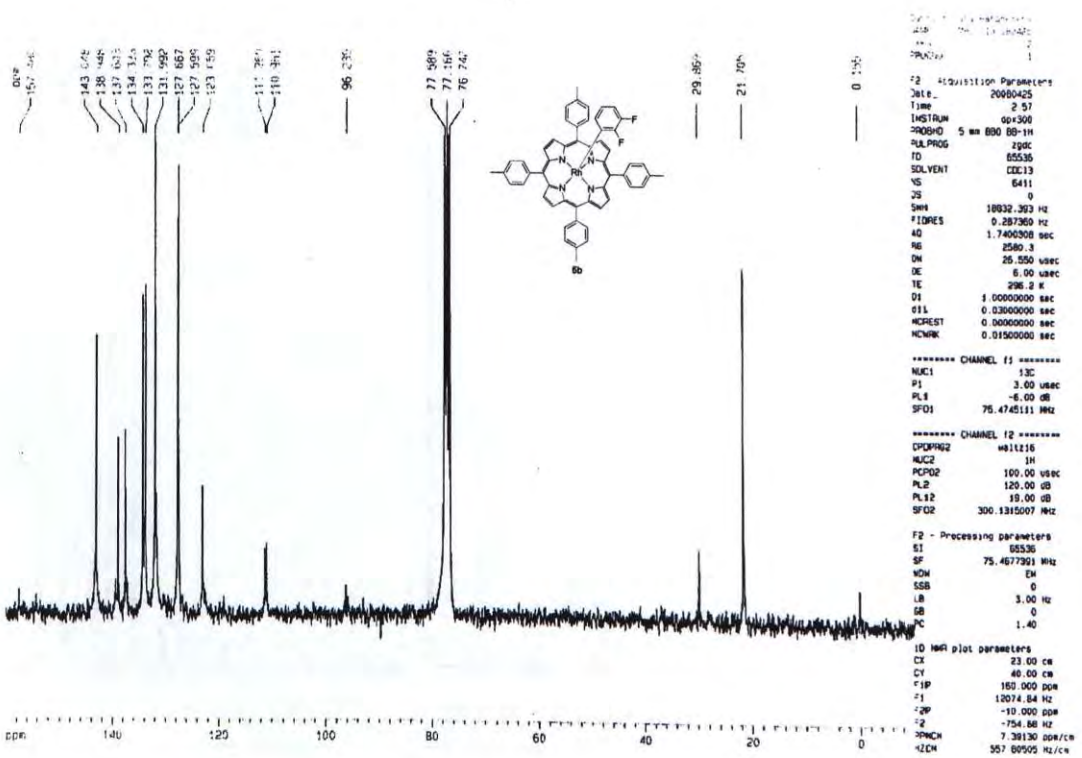

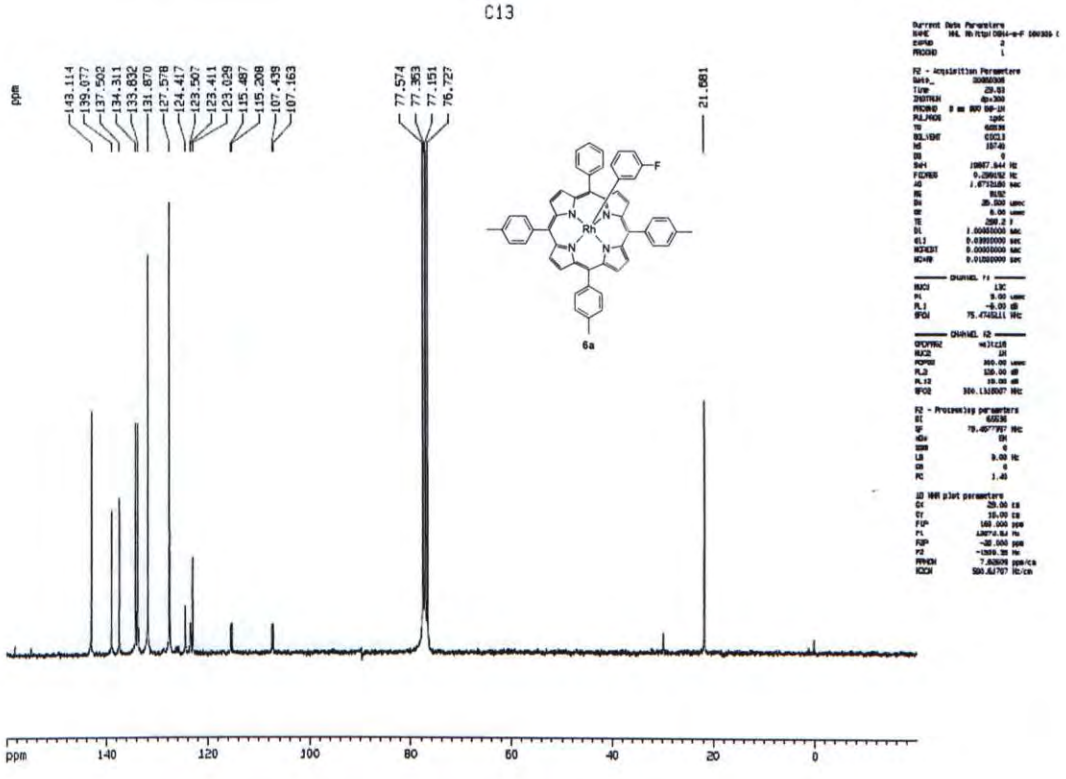
C13
ppm
143.114
139.077
137.502
134.311
133.832
131.870
127.578
124.417
123.507
123.411
123.029
115.497
115.208
107.439
107.163
77.574
77.363
77.151
76.727
21.081
6a
ppm
140
120
100
80
60
40
20
0

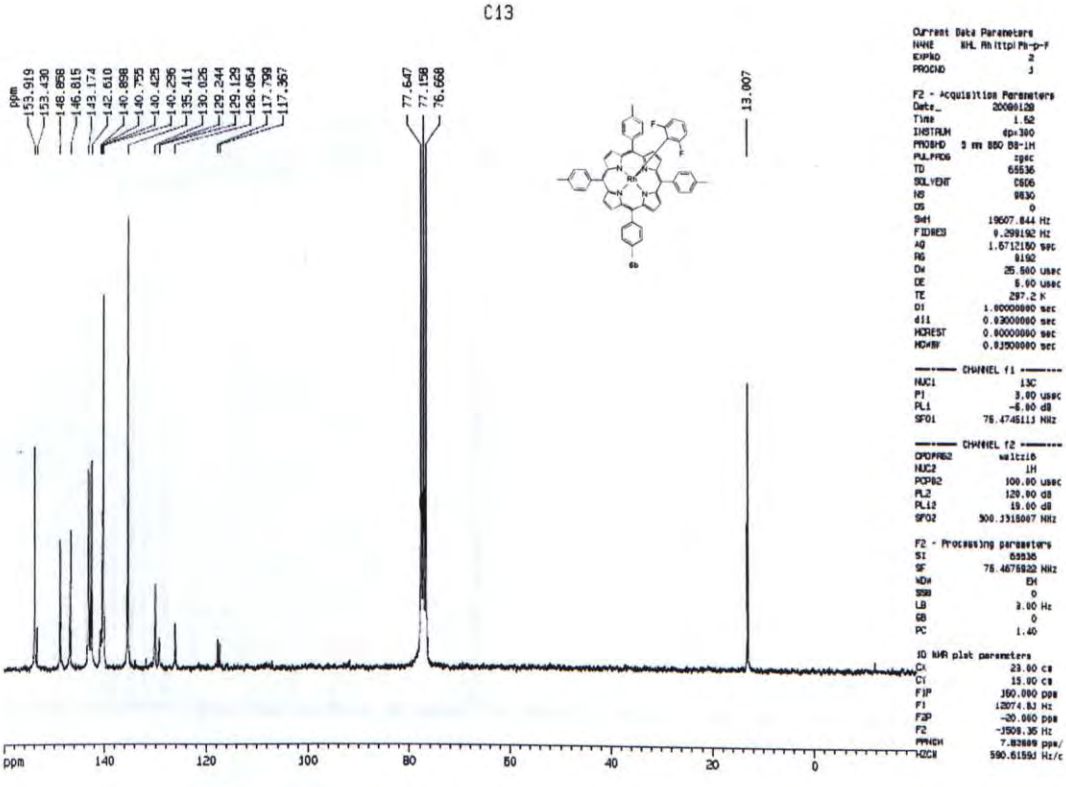
C13
ppm
153.919
153.430
146.868
146.815
143.174
142.610
140.898
140.755
140.425
140.296
135.411
130.026
129.244
129.129
126.854
117.799
117.367
77.647
77.158
76.668
13.007
6b
ppm
140
120
100
80
60
40
20
0

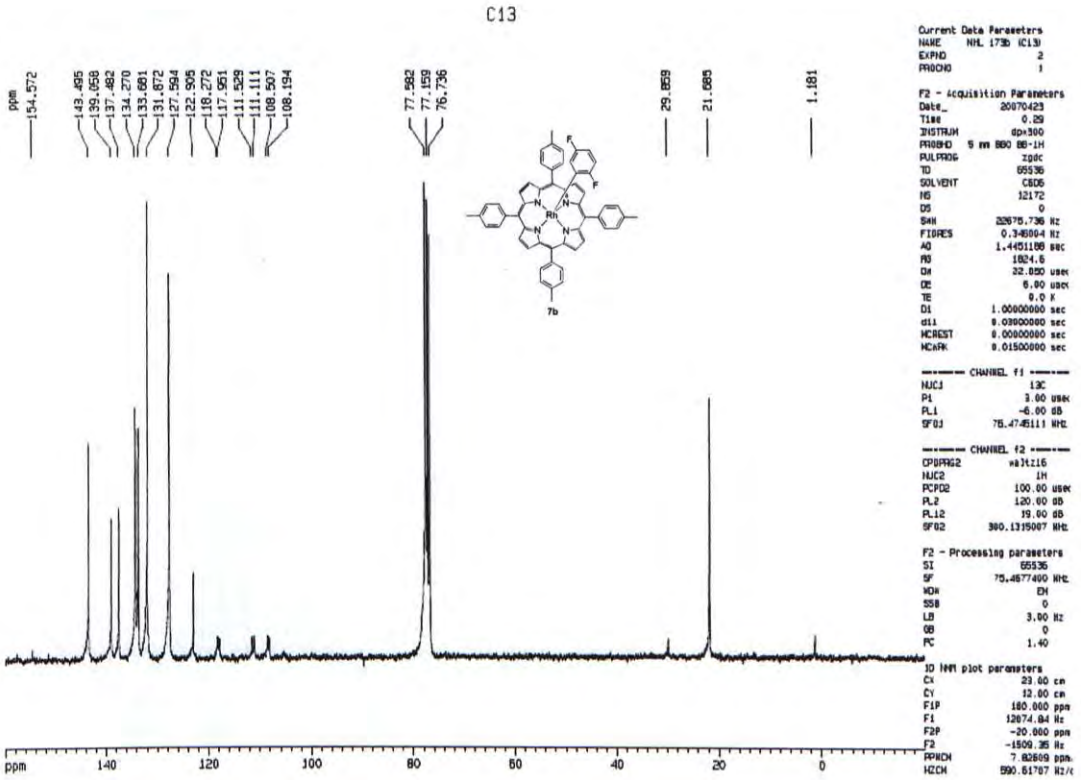
C13
ppm
154.572
143.495
139.058
137.482
134.270
133.681
131.672
127.594
122.906
118.272
117.951
111.529
111.111
108.507
108.194
77.582
77.159
76.736
29.859
21.085
1.181
7b
ppm
140
120
100
80
60
40
20
0
Current Data Parameters
NAME NHL 1736 IC13
EXPNO 2
PROCNO 1
F2 - Acquisition Parameters
Date_ 20070423
Time 0.29
INSTRUM dpx300
PROBHD 5 mm BBO BB-1H
PULPROG zgpg
TD 65536
SOLVENT CDCl3
NS 12172
DS 0
SWH 22675.736 Hz
FIDRES 0.346004 Hz
AQ 1.4451188 sec
RG 1024.6
DW 22.050 usec
DE 6.00 usec
TE 0.0 K
D1 1.00000000 sec
d11 0.03000000 sec
MCREST 0.00000000 sec
MCWRK 0.01500000 sec
CHANNEL f1
NUC1 13C
P1 3.00 usec
PL1 -6.00 dB
SFO1 75.4745111 MHz
CHANNEL f2
CPDPRG2 waltz16
NUC2 1H
PCPD2 100.00 usec
PL2 120.00 dB
PL12 19.00 dB
SFO2 300.1315007 MHz
F2 - Processing parameters
SI 65536
SF 75.4677400 MHz
WDW EM
SSB 0
LB 3.00 Hz
GB 0
PC 1.40
1D NMR plot parameters
CX 23.00 cm
CY 12.00 cm
F1P 180.000 ppm
F1 12074.84 Hz
F2P -20.000 ppm
F2 -1509.35 Hz
PPMCM 7.82809 ppm/cm
HZCM 590.61787 Hz/cm

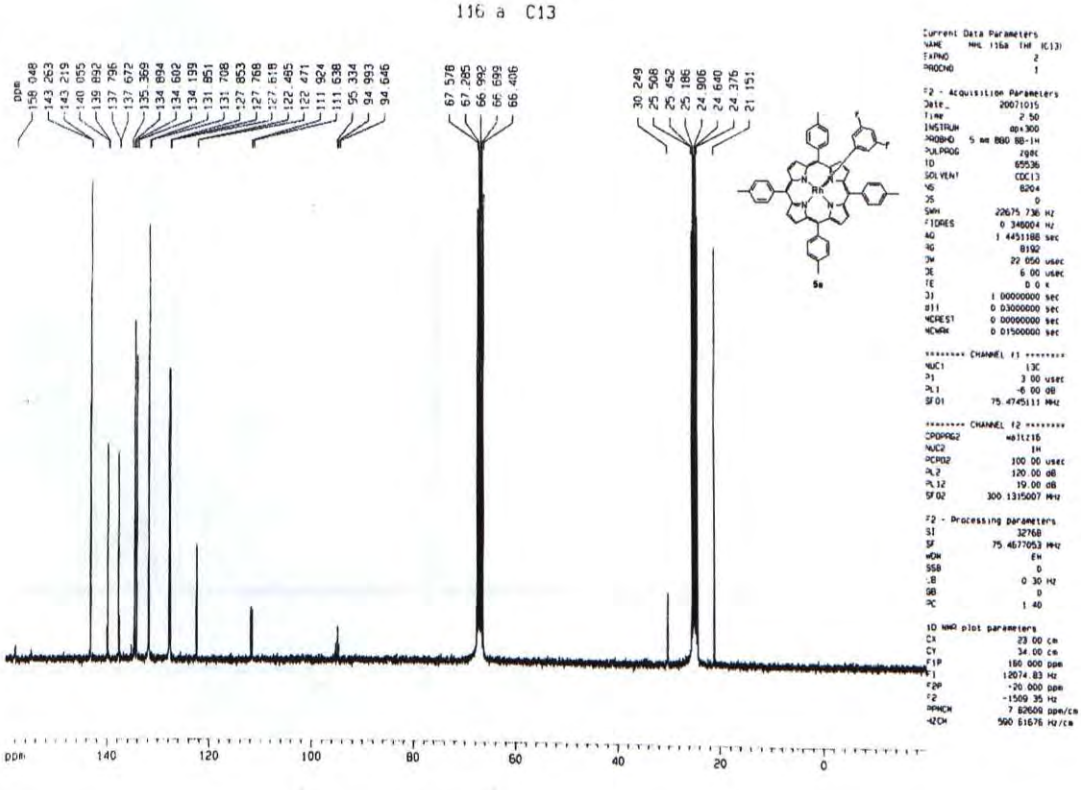
116 a C13
ppm
158.048
143.263
143.219
140.055
139.892
137.796
137.672
135.369
134.894
134.602
134.199
131.851
131.708
127.853
127.768
127.618
122.485
122.471
111.924
111.638
95.334
94.993
94.646
67.578
67.285
66.992
66.699
66.406
30.249
25.508
25.452
25.186
24.906
24.640
24.376
21.151
5a
ppm
140
120
100
80
60
40
20
0
Current Data Parameters
NAME NHL 116a (NF IC13)
EXPNO 2
PROCNO 1
F2 - Acquisition Parameters
Date_ 20071015
Time 2.50
INSTRUM dpx300
PROBHD 5 mm BBO BB-1H
PULPROG zgpg
TD 65536
SOLVENT CDCl3
NS 8204
DS 0
SWH 22675.736 Hz
FIDRES 0.346004 Hz
AQ 1.4451188 sec
RG 8192
DW 22.050 usec
DE 6.00 usec
TE 0.0 K
D1 1.00000000 sec
D11 0.03000000 sec
MCREST 0.00000000 sec
MCWRK 0.01500000 sec
CHANNEL f1
NUC1 13C
P1 3.00 usec
PL1 -6.00 dB
SFO1 75.4745111 MHz
CHANNEL f2
CPDPRG2 waltz16
NUC2 1H
PCPD2 100.00 usec
PL2 120.00 dB
PL12 19.00 dB
SFO2 300.1315007 MHz
F2 - Processing parameters
SI 32768
SF 75.4677053 MHz
WDW EM
SSB 0
LB 0.30 Hz
GB 0
PC 1.40
1D NMR plot parameters
CX 23.00 cm
CY 14.00 cm
F1P 180.000 ppm
F1 12074.83 Hz
F2P -20.000 ppm
F2 -1509.35 Hz
PPMCM 7.82609 ppm/cm
HZCM 590.61676 Hz/cm

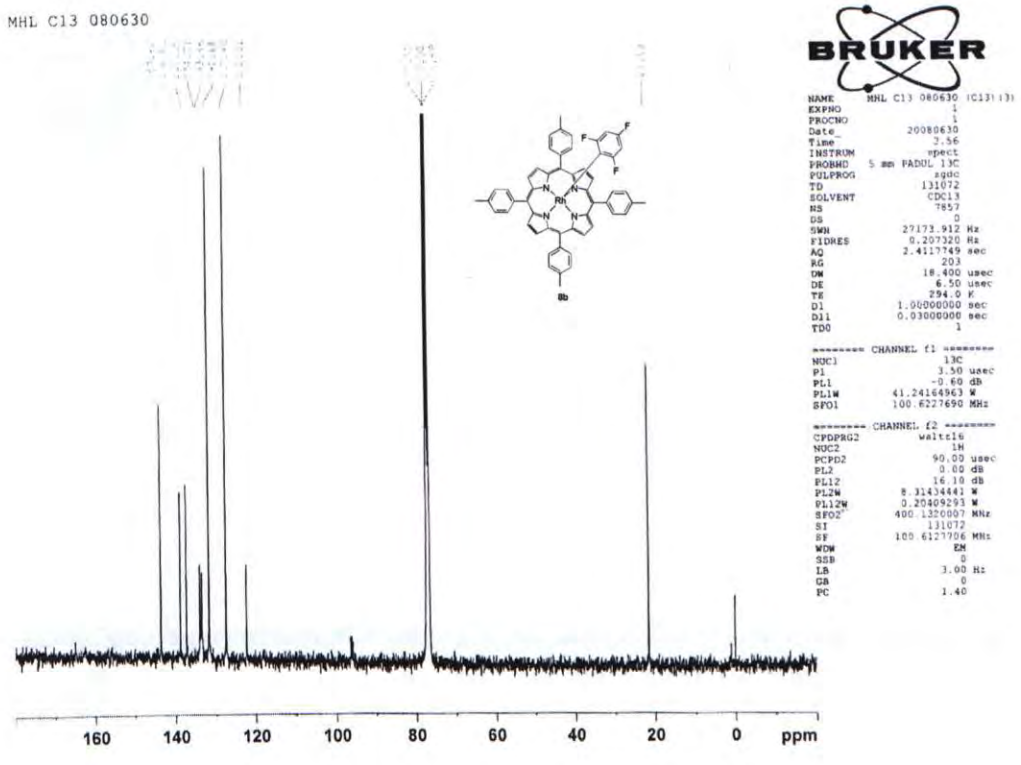
MHL C13 080630
BRUKER
NAME MHL C13 080630 (C13)(13)
EXPNO 1
PROCNO 1
Date_ 20080630
Time_ 2.56
INSTRUM spect
PROBHD 5 mm PADUL 13C
PULPROG zgdc
TD 131072
SOLVENT CDCl3
NS 7857
DS 0
SWH 27173.912 Hz
FIDRES 0.207320 Hz
AQ 2.4117749 sec
RG 203
DW 18.400 usec
DE 6.50 usec
TE 294.0 K
D1 1.00000000 sec
D11 0.03000000 sec
TD0 1
======== CHANNEL f1 ========
NUC1 13C
P1 3.50 usec
PL1 -0.60 dB
PL1W 41.24164963 W
SFO1 100.6227690 MHz
======== CHANNEL f2 ========
CPDPRG2 waltz16
NUC2 1H
PCPD2 90.00 usec
PL2 0.00 dB
PL12 16.10 dB
PL2W 8.31434441 W
PL12W 0.20409293 W
SFO2 400.1320007 MHz
SI 131072
SF 100.6127706 MHz
WDW EM
SSB 0
LB 3.00 Hz
GB 0
PC 1.40
8b
160
140
120
100
80
60
40
20
0
ppm

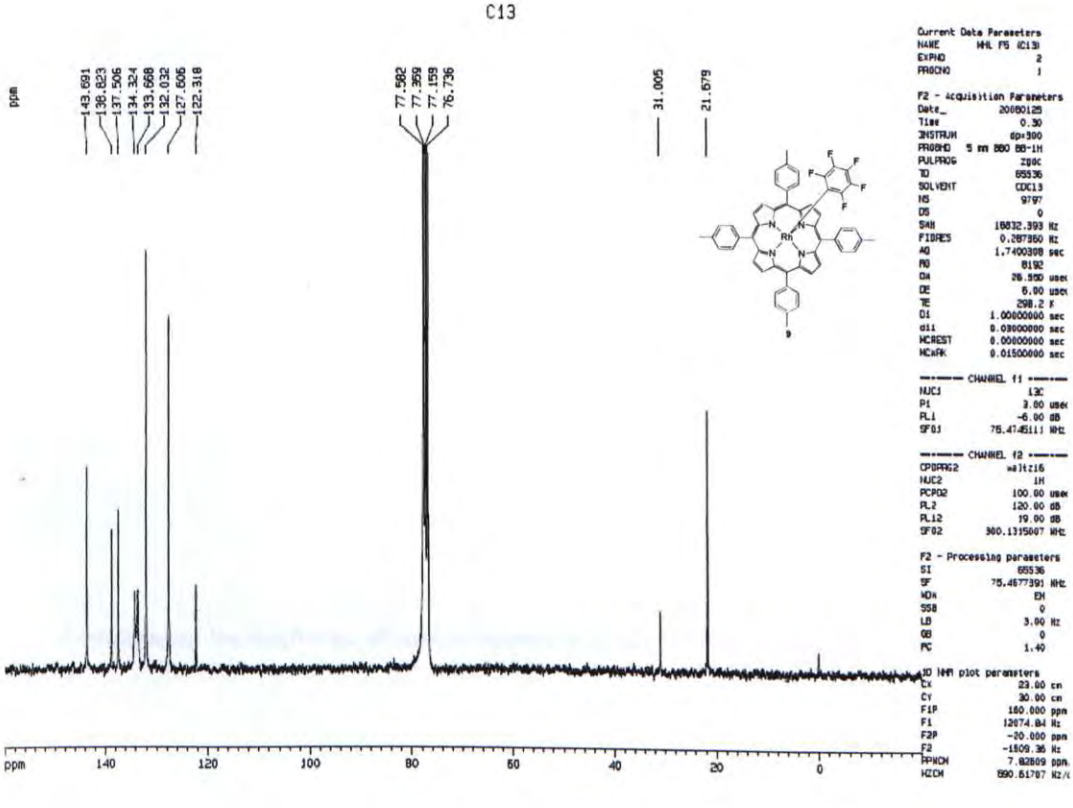
C13
ppm
143.691
138.823
137.506
134.324
133.668
132.032
127.606
122.318
77.582
77.359
77.159
76.736
31.005
21.679
9
Current Data Parameters
NAME MHL F5 (C13)
EXPNO 2
PROCNO 1
F2 - Acquisition Parameters
Date_ 20080125
Time 0.30
INSTRUM spect
PROBHD 5 mm BBO BB-1H
PULPROG zgdc
TD 65536
SOLVENT CDCl3
NS 9797
DS 0
SWH 18832.393 Hz
FIDRES 0.287360 Hz
AQ 1.7400309 sec
RG 8192
DW 26.550 usec
DE 6.00 usec
TE 298.2 K
D1 1.00000000 sec
d11 0.03000000 sec
MCREST 0.00000000 sec
MCWRK 0.01500000 sec
======== CHANNEL f1 ========
NUC1 13C
P1 3.80 usec
PL1 -6.00 dB
SFO1 75.4745111 MHz
======== CHANNEL f2 ========
CPDPRG2 waltz16
NUC2 1H
PCPD2 100.00 usec
PL2 120.00 dB
PL12 19.00 dB
SFO2 300.1315007 MHz
F2 - Processing parameters
SI 65536
SF 75.4677391 MHz
WDW EM
SSB 0
LB 3.00 Hz
GB 0
PC 1.40
1D NMR plot parameters
CX 23.00 cm
CY 30.00 cm
F1P 160.000 ppm
F1 12074.84 Hz
F2P -20.000 ppm
F2 -1509.36 Hz
PPMCM 7.82809 ppm/
HZCM 590.61787 Hz/
ppm
140
120
100
80
60
40
20
0

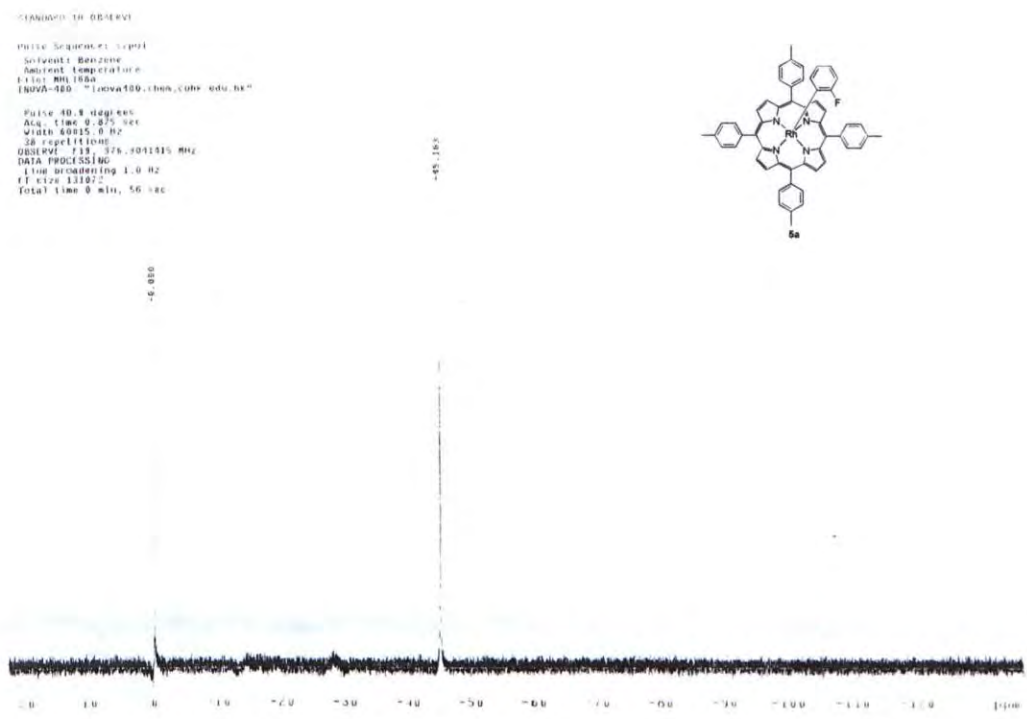
Pulse Sequence: s2pul
Solvent: Benzene
Ambient temperature
File: MHL186a
INOVA-400 "inova400.chem.cuhk.edu.hk"
Pulse 40.8 degrees
Acq. time 0.875 sec
Width 60015.0 Hz
38 repetitions
OBSERVE F19, 376.3041815 MHz
DATA PROCESSING
Line broadening 1.0 Hz
FT size 131072
Total time 0 min, 56 sec
-45.163
-6.050
5a
ppm

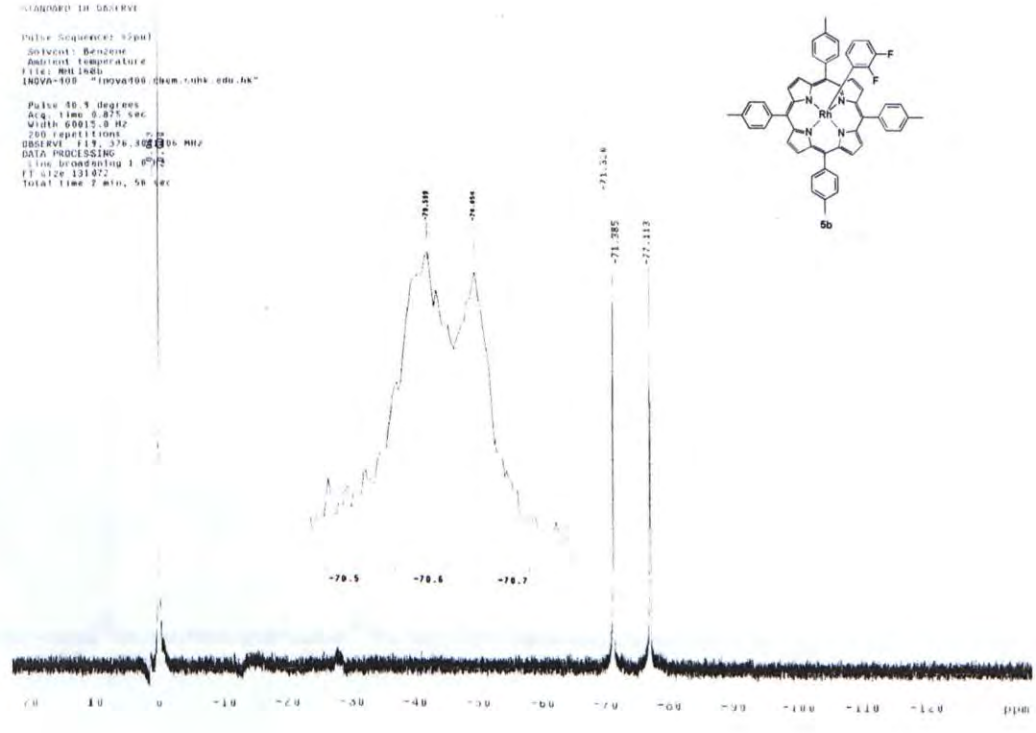
Pulse Sequence: s2pul
Solvent: Benzene
Ambient temperature
File: MHL186b
INOVA-400 "inova400.chem.cuhk.edu.hk"
Pulse 40.9 degrees
Acq. time 0.875 sec
Width 60015.0 Hz
200 repetitions
DATA PROCESSING
Line broadening 1.0 Hz
FT size 131072
Total time 2 min, 58 sec
-71.385
-72.113
-70.5
-70.6
-70.7
5b
ppm

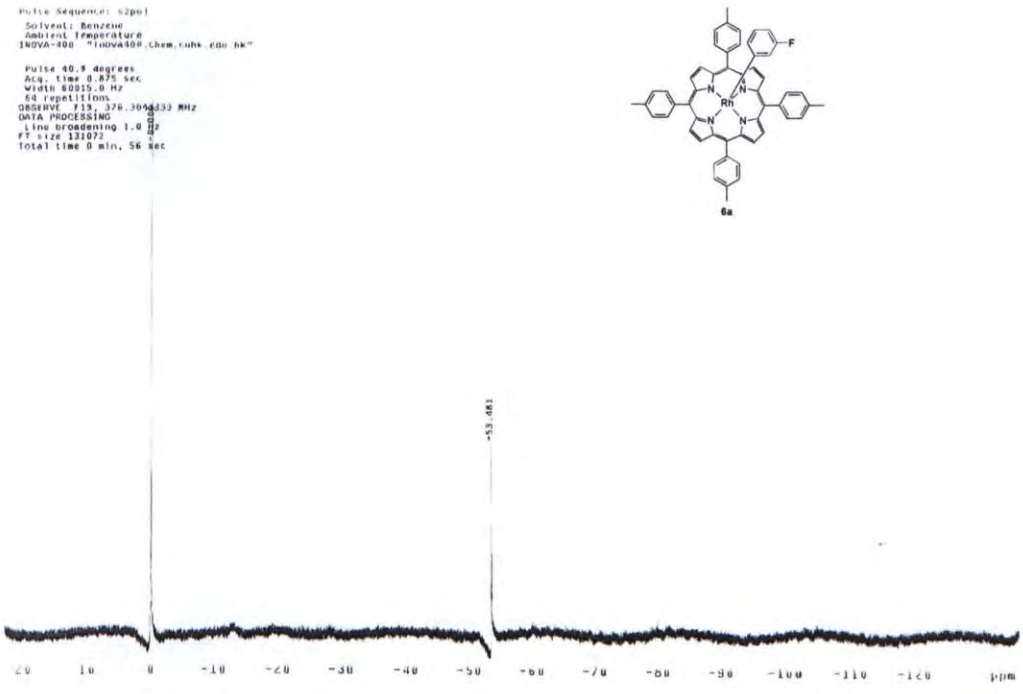
Pulse Sequence: s2pul
Solvent: Benzene
Ambient temperature
INOVA-400 "inova400.chem.cuhk.edu.hk"
Pulse 40.9 degrees
Acq. time 0.875 sec
Width 60015.0 Hz
64 repetitions
OBSERVE F19, 376.3048833 MHz
DATA PROCESSING
Line broadening 1.0 Hz
FT size 131072
Total time 0 min, 56 sec
-53.681
F
Rh
6a
20 10 0 -10 -20 -30 -40 -50 -60 -70 -80 -90 -100 -110 -120 ppm

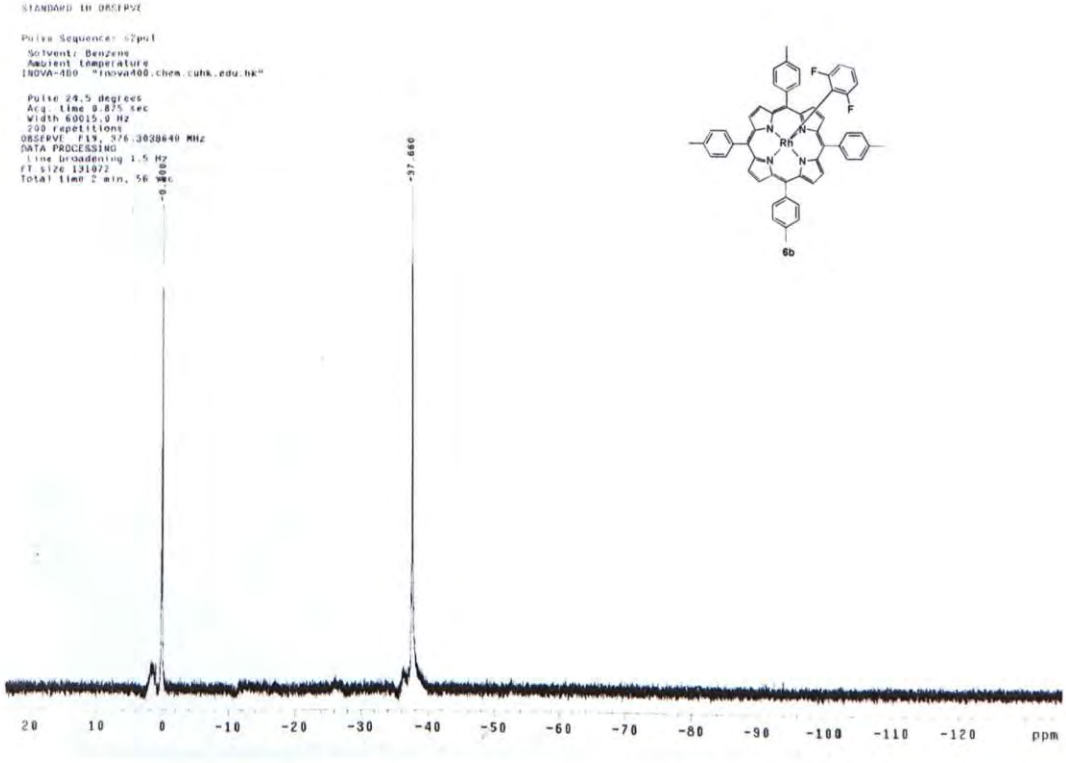
STANDARD IN OBSERVE
Pulse Sequence: s2pul
Solvent: Benzene
Ambient temperature
INOVA-400 "inova400.chem.cuhk.edu.hk"
Pulse 24.5 degrees
Acq. time 0.875 sec
Width 60015.0 Hz
200 repetitions
OBSERVE F19, 376.3038640 MHz
DATA PROCESSING
Line broadening 1.5 Hz
FT size 131072
Total time 2 min, 56 sec
-0.000
-37.660
F
F
Rh
6b
20 10 0 -10 -20 -30 -40 -50 -60 -70 -80 -90 -100 -110 -120 ppm

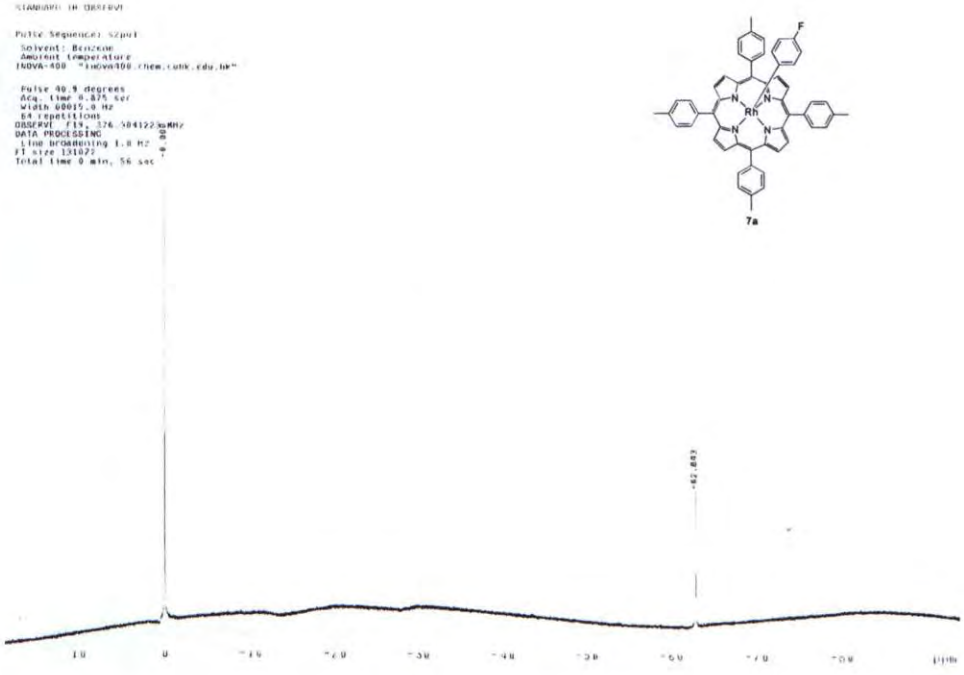
F
Rh
7a
-62.683
10
0
-10
-20
-30
-40
-50
-60
-70
-80
ppm

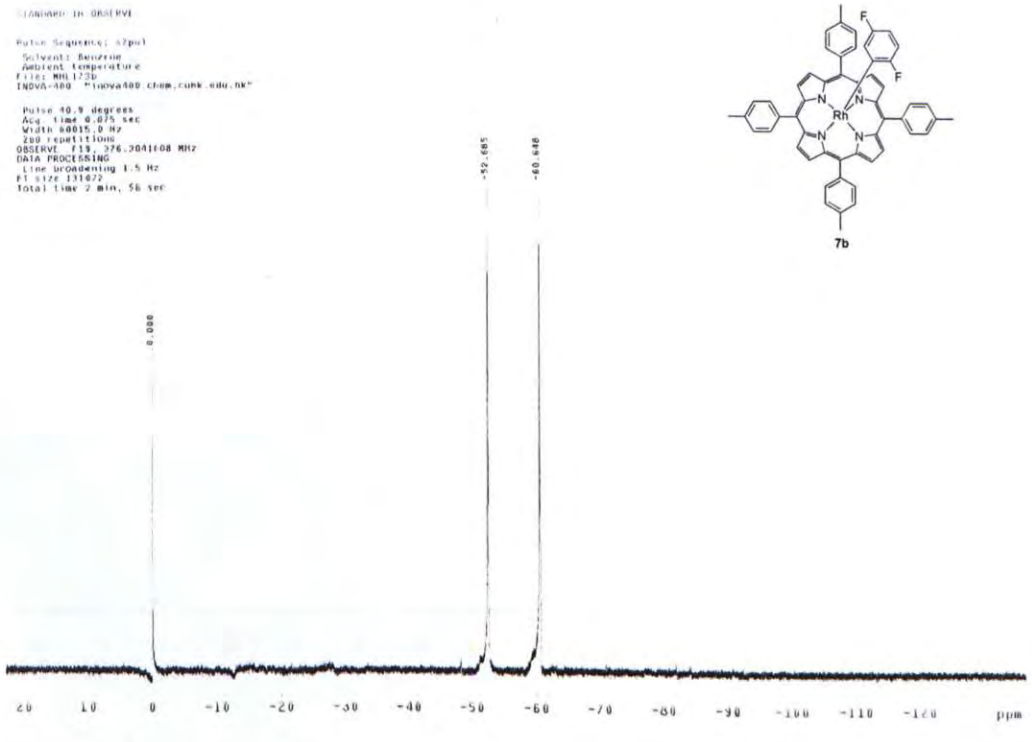
F
F
Rh
7b
-52.685
-60.640
20
10
0
-10
-20
-30
-40
-50
-60
-70
-80
-90
-100
-110
-120
ppm

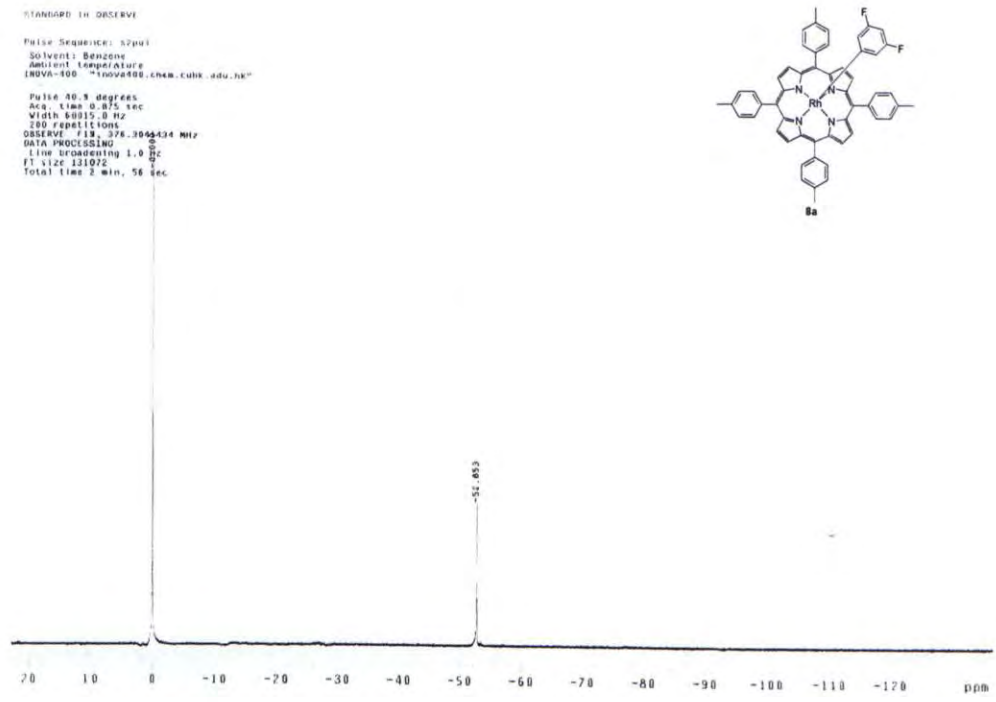
STANDARD 1H OBSERVE
Pulse Sequence: s2pul
Solvent: Benzene
Ambient temperature
INOVA-400 "inova400.chem.cuhk.edu.hk"
Pulse 40.9 degrees
Acq. time 0.875 sec
Width 60015.0 Hz
200 repetitions
DATA PROCESSING
Line broadening 1.0 Hz
FT size 131072
Total time 2 min, 56 sec
-51.653
20 10 0 -10 -20 -30 -40 -50 -60 -70 -80 -90 -100 -110 -120 ppm

8a

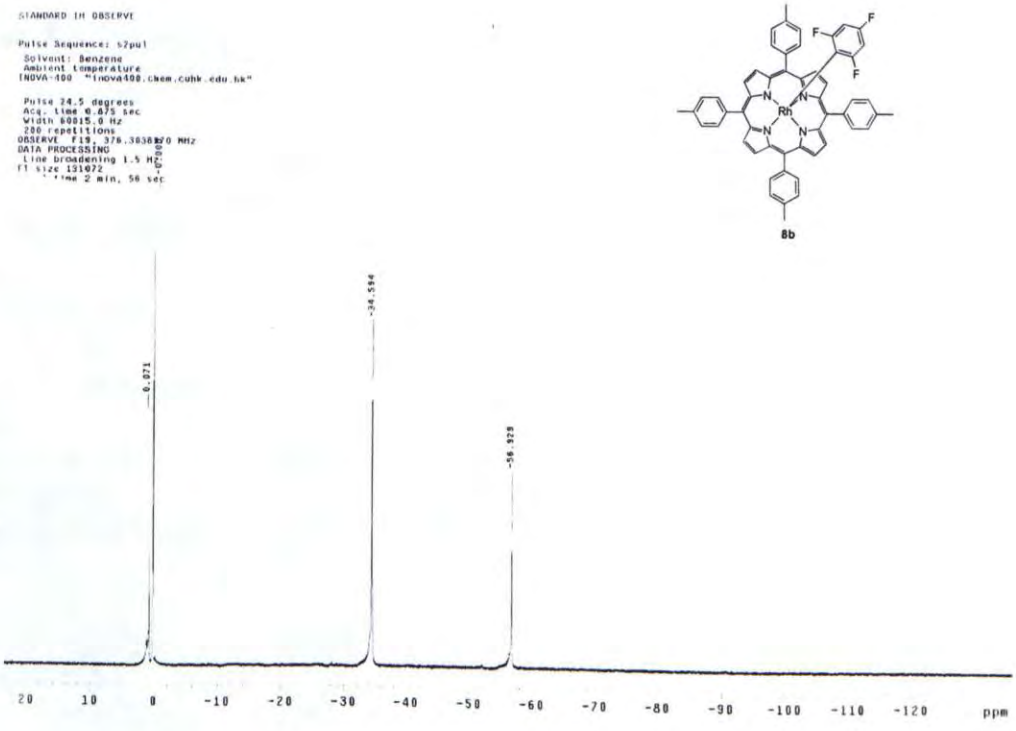
STANDARD 1H OBSERVE
Pulse Sequence: s2pul
Solvent: Benzene
Ambient temperature
INOVA-400 "inova400.chem.cuhk.edu.hk"
Pulse 24.5 degrees
Acq. time 0.875 sec
Width 60015.0 Hz
200 repetitions
DATA PROCESSING
Line broadening 1.5 Hz
FT size 131072
Total time 2 min, 56 sec
0.071
-34.584
-56.928
20 10 0 -10 -20 -30 -40 -50 -60 -70 -80 -90 -100 -110 -120 ppm

8b

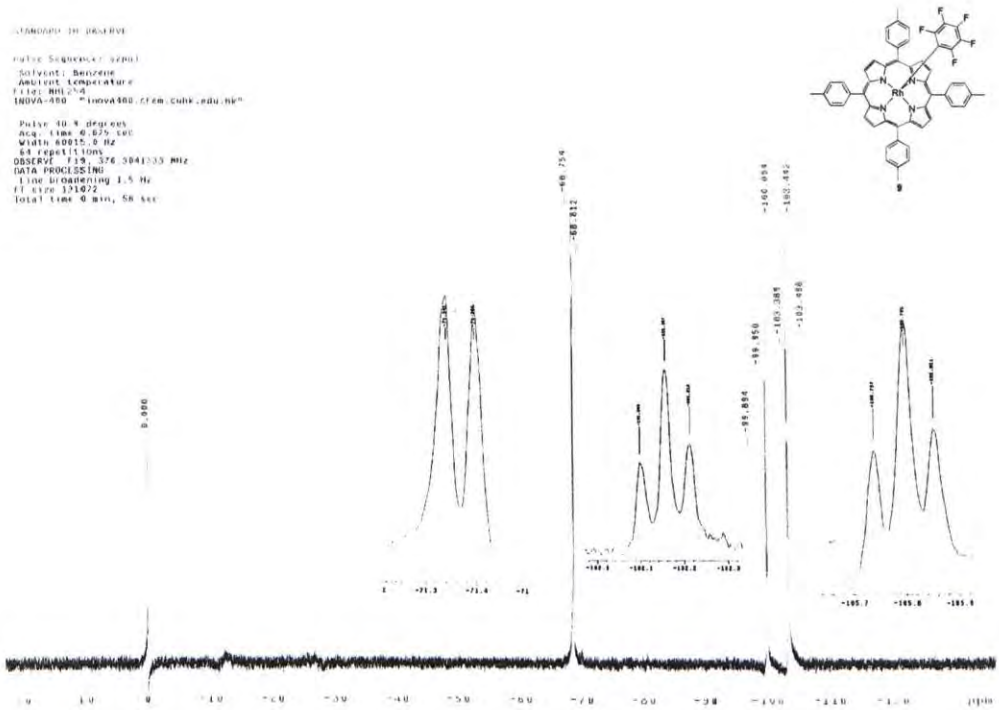

Table 3.3 Chemical Shift and Coupling Constant of various products obtained in ^{19}F NMR

Compound	*o*-F		*m*-F		*p*-F	
	Chemical shift / ppm	$^3J_{F-F}$ / Hz	Chemical shift / ppm	$^3J_{F-F}$ / Hz	Chemical shift / ppm	$^3J_{F-F}$ / Hz
(*o*-F)C_6H_4Rh(ttp) **5a**	-45.15	Nil	Nil	Nil	Nil	Nil
(2,3-F_2)C_6H_3 Rh(ttp) **5b**	-71.35	22.2	-77.14	22.2	Nil	Nil
(*m-F*)C_6H_4Rh(ttp) **6a**	Nil	Nil	-52.85	Nil	Nil	Nil
(2,6-F_2)C_6H_3 Rh(ttp) **6b**	-37.66	Nil	Nil	Nil	Nil	Nil
(*p*-F)C_6H_4Rh(ttp) **7a**	Nil	Nil	Nil	Nil	-62.84	Nil
(2,5-F_2)C_6H_3 Rh(ttp) **7b**	-52.69	Nil	-60.67	Nil	Nil	Nil
(3,5-F_2)C_6H_3 Rh(ttp) **8a**	Nil	Nil	-52.86	Nil	Nil	Nil
(2,4,6-F_3)C_6H_2 Rh(ttp) **8b**	-34.53	Nil	Nil	Nil	-56.93	Nil
C_6F_5Rh(ttp) **9**	-71.36	22.0	-102.16	22.8	-105.80	22.8